

AD 687852

AMRL-TR-68-105



## CRYOGENIC SOLID OXYGEN STORAGE AND SUBLIMATION INVESTIGATION

JOHN E. AHERN  
TRUMAN W. LAWSON, JR.  
*Aerojet General Corporation*

DECEMBER 1968

---

This document has been approved for public  
release and sale; its distribution is unlimited.

---

JUN 8 1969

AEROSPACE MEDICAL RESEARCH LABORATORIES  
AEROSPACE MEDICAL DIVISION  
AIR FORCE SYSTEMS COMMAND  
WRIGHT-PATTERSON AIR FORCE BASE, OHIO

## NOTICES

When US Government drawings, specifications, or other data are used for any purpose other than a definitely related Government procurement operation, the Government thereby incurs no responsibility nor any obligation whatsoever, and the fact that the Government may have formulated, furnished, or in any way supplied the said drawings, specifications, or other data, is not to be regarded by implication or otherwise, as in any manner licensing the holder or any other person or corporation, or conveying any rights or permission to manufacture, use, or sell any patented invention that may in any way be related thereto.

Federal Government agencies and their contractors registered with Defense Documentation Center (DDC) should direct requests for copies of this report to:

DDC  
Cameron Station  
Alexandria, Virginia 22314

Non-DDC users may purchase copies of this report from:

Chief, Storage and Dissemination Section  
Clearinghouse for Federal Scientific & Technical Information (CFSTI)  
Sills Building  
5285 Port Royal Road  
Springfield, Virginia 22151

Organizations and individuals receiving reports via the Aerospace Medical Research Laboratories' automatic mailing lists should submit the addressograph plate stamp on the report envelope or refer to the code number when corresponding about change of address or cancellation.

Do not return this copy. Retain or destroy.

ADDITIONAL TO  
WHITE SECTION  
BLUE SECTION  
DISTRIBUTION AVAILABILITY CODES  
DIST. AVAIL. SEC. OR SPECIAL  
600 - March 1969 - CO455 70-1541

AD 687852

AMRL-TR-68-105

**CRYOGENIC SOLID OXYGEN STORAGE  
AND SUBLIMATION INVESTIGATION**

*JOHN E. AHERN*  
*TRUMAN W. LAWSON, JR.*

This document has been approved for public  
release and sale; its distribution is unlimited.

## FOREWORD

This program was conducted by Aerojet-General Corporation, Azusa, California, during the period from 1 July 1967 through 31 March 1968, under Contract F33615-67-C-1849 and in support of Project 6373, "Equipment for Life Support," Task 637302, "Respiratory Support Equipment." The program was sponsored by the Aerospace Medical Research Laboratories and monitored by Mr. Konrad Weiswurm of the Biotechnology Branch, Life Support Division, Biomedical Laboratory, Aerospace Medical Research Laboratories, Wright-Patterson Air Force Base, Ohio. This report has been catalogued as Report No. 3545 by Aerojet.

The Principal Investigator at Aerojet-General Corporation, Azusa, California, was Mr. Norman Plaks, who was supported in this program by T. W. Lawson in the analytical phase, U. E. Gross, and E. Ogg in the experimental phase, and J. E. Ahern. The program was conducted under the management supervision of Mr. Lloyd Candell, Head of the Thermal and Environmental Systems Design Group.

This technical report has been reviewed and is approved.

C. H. KRATOCHVIL, Colonel, USAF, MC  
Commander  
Aerospace Medical Research Laboratories

## SUMMARY

The objectives of this program were (1) to determine analytically the advantages of using solid oxygen for long-term storage compared to subcritical liquid and supercritical oxygen for space systems, and (2) to determine the feasibility of transporting oxygen from the solid state to a condition suitable for breathing.

The analysis was made for two conditions of oxygen storage - with continuous use by crew members, and under conditions where oxygen is not being continuously used during the storage period. Practical storage vessel designs were selected for the study having supports to withstand two different G loads. Both multilayer and multiple-shield insulations were used in the study. Equations were developed to determine the initial storage system weight and the oxygen supply duration as a function of the type of oxygen storage - solid, saturated liquid, and supercritical fluid. In the case of continuous use of the oxygen for space cabin supply, the number of crew members and cabin leakage were additional independent parameters. The equations were programmed for the IBM 360 and cases were run over a range of potential space missions conditions.

For the case of continuous consumption by crew members, the results indicated that solid oxygen had a small performance advantage over the presently used subcritical oxygen supply system. This advantage would be nullified by the need for additional equipment to transport the solid oxygen to a breathable state. In this application, the need to draw off oxygen at a given rate for crew consumption nullified the major advantage of solid oxygen - the greater heat absorbing capability of solid oxygen over the liquid and supercritical state.

When the oxygen was not being continuously used to supply a space cabin atmosphere for crew members, storage of oxygen in the solid state was found to be significantly better from a duration standpoint than storing the oxygen as a saturated liquid for a supercritical fluid. The gain is significant enough to seriously consider solid oxygen in place of subcritical or supercritical oxygen for long-term storage under these conditions. Supercritical oxygen was shown to be poor for long-term storage due to the lower specific heat of the fluid in the supercritical condition. The better performance of solid oxygen, more than twice the storage life in this case, is due to the fact that advantage is taken of the heat of fusion, heats of transition, and the additional sensible heat in solid oxygen to extend the storage life.

Experimental studies were conducted on transporting oxygen from the vacuum storage condition to a condition suitable for breathing. Oxygen was solidified for these experiments by cooling with solid nitrogen under vacuum conditions. Two transport methods were evaluated. One method was to adsorb the vapor subliming from the solid oxygen on molecular-sieve cryosorption pumps cooled to liquid nitrogen temperature. After the pump is saturated with oxygen vapor, it is isolated from the vacuum storage vessel and heated to de-adsorb the oxygen into the space cabin atmosphere. The experiments showed that this method is feasible. However, low vapor flow conductance and slow cryosorption pump cooldown rates were encountered in the experimental work. Practical application of this transport method to space systems will require system designs that avoid these problems.

The other transport method which was experimentally evaluated was to physically move a solid piece of oxygen from the vacuum storage vessel to the space cabin atmosphere. An airlock system was used to maintain a vacuum in the storage vessel during the transfer. During transfer, one valve is opened between the airlock chamber and the storage vessel. The solid oxygen block is mechanically moved into the airlock chamber. When the valve is closed between the airlock chamber and the storage vessel, and the valve opened between the airlock chamber and the cabin atmosphere, the solid oxygen melts and vaporizes into the cabin atmosphere. Initial transfer of the solid oxygen was attempted by using a magnet since oxygen possesses paramagnetic properties. Although the oxygen could be picked up and moved, these preliminary results were inconclusive because of secondary adhesion effects due to the oxygen freezing to the magnet. The solid oxygen block could be readily picked up with a hook or with a magnet if a wire was frozen into the oxygen block. There appeared to be no problem in adapting this transport method to a space system.

Storage of oxygen in the solid form was shown to have significant advantages over the liquid or supercritical fluid when the oxygen was consumed only intermittently. Transport of the solid oxygen in blocks through an airlock valve was also found to be feasible. These methods could be used in a practical oxygen storage system as an emergency or reserve supply or for extra-vehicular activities.

TABLE OF CONTENTS

	<u>Page</u>
SECTION I	
INTRODUCTION . . . . .	1
PROGRAM OBJECTIVES . . . . .	1
Analytical Study . . . . .	1
Experimental Study . . . . .	1
BACKGROUND TECHNOLOGY . . . . .	2
SECTION II	
PROGRAM PLAN . . . . .	3
EXPERIMENTAL PLAN . . . . .	3
ANALYTICAL PLAN . . . . .	3
GENERAL OXYGEN PROPERTIES . . . . .	5
SECTION III	
EXPERIMENTAL STUDY . . . . .	8
OXYGEN TRANSPORT BY THE ADSORPTION METHOD . . . . .	8
Solid Oxygen Sublimation Laboratory Tests . . . . .	8
Test Apparatus . . . . .	8
Test Operations . . . . .	8
Procedure . . . . .	8
Shakedown Operation . . . . .	12
Test Runs . . . . .	16
Test Results . . . . .	18
Cryosorption Pump Adsorption Laboratory Tests . . . . .	18
Test Apparatus . . . . .	18
Test Operations . . . . .	19
Test Results . . . . .	20

Table of Contents (Continued)

	<u>Page</u>
Evaluation and Application of Results . . . . .	22
OXYGEN TRANSPORT BY MECHANICAL MANIPULATION . . . . .	25
Laboratory Tests . . . . .	25
Preliminary Experiment . . . . .	28
Test Operations . . . . .	34
Discussion of Test Results . . . . .	39
Evaluation and Application of Results . . . . .	39
DISCUSSION OF EXPERIMENTAL RESULTS . . . . .	39

SECTION IV

ANALYTICAL STUDY . . . . .	41
OBJECTIVE . . . . .	41
BACKGROUND TECHNICAL AREA . . . . .	42
STORAGE SYSTEM DESIGN FOR THE ANALYTICAL STUDY . . . . .	45
STORAGE OF OXYGEN WITH NO USAGE . . . . .	49
Analytical Procedures . . . . .	49
Results of the Analyses . . . . .	49
Discussion of Results . . . . .	50
STORAGE OF OXYGEN WITH USAGE . . . . .	64
Analytical Procedure . . . . .	64
Results of the Analyses . . . . .	65
Discussion of Results . . . . .	77
SOLID OXYGEN STORAGE AND SUPPLY SYSTEMS . . . . .	79
Systems for Space Cabin Oxygen Supply . . . . .	79
Systems for Long-Term Storage . . . . .	80
Systems for Extra-Vehicular Activity Supply . . . . .	84

Table of Contents (Continued)

	<u>Page</u>
SECTION V	
CONCLUSIONS . . . . .	86
SECTION VI	
RECOMMENDATIONS . . . . .	87
APPENDIX I - ANALYSIS OF HEAT TRANSFER TO THE STORED OXYGEN . . . . .	88
APPENDIX II - HEATING REQUIREMENTS FOR OXYGEN DELIVERY . . . . .	117
APPENDIX III - ANALYTIC STUDY, COMPARISON OF LIQUID VERSUS SOLID OXYGEN STORAGE . . . . .	124
APPENDIX IV - ANALYSIS OF WEIGHTS FOR OXYGEN STORAGE SYSTEMS . . . . .	137
APPENDIX V - ANALYSIS OF OXYGEN USAGE . . . . .	154

Table

LIST OF TABLES

I	Test System Pump Down Oxygen Transport by Absorption Method . . .	17
II	Molal Volumes and Densities of Solid Oxygen . . . . .	43
III	Heats of Sublimation and Vaporization for Oxygen . . . . .	44

## LIST OF ILLUSTRATIONS

<u>Figure</u>		<u>Page</u>
1	Program Schedule Contract F33615-67-C-1849 . . . . .	4
2	Vapor Pressure of Solid Oxygen . . . . .	6
3	Heat Capacity of Oxygen in the Solid and Liquid States . . . . .	7
4	Experimental Setup-Transport by Adsorbents . . . . .	9
5	Solidified Oxygen Storage Container . . . . .	10
6	Experimental Apparatus - Transport by Adsorbents . . . . .	11
7	Test Results for Heat Transfer Evaluation . . . . .	14
8	Modification of Apparatus to Improve Heat Transfer . . . . .	15
9	Schematic of Test Apparatus for Oxygen Adsorption Tests . . . . .	19
10	Adsorption Isotherm, O <sub>2</sub> , on Molecular Sieve at 77 K and 195 K . . . . .	21
11	Adsorption Rate of 10X Sieve at 77 K and 195 K . . . . .	23
12	Adsorbent Weight as a Function of Cycle Time . . . . .	24
13	Adsorbent Weight Required as a Function of Oxygen Flow Rate . . . . .	26
14	Cooldown Rate of Cryosorption Pump . . . . .	27
15	Preliminary Apparatus for Preparing Solid Oxygen . . . . .	29
16	Overall View of Preliminary Solid Oxygen Experiment . . . . .	30
17	Solid Oxygen Crystals Being Raised with Magnet . . . . .	31
18	Initial Design of Test Apparatus - Solid Oxygen Mechanical Transports . . . . .	32
19	Modifications to Test Apparatus . . . . .	33
20	Final Test Arrangement - Solid Oxygen Mechanical Transports . . . . .	35
21	Internal Arrangement of Solid Oxygen Mechanical Transport Test System . . . . .	36
22	Overall View of Solid Oxygen Mechanical Transport Test System . . . . .	37
23	Solid Oxygen in Pressure Chamber . . . . .	38
24	Latent Heat of Vaporization and Sublimation of Oxygen as a Function of Temperature . . . . .	46
25	Cut-Away View of the Oxygen Storage Dewar-Analytical Study . . . . .	47

List of Illustrations (Continued)

<u>Figure</u>		<u>Page</u>
26	Extended Storage Time of Liquid Oxygen by Subliming and Melting Solid Oxygen as a Function of Inner Container Radius (Solid Oxygen Storage 54.36 K, Flexible Multilayer Insulation) . . . . .	51
27	Extended Storage Time of Liquid Oxygen by Subliming and Melting Solid Oxygen as a Function of Inner Container Radius (Solid Oxygen Storage at 54.36 K, Rigid Shield Insulation . . .	52
28	Extended Storage Time of Liquid Oxygen by Subliming and Melting Solid Oxygen as a Function of Inner Container Radius (Solid Oxygen Storage at 43.8 K, Flexible Multilayer Insulation)	53
29	Extended Storage Time of Liquid Oxygen by Subliming and Melting Solid Oxygen as a Function of Inner Container Radius (Solid Oxygen Storage at 43.8 K, Rigid Shield Insulation) . . .	54
30	Comparison of Solid as a Function of Liquid Oxygen Storage Times, Flexible Multilayer Insulation $R_1 = 30$ CM, $T_{INS} = 1.0$ CM, 86.6 G . . . . .	55
31	Comparison of Solid as a Function of Liquid Oxygen Storage Times, Flexible Multilayer Insulation $R_1 = 30$ CM, $T_{INS} = 1.0$ CM, 10.0 G . . . . .	56
32	Comparison of Solid as a Function of Liquid Oxygen Storage Times, Flexible Multilayer Insulation $R_j = 30$ CM, $T_{INS} = 1.0$ CM, 86.6 G . . . . .	57
33	Comparison of Solid as a Function of Liquid Oxygen Storage Times, Flexible Multilayer Insulation $R_j = 70$ CM, $T_{INS} = 1.0$ CM, 86.6 G . . . . .	58
34	Comparison of Solid as a Function of Liquid Oxygen Storage Times, Rigid Shield Insulation $R_j = 39$ CM, $N = 0$ , 86.6 G . .	59
35	Comparison of Solid as a Function of Liquid Oxygen Storage Times, Rigid Shield Insulation $R_j = 30$ CM, $N = 0$ , 10 G . . .	60
36	Comparison of Solid as a Function of Liquid Oxygen Storage Times, Rigid Shield Insulation $R_j = 30$ CM, $N = 2$ , 86.6 G . .	61
37	Comparison of Solid as a Function of Liquid Oxygen Storage Times, Rigid Shield Insulation $R_j = 30$ CM, $N = 2$ , 10 G . . .	62
38	Required Initial Oxygen Weight as a Function of Mission Length and Number of Men and Heat Transfer Into the Container for Solid Oxygen Storage - 86.6 G . . . . .	66

List of Illustrations (Continued)

<u>Figure</u>		<u>Page</u>
39	Required Initial Oxygen Weight as a Function of Mission Length and Number of Men and Heat Transfer Into the Container for Liquid Oxygen Storage - 86.6 G . . . . .	67
40	Required Initial Oxygen Weight as a Function of Mission Length and Number of Men and Heat Transfer Into the Container for Supercritical Oxygen Storage - 86.6 G . . .	68
41	Required Initial Oxygen Weight as a Function of Mission Length and Number of Men and Heat Transfer Into the Container for Solid Oxygen Storage - 10.0 G . . . . .	69
42	Required Initial Oxygen Weight as a Function of Mission Length and Number of Men and Heat Transfer Into the Container for Liquid Oxygen Storage - 10.0 G . . . . .	70
43	Required Initial Oxygen Weight as a Function of Mission Length and Number of Men and Heat Transfer Into the Container for Supercritical Oxygen Storage - 10.0 G . . .	71
44	Mission Length Without Dumping Oxygen as a Function of Insulation Thickness (One Man Usage) . . . . .	72
45	Mission Length Without Dumping Oxygen as a Function of Insulation Thickness (Three Men Usage) . . . . .	73
46	Mission Length Without Dumping Oxygen as a Function of Insulation Thickness (Seven Men Usage) . . . . .	74
47	Total Weight as a Function of Mission Length and Number of Men (Insulation Thickness = 0.5 Centimeters, Flexible Multilayer Type). . . . .	75
48	Total Weight as a Function of Mission length and Number of Men (Insulation Thickness = 5.0 Centimeters, Flexible Multilayer Type). . . . .	76
49	Three Cryosorption Pump Transfer System . . . . .	81
50	Maximum Rate of Sublimation of Oxygen . . . . .	82
51	Flow Conductance of Subliming Oxygen Vapor Zero Flow Length Assumed (Orifice) . . . . .	83
52	Cross-Section View of Oxygen Container Illustrating Insulation Shielding Geometry . . . . .	92
53	Flexible Multilayer Thermal Conduction Parameter (T, 298) (298-T) . . . . .	93

List of Illustrations (Continued)

<u>Figure</u>		<u>Page</u>
54	Hemispherical and Normal Emittance and Absorptance of Gold . .	94
55	Thermal Conductivity of Titanium Alloy vs Temperature . . . .	105
56	Total Heat Transfer Through Insulation and Supports as a Function on Internal Container Radius - Solid Oxygen Storage .	111
57	Total Heat Transfer Through Insulation and Supports vs Internal Container Radius - Liquid Oxygen Storage . . . . .	112
58	Total Heat Transfer Through Insulation and Supports vs Internal Container Radius - Supercritical Oxygen Storage, Initial Storage . . . . .	113
59	Total Heat Transfer Through Insulation and Supports vs Internal Container Radius - Supercritical Oxygen Storage, at Minimum Required Heating . . . . .	114
60	Specific Heat Input for Constant Pressure Delivery - Supercritical Oxygen Storage . . . . .	115
61	Fluid Temperature for Constant Pressure Delivery - Supercritical Oxygen Storage . . . . .	116
62	Procedure I: Oxygen Initially Stored as a Solid at the Triple Point . . . . .	125
63	Procedures II and III: Oxygen Initially Stored as a Solid at 43.79 K (Phase II), and 12 K (Phase III), Respectively . . . . .	126
64	Oxygen Container . . . . .	138
65	Inner Container Radius vs. Stored Oxygen Weight . . . . .	141
66	Oxygen Usage Rate as a Function of Number of Men, Leakage Rate and Air-Lock Usage Factor - 150 Torr. . . . .	157
67	Oxygen Usage Rate as a Function of Number of Men Leakage Rate and Air-Lock Usage Factor - 250 Torr. . . . .	158

## SECTION I

### INTRODUCTION

The oxygen storage and supply system is a critical component of a manned space vehicle. The larger number of crew members now being considered for advance space vehicles will impose severe requirements on the environmental control system from the standpoint of reliable long-term storage of oxygen. Oxygen is conventionally stored as a liquid in either the subcritical or supercritical conditions. However, volume storage capacity of oxygen can be reduced if the oxygen is stored as a solid. Certain benefits appear to exist for solid oxygen in terms of transporting oxygen under zero-G condition and for long-term dead storage of oxygen.

Under the sponsorship of the Aerospace Medical Research Laboratories, Aerojet-General has performed a 10-month program encompassing both analytical and experimental tasks to evaluate the use of solid oxygen for the environment oxygen supply of a manned space vehicle. This report represents the culmination of the program effort and contains the results of the analytical and experimental studies. The information provided by this study will allow the selection of practical approaches for further study with respect to their application to existing and future system requirements.

#### PROGRAM OBJECTIVES

##### Analytical Study

The basic objective of the analytical study was to evaluate the storage capability of solid oxygen in comparison with storage of oxygen in the subcritical and supercritical condition. The comparison was to be made using realistic cryogenic storage vessels having a range of insulation characteristics and designed to survive high launch G-loads. Two storage conditions are of interest for solid oxygen: (1) comparatively long-term storage without using the oxygen followed by a period of usage and (2) short-term storage where the oxygen will be used for crew breathing as soon as the vehicle is in orbit. A comparison of solid oxygen with subcritical and supercritical oxygen for these two conditions is of interest. The evaluation of these analytical comparisons will indicate the practical applications of solid oxygen as well as the potential gain in performance by using solid oxygen.

##### Experimental Study

The basic objective of the experimental program was to demonstrate the feasibility of transporting the oxygen from the solid storage conditions to the conditions suitable for use by crew members, i.e., an oxygen pressure of about 150 torr at ambient temperature. Two methods appeared to be of interest; one method involves the adsorption and desorption of the oxygen vapor on an adsorbent, and the second method involves the mechanical movement of the solid oxygen through an airlock between the two pressure and temperature conditions. The tests were directed toward establishing the feasibility of these methods and obtaining data for a preliminary evaluation of the practicality of using these approaches in an operating system.

## BACKGROUND TECHNOLOGY

Solid cryogenics have found many uses in advanced technology areas, primarily for space and airborne applications. Many of these applications involve the use of the cryogen for cooling (Plaks, 1966; Gross et al, 1962; and Gross et al, 1964). Slush or solid hydrogen have also been considered for improving propellant storage in hydrogen-fueled vehicles. The major factor involved in the consideration of the solid phase is the fact that many problems associated with storage of the liquid or gas can be avoided. These include liquid sloshing during vehicle maneuver, zero-G two-phase supply problems with subcritical liquid, and high pressure tankage requirements for the supercritical liquid and gas storage.

Solid storage of oxygen has not been extensively studied. However, considerable work has been accomplished on solid storage of nitrogen, hydrogen, methane, and neon. The technology developed from working with these cryogenics is directly applicable to solid oxygen. Of particular interest is that the technology of insulating and supporting cryogenic tanks is available to design a thermally practical, solid-oxygen storage system.

The basic technology for preliminary evaluation of the solid oxygen storage and supply system is available. The specific problems in applying this technology to the solid oxygen system must be ascertained.

## SECTION II

### PROGRAM PLAN

The objectives of this program dictated that the analytical and experimental parts of the program could be essentially independent of each other. To assure that the analytical study would take advantage of any technology developed in the experimental study, the analytical study was to start later in the program with the experimental work on oxygen transport preceding the analytical study. The general program schedule is shown in figure 1.

#### EXPERIMENTAL PLAN

The experimental effort was divided into two phases as shown in figure 1. The initial phase involved the evaluation of the adsorption-desorption method of transporting oxygen from a subliming vapor at low pressures and temperatures to a vapor under the pressure and temperature conditions of a space cabin. This work was to take the form of experiments to determine the feasibility of the approach and to provide data to make a preliminary evaluation of the practicability of the approach. Tests were planned in which the adsorption of oxygen vapor subliming from solid oxygen would be demonstrated. Tests were also planned to provide the adsorption rate of cold oxygen vapor for various temperatures of the cryosorption pump. The work was to be done on a laboratory scale using solid nitrogen to prepare the solid oxygen.

The second phase of the experimental work was to demonstrate the transport of solid oxygen by mechanical transport from the low-pressure, low-temperature storage area to a chamber where the oxygen could be transformed to a breathable condition. The tests would disclose major problems in this approach and, thereby, provide preliminary information to indicate the best mechanical method to use. This work was to be done on a laboratory scale using solid nitrogen to prepare the solid oxygen.

From a temperature difference standpoint, the best method of solidifying oxygen is with liquid helium. However, liquid helium is expensive, and its use becomes impractical for the scope of this feasibility program since the quantities of solid oxygen required could be prepared using solid nitrogen.

#### ANALYTICAL PLAN

The basic plan for the analytical phase of the program was to evaluate the use of solid oxygen for application in manned space systems for storage and supply of breathable oxygen. The study was to evaluate the use of solid oxygen to improve the storage life of oxygen when it is not being consumed, as well as the use of solid oxygen for storage and supply systems during continuous use by crew members. The application potential of solid oxygen was to be developed by comparison with the use of subcritical and supercritical oxygen storage.

The work involved in the analytical phase would initially require developing the analytical procedures and then programming these procedures for use on the IBM 360 digital computer.

	1967							1968		
	EVAL.	JUL	AUG	SEP	OCT	NOV	DEC	JAN	FEB	MAR
<b>PHASE I EXPERIMENTAL</b>										
1. EXPERIMENT PLANNING		■	■							
2. FABRICATION			■	■	■	■	■			
3. TRANSPORT BY ABSORBANTS				■	■	■	■			
4. TRANSPORT BY MECHANICAL MANIPULATION							■	■		
<b>PHASE II ANALYTIC</b>										
1. ANALYSIS AND PARAMETRIC STUDY							■	■	■	■

Figure 1. Program Schedule Contract F33615-67-C-1849

The basis for the study was to be an oxygen storage vessel, thermally insulated, and having thermal isolation supports to handle realistic launch G-loads. The insulation and support methods were to be considered for all three oxygen storage methods (solid, subcritical, and supercritical) so that comparison of optimum designs for each method can be made.

#### GENERAL OXYGEN PROPERTIES

The physical and thermodynamic properties of oxygen in the liquid and solid state are important in developing the storage and transport systems analytically, and for establishing the conditions that are used in the experimental work. Data in the liquid and gaseous state is readily available in the literature. Information on solid oxygen, however, is not extensively available. Properties of solid oxygen given in Mullins et al (1965) were used in this study since it was the most complete compilation of solid oxygen data available in the literature. The vapor pressure of solid oxygen is shown in figure 2, and the specific heat of the solid oxygen is shown in figure 3.

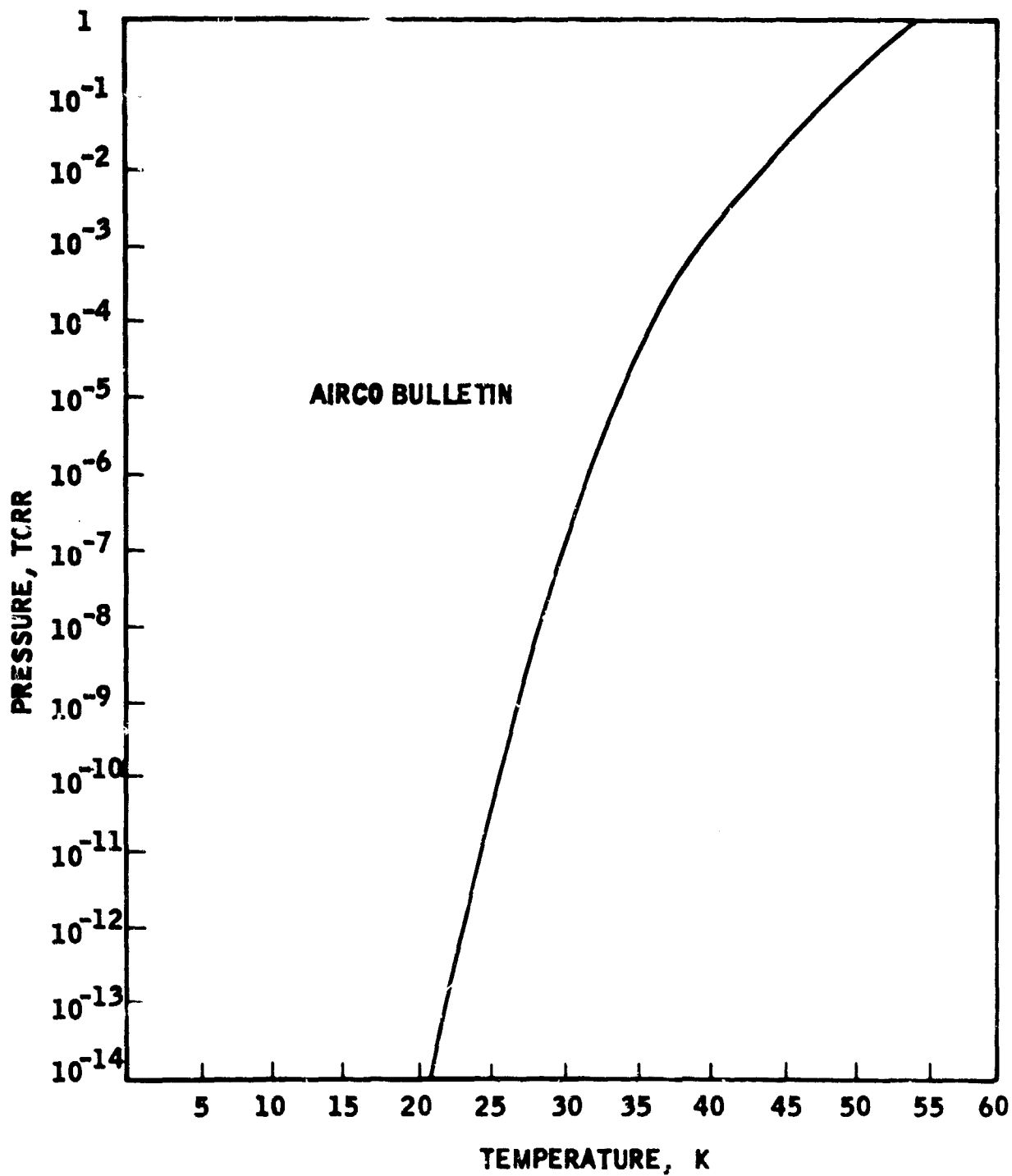


Figure 2. Vapor Pressure of Solid Oxygen

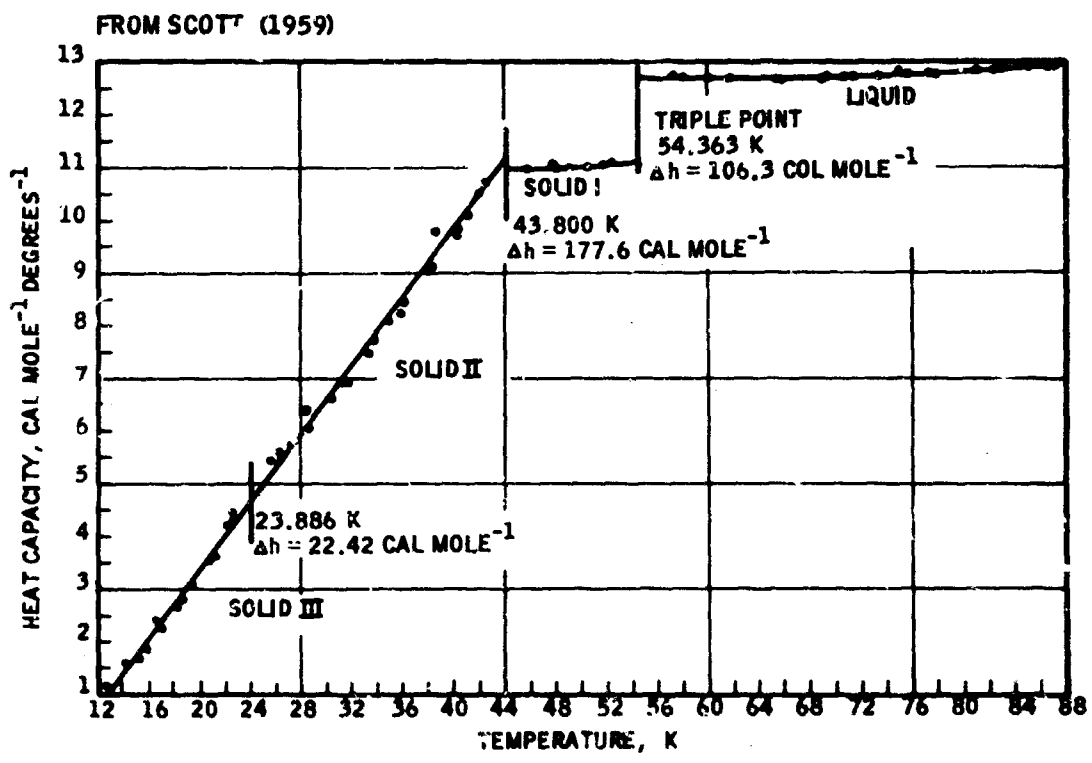


Figure 3. Heat Capacity of Oxygen in the Solid and Liquid States

SECTION III  
EXPERIMENTAL STUDY

OXYGEN TRANSPORT BY THE ADSORPTION METHOD

Solid Oxygen Sublimation Laboratory Tests

The purpose of the initial tests was to determine important parameters involved in the transport of oxygen from a stored solid to a breathable state by the use of molecular sieve adsorbents that have been cooled to temperatures obtainable by passive radiation to space.

Test Apparatus

The basic arrangement for this first experimental test is shown schematically in figure 4, and the working vessel for preparing and storing the solid oxygen is shown schematically in figure 5. A photograph of the complete test system for transport by adsorbents is shown in figure 6.

The working vessel consists of a double-wall container with associated filling and evacuation lines, a pressure sensing tube, and an evacuation line leading into the space between the double walls. The space between the double walls can be evacuated to provide an insulation space or filled with helium gas to serve as a thermal conductor. The pressure sensing tube from the oxygen container was connected to a pressure gauge to indicate the state of the oxygen.

The cryosorption pump provides a low pressure over the stored oxygen and acts as a collector and pressure raising device for the subliming oxygen. Valves are provided so that the pumps can be alternately and sequentially removed from the low-temperature bath for measurement of the amount of oxygen evolved at a breathable pressure. By using three cryosorption pumps, this can be done on a continuous basis.

The gaseous oxygen de-absorbed from the cryosorption pumps by heating was condensed and measured. This was done in the collection and measuring apparatus shown in figure 6. Condensing was accomplished by surrounding the oxygen collection tube with liquid nitrogen. The amount transferred was determined by measuring the level of the liquified oxygen with a cathetometer.

Test Operations

Procedure

The procedure for operation of the test system was as follows (see figure 4):

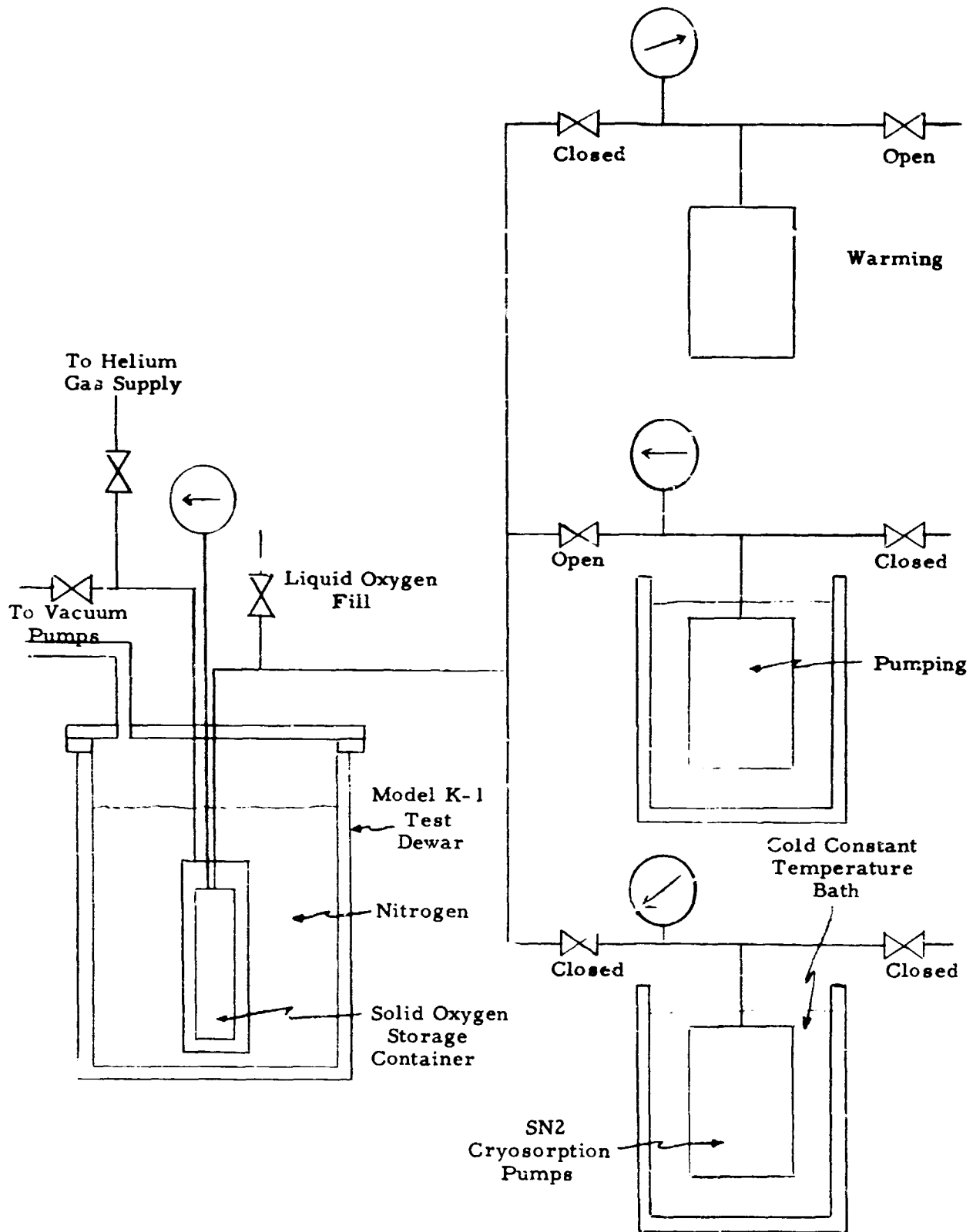


Figure 4. Experimental Setup-Transport by Adsorbents

Stainless Steel Tube  
1.25 cm ID, 0.25 mm Wall Thickness

Stainless Steel Tube  
0.95 cm ID,  
0.25 mm Wall Thickness

Stainless Steel  
Capillary Tube:  
0.5 mm OD

O-Ring

K-1 Dewar

Stainless  
Steel Inner  
Container  
0.5-mm  
Thick Wall

Solidified  
Nitrogen

Copper Outer  
Container  
2.5 mm  
Thick Wall

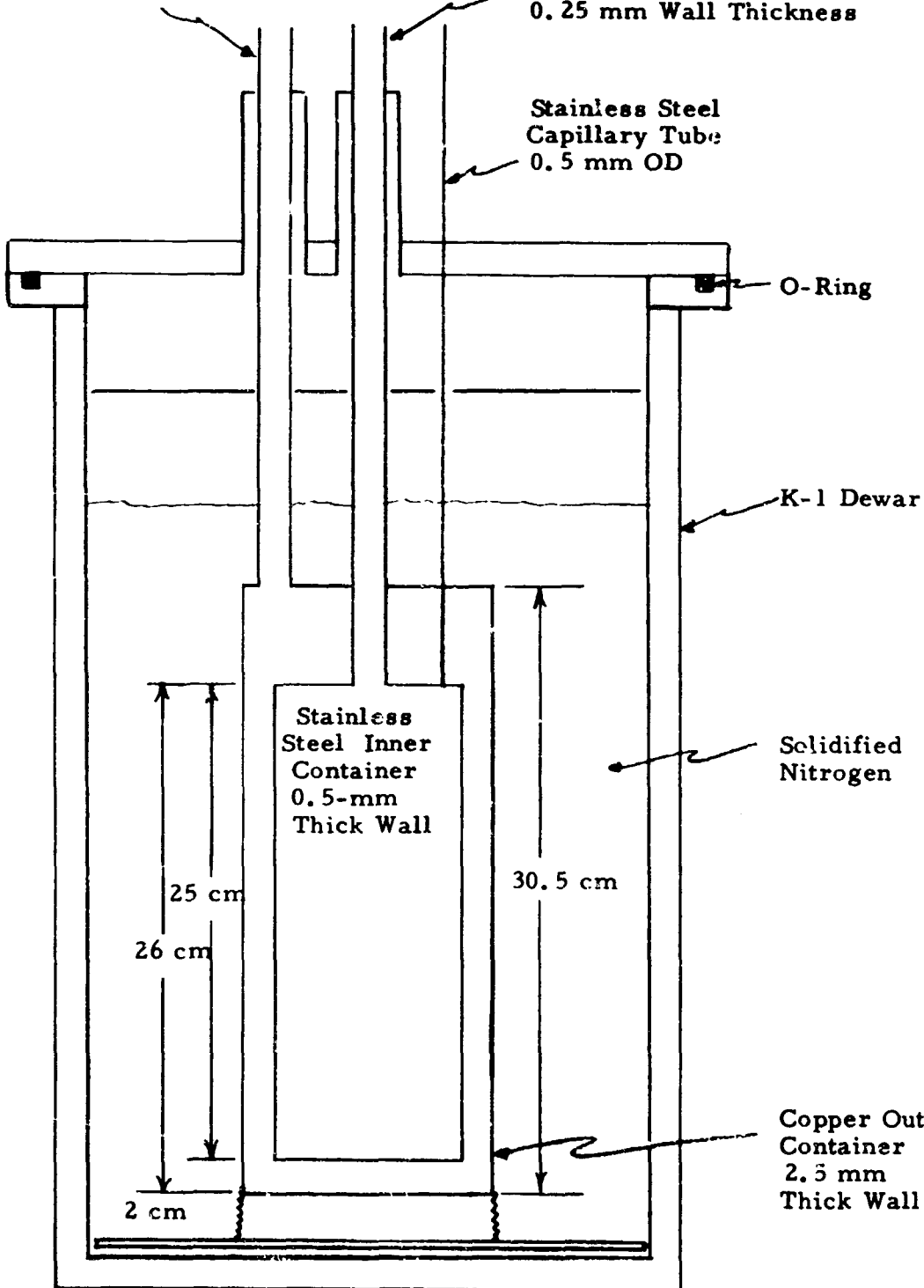


Figure 5. Solidified Oxygen Storage Container



Figure 6. Experimental Apparatus - Transport by Adsorbents

1. The test Dewar is partially filled with liquid nitrogen.
2. The space between the double walls of the working vessel is evacuated, and the working vessel and Dewar cover are installed in the test Dewar.
3. The inner container of the working vessel is filled with liquid oxygen and the fill line sealed.
4. The space between the double walls of the working vessel is filled with helium that provides a thermal conduction path and allows the liquid oxygen to cool to the liquid nitrogen temperature.
5. Vacuum pumping reduces the pressure in the test Dewar, causing the nitrogen to solidify and cool to temperatures of about 48 to 50K.
6. The solid nitrogen then cools the liquid oxygen through the helium space to a temperature where it solidified (54.36K).
7. After the oxygen is solidified, the helium is evacuated from between the double walls of the working vessel, and the solid oxygen, under vacuum storage conditions, is now available for the adsorption experiments.
8. The cryosorption pumps are then cooled and connected in sequence to the solid oxygen storage container. The pumps are allowed to adsorb the sublimed oxygen at a pressure of 1.14 torr or less. After adsorption on a pump is completed, the pump is isolated from the solid oxygen container by means of valves, and the pump is warmed to desorb the oxygen at a considerably higher pressure than the vapor pressure of the solid. The desorption pressure was 150 torr for these tests (the vapor pressure of oxygen at 77K).

#### Shakedown Operation

Initial operations with the test system disclosed two areas in the test apparatus requiring modifications.

First of all, the solid nitrogen in the test Dewar surrounding the working vessel could not be cooled by vacuum pumping to a temperature sufficiently low to solidify the oxygen using the existing equipment. The lowest temperature that can be achieved by vacuum pumping over a solid such as nitrogen is a function of its evaporation rate. To lower the sublimation temperature of the solid the vacuum pumping system should be increased in size, and/or the heat leak into the vessel reduced. The system was modified by increasing the capacity of the vacuum pump from 14.2 to 38 liters per second, and a low-emissivity shield was placed between the surface of the nitrogen

and the cover of the test Dewar. These modifications increased the evaporation rate and reduced the heat leak rate to the point where a nitrogen temperature of 50K was obtained as shown by the pressure measured over it of 3 torr. This temperature is sufficiently lower than the 54.36K required for solidifying oxygen.

The second problem was that the oxygen in the inner container of the working vessel would not solidify in a reasonable length of time when the solid nitrogen temperature was around 50K. The heat transfer rate between the solid nitrogen and the oxygen was not sufficient. The two major causes of a low heat-transfer rate are the thermal resistance of the helium transfer gas and the thermal resistance of the gap created by the solidifying nitrogen.

To evaluate the cause of the heat transfer problem, a special test was conducted using liquid nitrogen in the inner container of the working vessel where oxygen is normally contained. The test Dewar was charged with about 75 liters of liquid nitrogen and the inner container was loaded with 0.88 liters of liquid nitrogen. The intermediate volume between the two nitrogen areas was filled with helium gas at a pressure of 1.06 kg/cm<sup>2</sup> absolute. The test Dewar containing the 75 liters of liquid nitrogen was then evacuated by connecting it to the vacuum pumps.

Figure 7 shows the temperatures observed in the test apparatus from the vapor pressure measurements in each nitrogen container. The pump-down curve for the evacuated nitrogen in the test Dewar is shown as curve II. The section of this curve from "a" to "b" shows nitrogen as a liquid; from "b" to "c" the nitrogen is solidifying, and from "c" to "d" the nitrogen is a solid and continues to drop in temperature with continued pumping. Curve I in figure 7 shows the temperatures during cool-down of the nitrogen in the inner container, and curve III shows the heat transfer rate between the nitrogen in the inner container and the nitrogen in the test Dewar as calculated from the temperatures and the properties of the materials. It is apparent from curve III that the rate of heat transfer decreases appreciably after the nitrogen in the Dewar solidifies, approaching 15 calories per minute after two hours. To determine whether the unexpected heat transfer resistance was through the helium gas or in the nitrogen, calculations were made. The heat transfer through the helium gas was over 30 calories per minute by conduction alone, and therefore the helium was not the source of the thermal resistance. The calculations indicated that a gap between the solid nitrogen and the inner container of about 0.01 cm would give a heat transfer rate of 15 calories per minute. Therefore, the reason for the high heat transfer resistance between the solid nitrogen and the inner container was the presence of a gap at this interface caused by the subliming nitrogen. To solve this problem by reducing the effects of gap resistance, copper conduction strips were attached to the bottom of the working vessel and extended into the solid nitrogen area in the test Dewar. A sketch of this modification is shown in figure 8. The

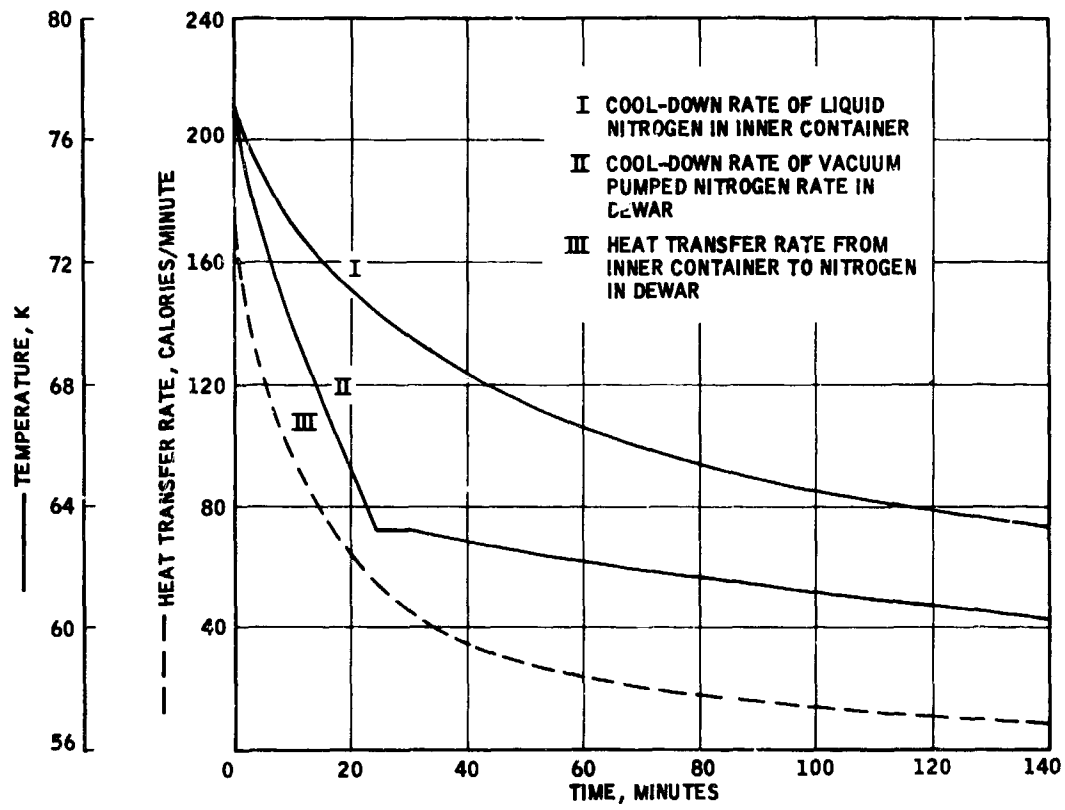


Figure 7. Test Results for Heat Transfer Evaluation

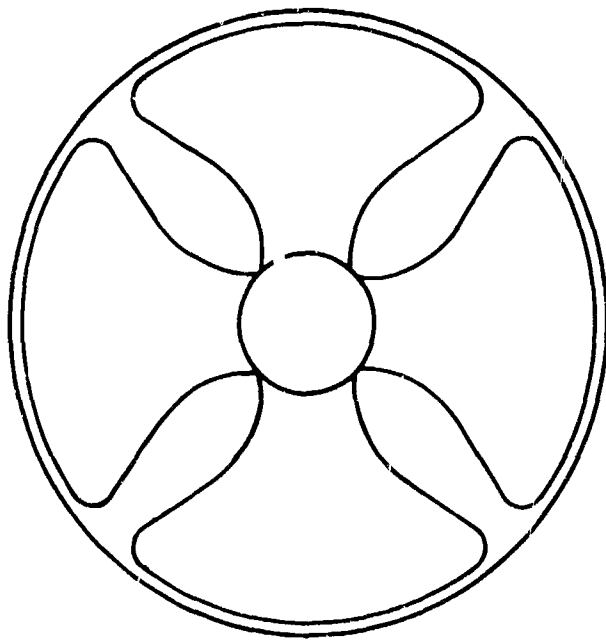
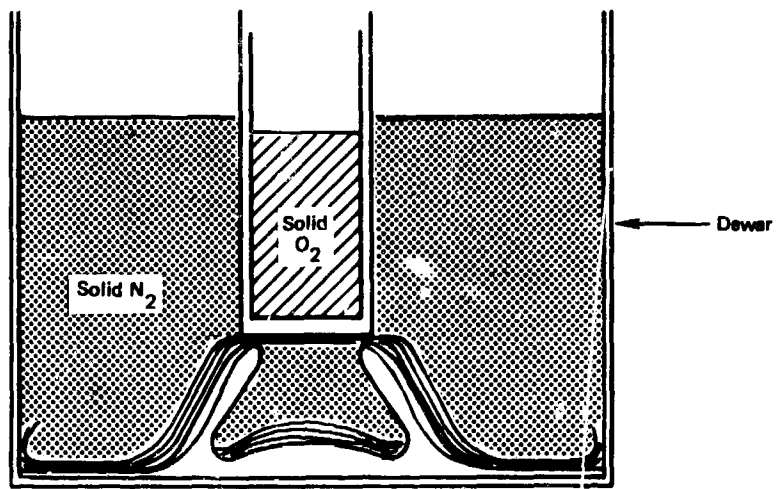


Figure 8. Modification of Apparatus to Improve Heat Transfer

tests described in the next section indicated that these problems were satisfactorily solved by the modifications that were made.

#### Test Runs

Two test runs were made in which solid oxygen was prepared in the working vessel and the subliming vapors collected on the cryosorption pumps. The oxygen in the pump was driven off by heating the pump. The amount of oxygen collected in the pumps was measured by condensing the vapors in a calibrated glass tube immersed in liquid nitrogen and determining the liquid level with a cathetometer.

#### Test Run No. 1

The test Dewar was filled with liquid nitrogen. Oxygen from a gas bottle flowed through a coil immersed in liquid nitrogen, where it was liquefied, and then it passed into the inner container of the working vessel. Helium gas was added to the space between the vessels to a pressure of one atmosphere. The test Dewar with the liquid nitrogen was then connected to the vacuum pump and evacuation started. Table I shows the pressures measured in the nitrogen Dewar and oxygen container during pump-down.

The helium was pumped out from the space between the solid cryogenes to thermally isolate the solid oxygen, and the cryosorption pump tests started. The pumps were connected to the solid oxygen in sequence, and after disconnecting, they were allowed to warm up. To accelerate the warm up of the pump, an electric heater was inserted in the center cavity of the pump, isolated from the molecular sieve by the casing. The oxygen was transferred to the measuring tubes by using the pumps until the pressures in the test system indicated that further transfer was impractical. The amount of gaseous oxygen transferred by the cryosorption pump in this test was about 3 cc in the condensed liquid state.

#### Test Run No. 2

This test run was similar to No. 1 except that the cryosorption pumps were more extensively activated to eliminate all traces of moisture in the molecular sieve. Activation was accomplished by heating the pumps to 240C under vacuum until the pressure on an absolute pressure gauge read zero. In this test, 10.0 cc of condensed liquid oxygen were transferred to the 0.625 cm ID and 2.19 cm ID oxygen measuring tubes as a gas.

#### Test Run No. 3

This test was a repeat of test run No. 2. In this test, 20.0 cc of condensed oxygen were transferred by using all three oxygen measuring tubes, the 0.625 cm ID, the 2.19 cm ID, and the 2.50 cm ID tubes.

TABLE I

TEST SYSTEM PUMP DOWN

OXYGEN TRANSPORT BY ABSORPTION METHOD

Run No. 1

<u>Time</u>	<u>Pressure of nitrogen in test dewar, mm Hg</u>	<u>Pressure of oxygen in working vessel container, mm Hg</u>
0857	83 - solid nitrogen	--
0932	42.3	80
0945	29.5	68.5
1007	13	57
1025	8.4	52
1040	6.5	49.4
1055	5.5	48
1120	4.5	46
1200	3.5	43.5
1300	3	42
1326	2.6	1.2 - solid oxygen
1327	2.6	1

## Test Results

The feasibility of transporting oxygen from the subliming solidified state, occurring at 1.14 torr or less, to a pressure sufficiently high to breathe was successfully demonstrated. An approximate 200:1 compression of the oxygen vapor was accomplished using thermal energy; no mechanical energy was used or required.

The rate of oxygen transport from the solidified condition by means of a 5A type molecular sieve (synthetic zeolite-calcium alumina silicate) was 0.0854 gram per minute for 0.725 kilogram adsorbent at 77K. For one man, 0.785 gram per minute are required, and the adsorbent weight requirement would be 6.7 kilograms.

Because the rate of oxygen transport was limited by the flow conductance of the apparatus tubing and the valves, and quantitative values obtained in these tests can not be considered optimum. This factor dictated that tests should be conducted to specifically obtain quantitative data on the adsorption capabilities of oxygen on the molecular sieve. This type of data would be useful in developing the practicality of the cryosorption method of oxygen transport. The next section describes the tests to obtain this data and the results of the tests.

### Cryosorption Pump Adsorption Laboratory Tests

The major factor determining the efficiency of the cryosorption pump, oxygen transport system is the effectiveness of the adsorbent. The previous tests provided preliminary data, but due to system limitations, the quantitative adsorption capabilities of the adsorbents could not be obtained. The tests described below were directed to obtaining the amount of oxygen that can be adsorbed per unit weight of molecular sieve at a given temperature.

### Test Apparatus

The test apparatus for these experiments used the cryosorption pumps from the previous test (see figure 6). The oxygen collection and measurement apparatus shown in figure 5 was used for the liquid oxygen supply and for measuring the quantity of oxygen adsorbed on the cryosorption pumps. The level of liquid oxygen in the precision bore tubes of the oxygen supply system was determined by using a cathetometer. A schematic of the test arrangement is shown in figure 9.

### Test Operations

Prior to each test, the molecular sieve was activated by heating to 477K for six hours while purging with dry nitrogen and then vacuum pumping for one hour at a pressure of  $10^{-2}$  torr.

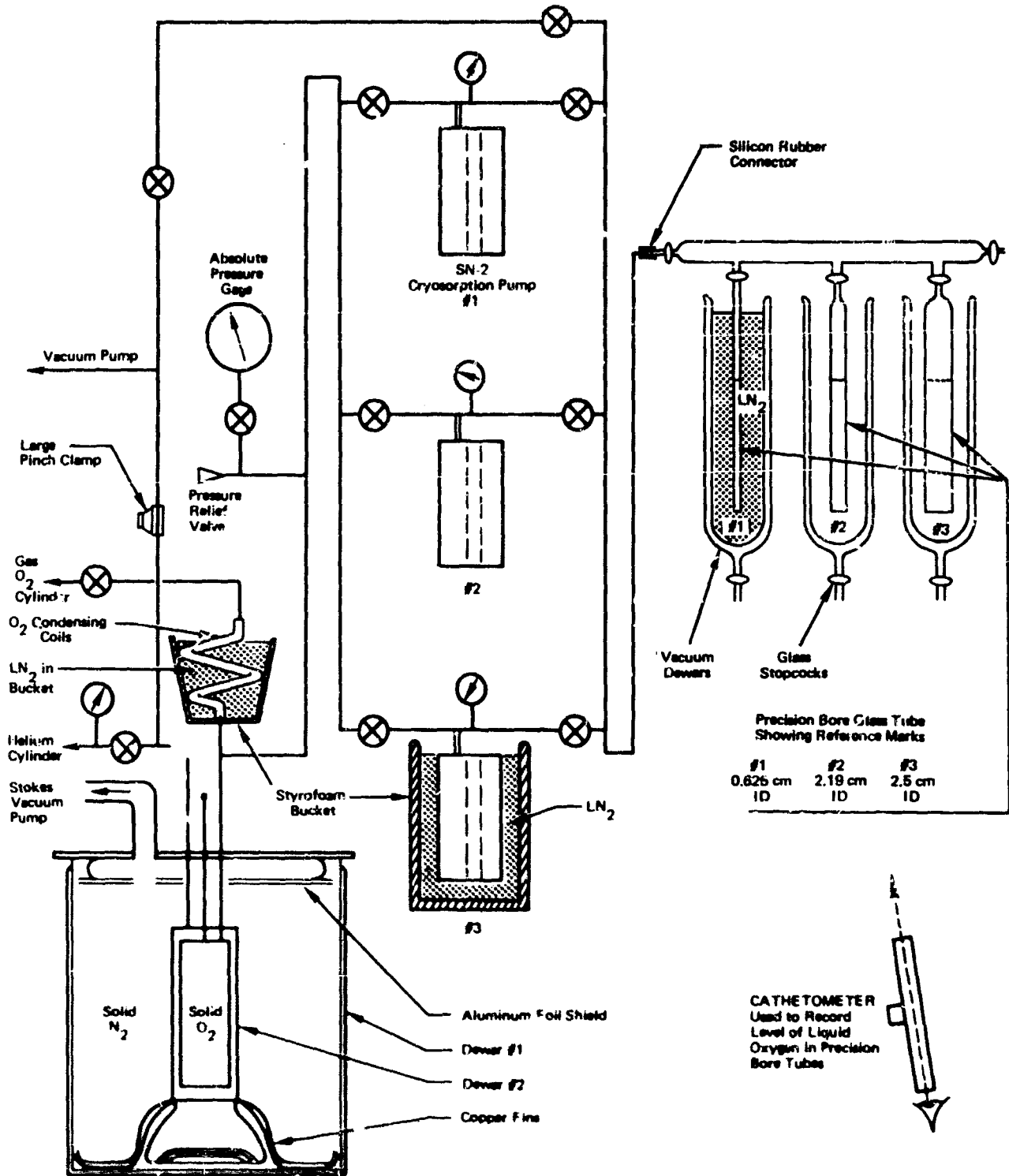


Figure 9. Schematic of Test Apparatus for Oxygen Adsorption Tests

The adsorption tests were conducted with the molecular sieves at two temperature levels. A temperature of 195K was obtained by submerging the cryosorption pump in a CO<sub>2</sub>-trichloroethylene bath, and a temperature of 77K was obtained by submerging the pump in a liquid nitrogen bath. Three molecular sieves, designated 5X, 10X, and 13X, were tested. These were standard molecular sieves as furnished by Linde and have 20 percent inert material as binder.

These tests were conducted in the following manner:

- a. The cryosorption pump was submerged in the coolant and the pump cooled to the test temperature level.
- b. The glass Dewar flasks surrounding the oxygen supply tubes were filled with liquid nitrogen.
- c. Gaseous bottled oxygen was put into the oxygen supply tubes and condensed by the liquid nitrogen.
- d. After the level of liquid oxygen was measured, the valve between the oxygen supply tube and the cryosorption pump was opened.
- e. The pressure in the pump was measured with a precision McLeod gage, and the liquid oxygen level was measured with a cathetometer at intervals during adsorption until equilibrium was achieved.

The initial tests indicated that this procedure was suitable for obtaining the data necessary to generate the desired performance. Each of the molecular sieves, type 5X (calcium alumina-silicate), type 10X (crystalline alumina-silicate), and type 13X (sodium alumina-silicate), was evaluated at temperatures of 195K and 77K. No problems occurred during the test operations.

#### Test Results

The results of the tests are presented in figure 10. The first important feature noted on the curves is the large difference in the quantity of oxygen adsorbed at the two temperature levels. This points out the importance of operating the cryosorption pumps at the lowest possible temperature level during the adsorption phase of operation.

The curves in figure 10 show a significant difference in performance of the three molecular sieves. The 10X type adsorbed approximately 10 percent more oxygen than the 13X type and about 25 percent more than the 5X type for a given pressure level at 77K. The 13X molecular sieve performed very poorly at 195K compared to the other two types. The quantity of oxygen adsorbed by the 13X sieve was almost negligible, although the 10X and 5X sieves only adsorbed about 1 gram of oxygen per 100 grams of adsorbent for these sieves at 77K.

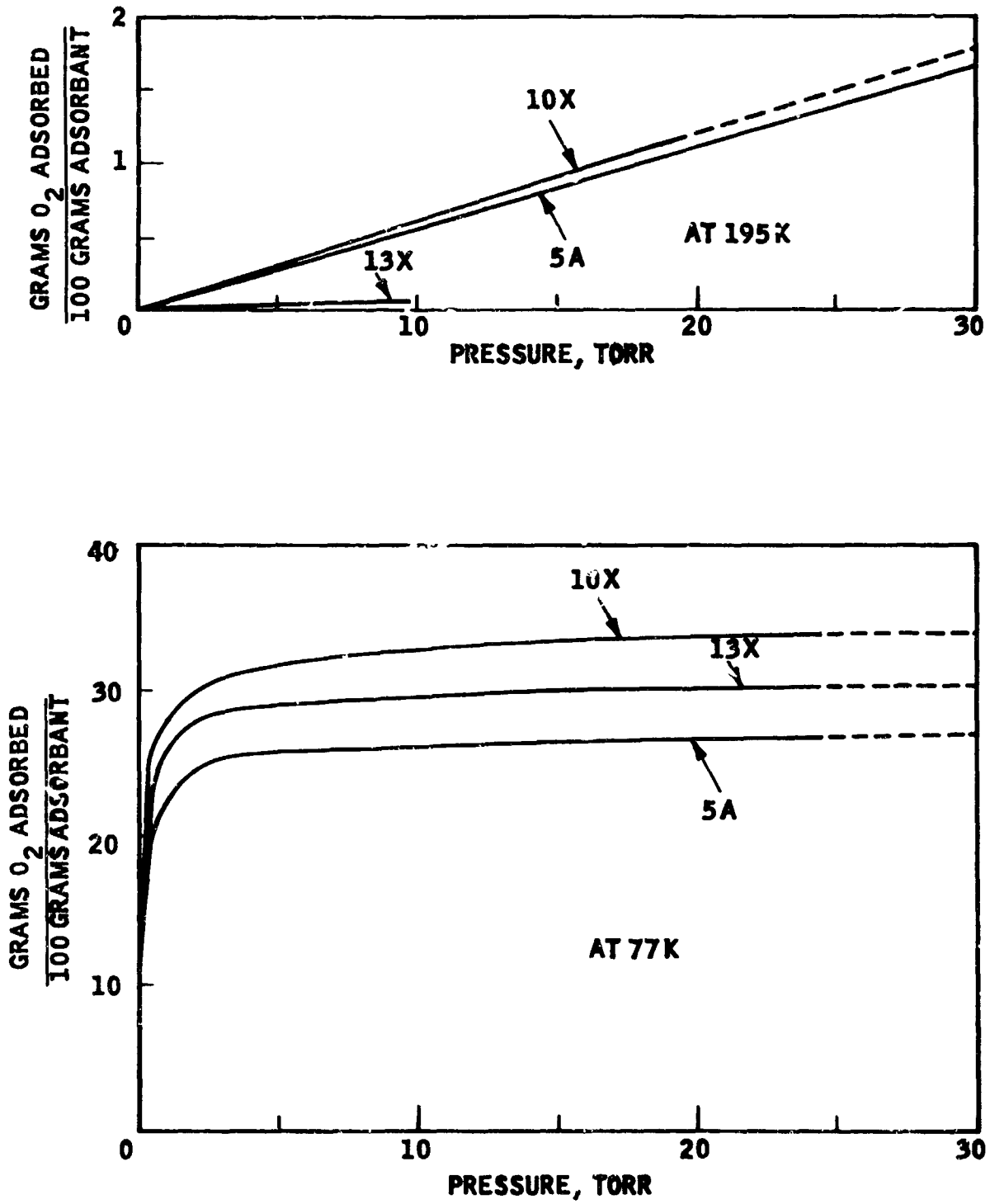


Figure 10. Adsorption Isotherm,  $O_2$ , on Molecular Sieve at 77K and 195K

The data shown in figure 10 indicates that of the three types tested the 10X molecular sieve is best suited for oxygen adsorption. The isotherms in figure 10 include the adsorption capability of the 10X sieve which should be used in the system study. Figure 11 is a plot of the oxygen adsorption rate for the 10X molecular sieve at 77K as determined from the test data. The information on the 10X molecular sieve in figures 10 and 11 can be used for preliminary performance evaluation of the cryosorption-pump, oxygen transport system.

#### Evaluation and Application of Results

The results obtained in these tests are suitable for preliminary evaluation of the performance of the cryosorption pump. The evaluation is limited to an operating temperature level for adsorption of 77K since only 77K and 195K temperature levels were evaluated in the tests, and the latter temperature level showed insignificant adsorption.

The information on the cryosorption pump performance that would be required for the oxygen transport system study includes the size of pump necessary for transporting a given amount of oxygen from the subliming condition to a breathable state. In addition, the rates of adsorption, desorption, and cool-down of the pump are necessary to establish practical cycling conditions and to determine the number of cryosorption pumps required.

Using the data from figures 10 and 11 for the 10X molecular sieve, the adsorption time required for various adsorbent weights can be developed for a given oxygen transport rate. A cyclic process is necessary for the cryosorption-pump transport method to maintain a constant oxygen supply rate. One pump is desorbing oxygen to the crew compartment while the other pump is adsorbing the oxygen that is subliming from the solid. The pumps are then switched over to the opposite process when the adsorbing pump is loaded with oxygen. Given an oxygen supply rate requirement of 2.26 kilograms per day, the cycle time and adsorbent weight requirements are shown in figure 12. This curve indicates that a minimum adsorbent weight exists for a cycle time of 6 hours. Operation with cycle times of less than 6 hours will result in less than optimum capacity of oxygen adsorbed on the molecular sieve (figure 11). With a cycle time greater than 6 hours, the rate of oxygen adsorption beyond the 6 hour period falls off as shown by figure 11, so that operation in this region becomes less efficient. It should be pointed out that the data in figure 11 was developed from one test and must be considered preliminary. The weight of the molecular sieve for one cryosorption pump is shown in figure 13 for various cycle times as a function of oxygen flow rate.

The other information required to evaluate the performance of the adsorbent transport system is the desorption rate of the molecular sieve and the cool-down rate of the cryosorption pump after it has been desorbed of oxygen and prior to the next adsorption cycle.

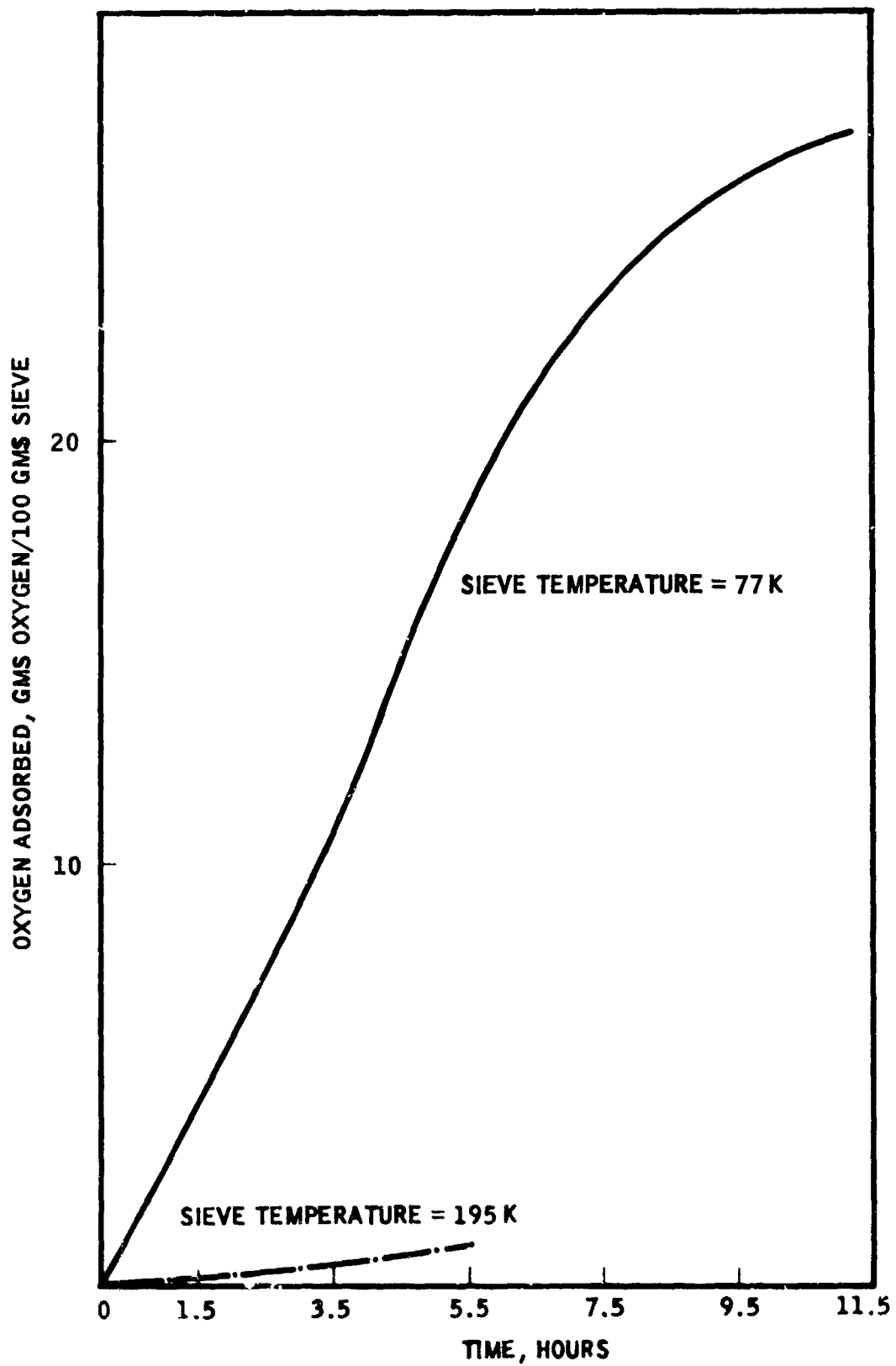


Figure 11. Adsorption Rate of 10X Sieve at 77K and 195K

ADSORBENT REQUIRED IN EACH OF TWO  
CRYOPUMPS TO SUPPLY 2.26 KG OXYGEN  
PER DAY  
(MOLECULAR SIEVE 10X AT 77 K)

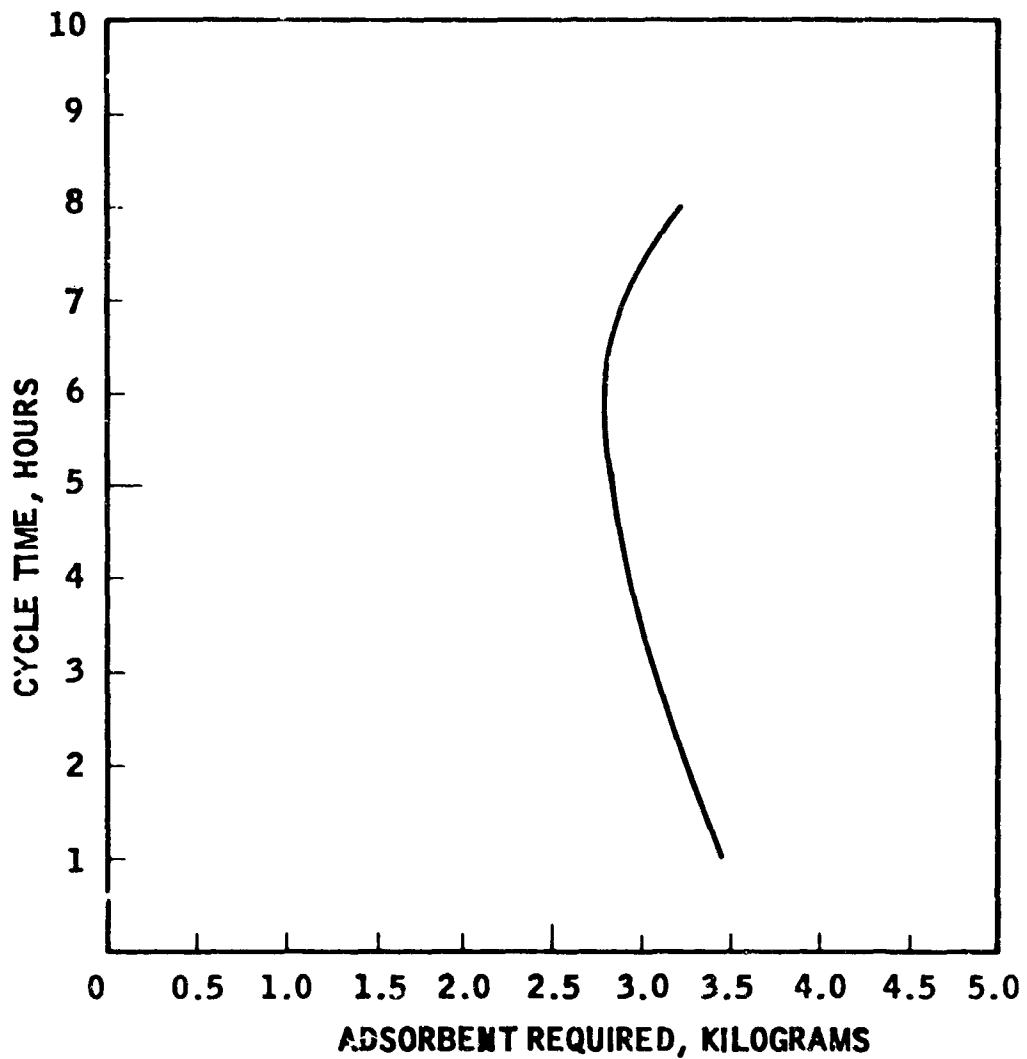


Figure 12. Adsorbent Weight as a Function of Cycle Time

The desorption of oxygen from the molecular sieve should be rapid at room temperature since figure 10 indicates that the adsorbed amount of oxygen in equilibrium with the 10X molecular sieve at 195K is almost negligible. The cool-down rate of the cryosorption pump used in the test was approximately determined from visual observations of the liquid nitrogen bubbling when the pump was immersed in liquid nitrogen for cooling. The liquid nitrogen bubbling essentially stopped after 30 minutes of immersion. A transient analysis for this annular sieve container gives a value of 45 minutes using a thermal diffusivity value of  $9.29\text{cm}^2/\text{hr}$ , and assuming that the thermal resistance between the pump and the coolant is negligible. Since this is reasonably close for approximate analysis, the cool-down rates for cylindrical cryosorption pumps of different sizes were calculated using these assumptions, and the results are shown in figure 14. The molecular sieve requires long cool-down times, 6 hours for a 0.5 kilogram cryosorption pump for example, and therefore, a three-pump system would be necessary for oxygen transport. One cryosorption pump is being cooled down, one pump is adsorbing oxygen, and one pump is desorbing oxygen. Therefore, to obtain the basic molecular sieve weight of the cryosorption-pump, oxygen transport system, it is necessary to multiply the weight in figure 13 by three for the three cryosorption pumps.

The cool-down rate can be improved by filling the molecular sieve with a material having high thermal conductivities, such as, aluminum or copper wire mesh, or else strip fins could be used to rapidly conduct the heat out of the adsorbent. These devices will add to the weight and the complexity of the structure. Further study of these methods would be required to establish the best method to use and the penalty associated with the modification.

The system analysis conducted in the analytical study assumes that the adsorption rate of oxygen on the molecular sieve dictates the cycle time and that a three-pump system is required. These are reasonable assumptions for a preliminary evaluation of the system, and further experimental and analytical study would be required on the desorption and cool-down phases for a complete system design study.

## OXYGEN TRANSPORT BY MECHANICAL MANIPULATION

### Laboratory Tests

The basic goal of this experiment was to demonstrate the feasibility of transporting solid oxygen by mechanical means from a vacuum storage space to a pressurized area via an air lock. In this latter condition, it would be available as breathing oxygen for crew use in a manned space vehicle and for extra-vehicular activity.

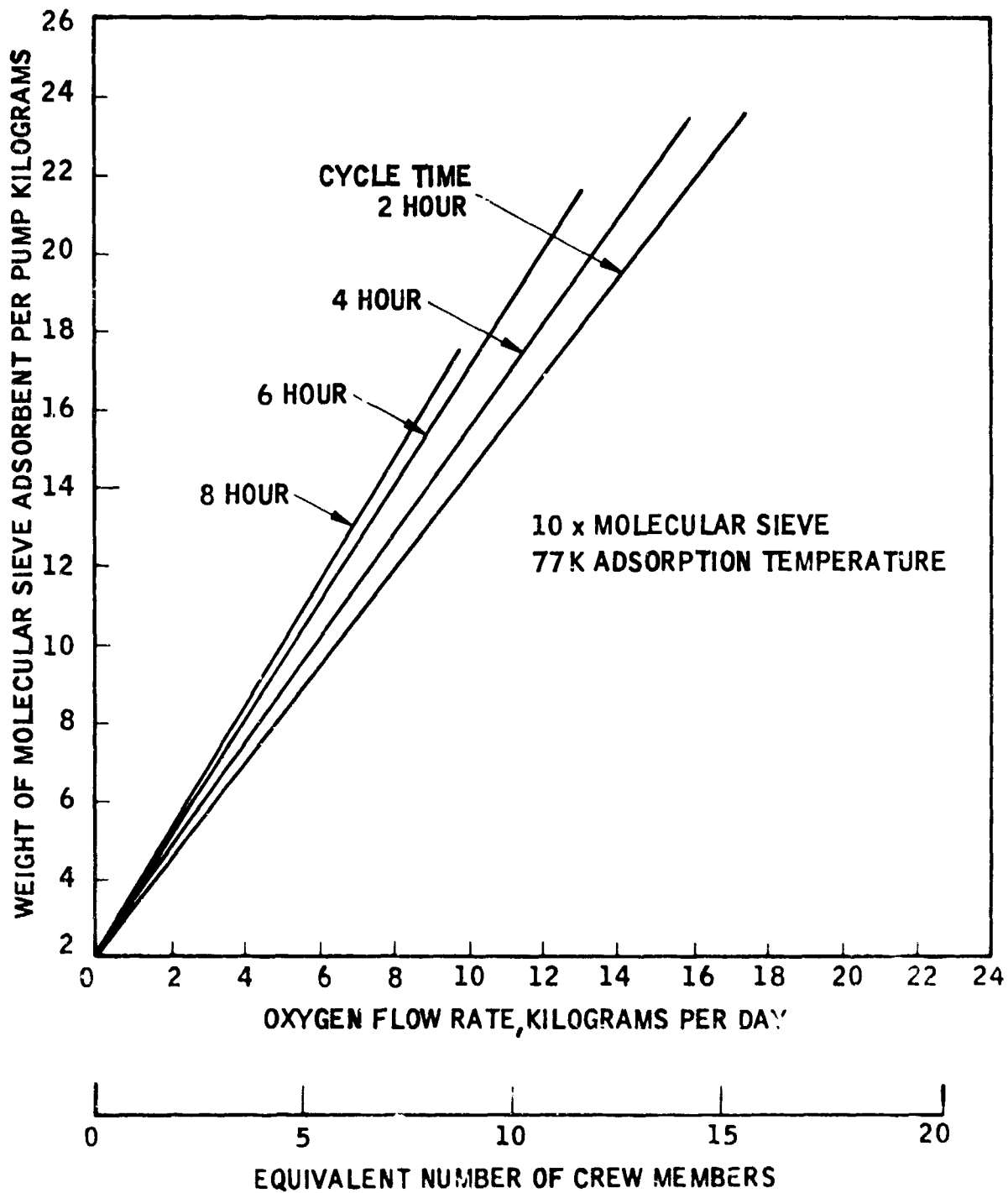


Figure 15. Adsorbent Weight Required as a Function of Oxygen Flow Rate

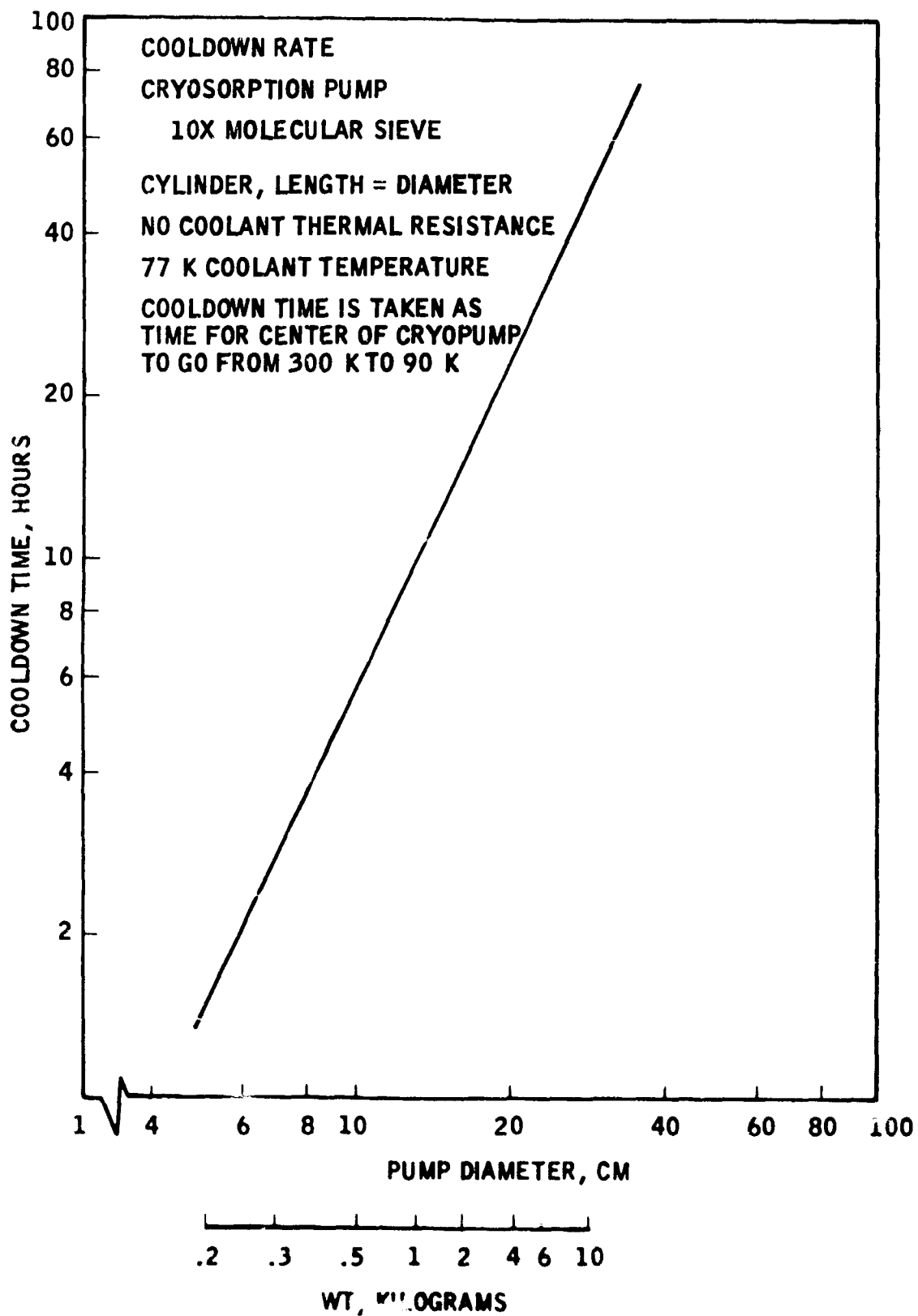


Figure 14. Cooldown Rate of Cryosorption Pump

### Preliminary Experiment

While the basic test apparatus for conducting these tests was being fabricated, a preliminary experiment was conducted with glass vessels (figure 15) to develop the method of preparing the solid oxygen and to visually observe some operations of moving the solid oxygen. Figures 16 and 17 show the solid oxygen formed in this system. The oxygen was condensed and cooled inside the inner vessel by the liquid nitrogen surrounding it. The atmosphere over the liquid oxygen was connected to a cryosorption pump which was cooled to 77K. The pressure over the oxygen was reduced to the point where the oxygen solidified (1.14 torr).

Since oxygen is paramagnetic, an attempt was made to pick up the solid oxygen with a magnet. As shown in figure 17, the solid oxygen was picked up by the magnet, but it is suspected that a major influence was played by the oxygen freezing on the magnet since the magnet was initially warm. The warm magnet melted a small amount of solid oxygen in contact with it, and then, after the magnet became cold, this liquid oxygen solidified on the magnet's surface.

The initial test apparatus was designed to solidify the oxygen by having the cavity of liquid oxygen in contact with solid nitrogen. When the pressure over the solid nitrogen is reduced below 1.14 torr, the temperature of the nitrogen is below 54.36K, sufficient to solidify the oxygen. Solid oxygen was formed under these conditions for the experiments after several modifications were made to the test apparatus to achieve the required temperature and pressure conditions in the oxygen. Initial tests with the system indicated a radiation heat leak to the oxygen and a loss of good thermal contact between the oxygen and the solid nitrogen when the nitrogen solidified. It was also found that because of the large mass of solid nitrogen in the system (figures 18 and 19a) and the limited pumping capacity of the vacuum pump, it was difficult to reduce the vapor pressure over the oxygen to the point where the oxygen would solidify (1.14 torr).

To resolve these problems, modifications were made to the system to reduce the mass of solid nitrogen used for cooling the oxygen (figure 19). The goal was to get the vapor pressure over the oxygen to below 1.14 torr while keeping its temperature below 54K. The first modification used a Fiberglas plate (figure 19b) on which a copper strip was mounted. Copper oxygen buckets and a container for  $N_2$  were located on this strip. Cooling of the oxygen buckets was accomplished by the solid nitrogen through the copper strip. This scheme made it possible to obtain a low vapor pressure, approximately 1 torr, over the oxygen, but the radiation heat transfer to the large copper strip surface was too great to lower the oxygen temperature much below the 54K required. A small amount of solid oxygen was formed but consistent formation of solid oxygen could not be accomplished.

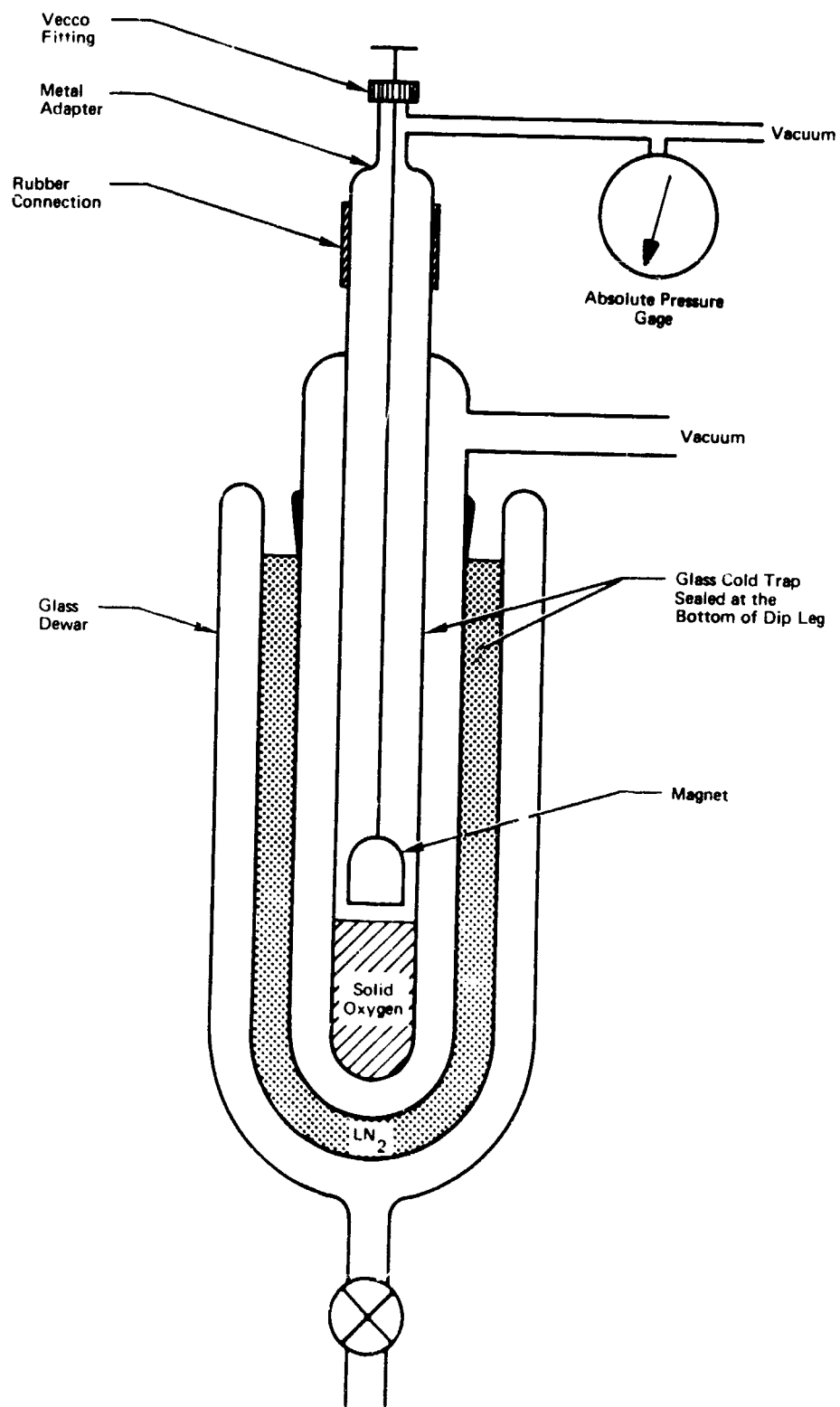


Figure 15. Preliminary Apparatus for Preparing Solid Oxygen

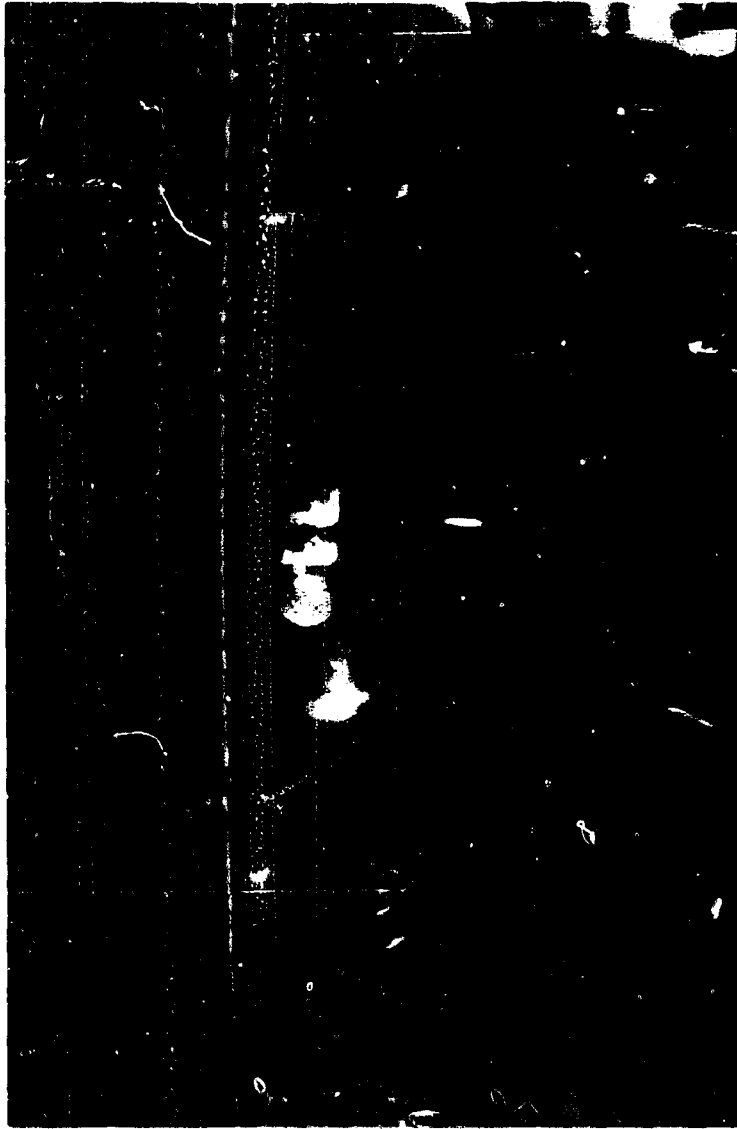


Figure 16. Overall View of Preliminary Solid Oxygen Experiment

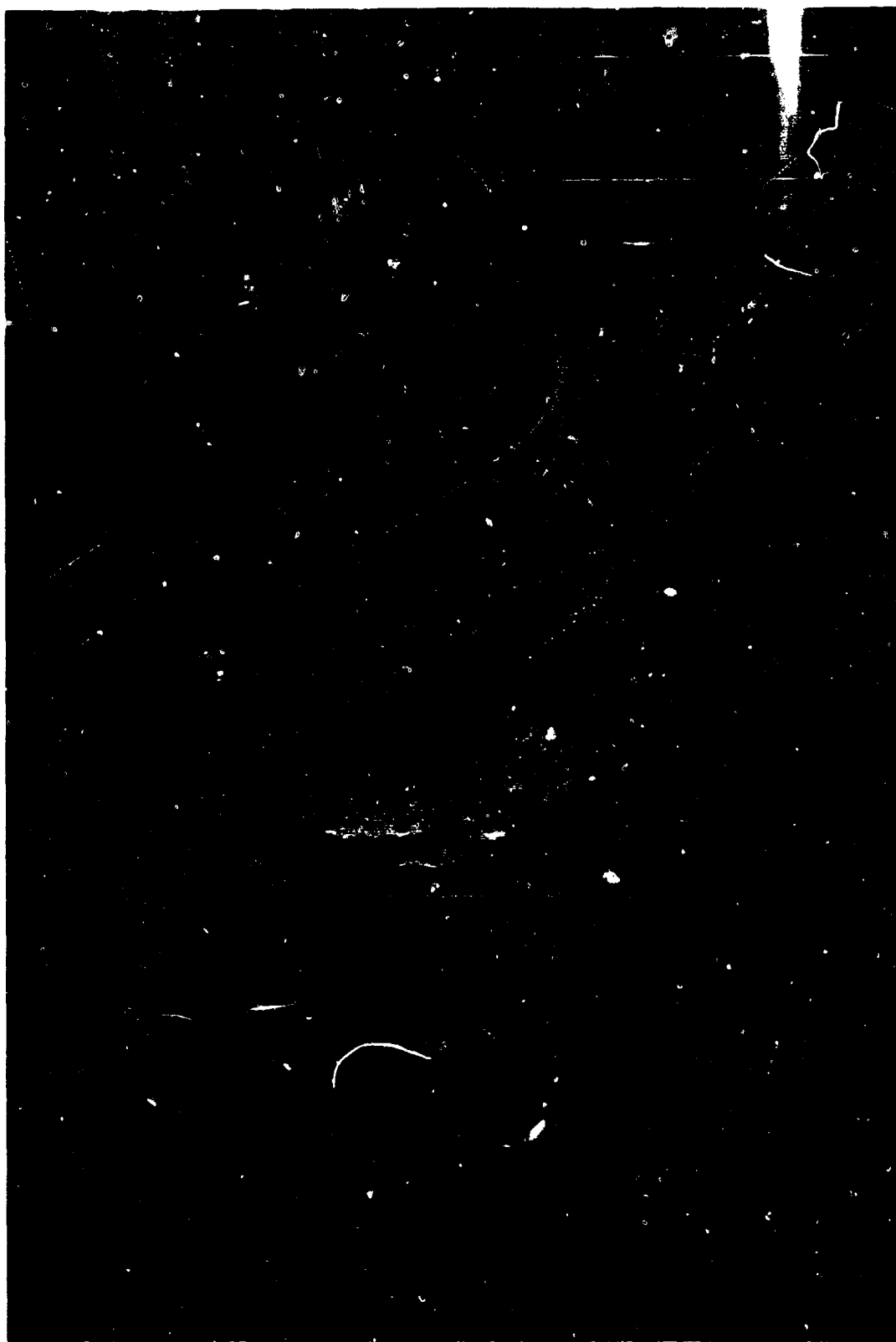


Figure 17. Solid Oxygen Crystals Being Raised with Magnet

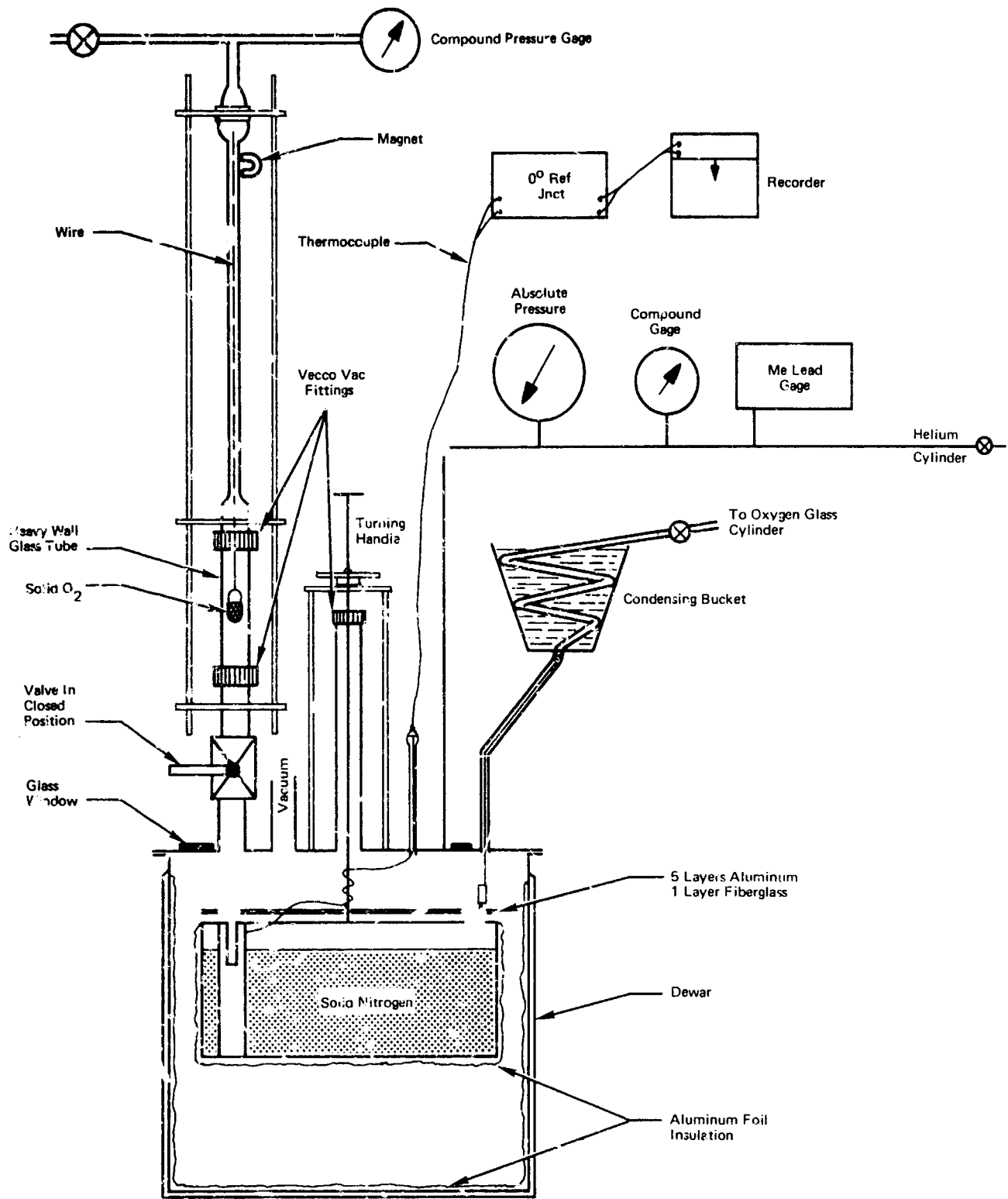
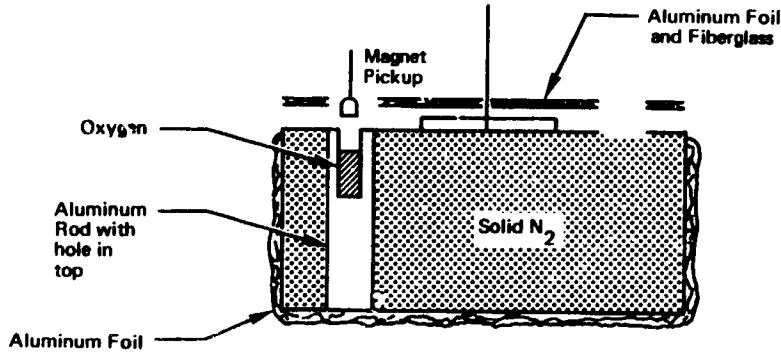
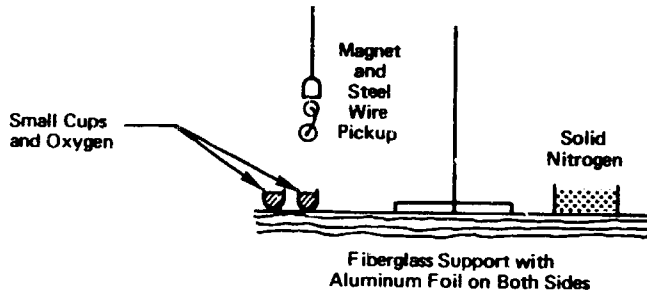


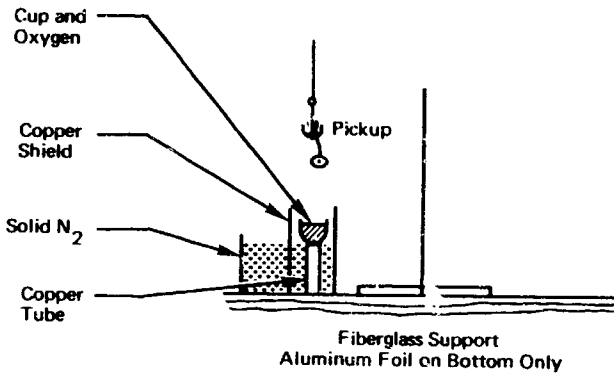
Figure 18. Initial Design of Test Apparatus - Solid Oxygen Mechanical Transports



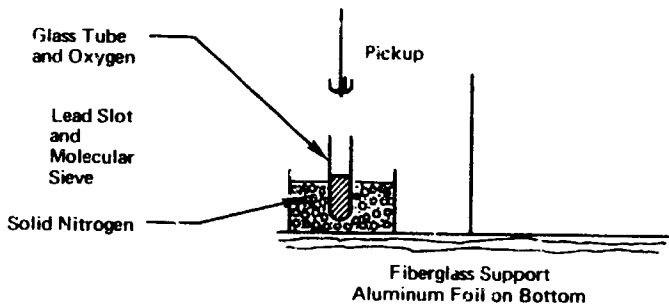
No Solid  
Too much heat leak even  
with foil insulation  
L<sub>2</sub> vapors too great to get  
low pressure



Only small amount of  
solid formed. Heat leak  
too great.



Improvement but heat  
leak caused oxygen to melt  
quickly as solid nitrogen  
sublimed away from copper  
tube.



All of the oxygen in the  
glass tube could be  
frozen.

Figure 10. Modifications to Test Apparatus

The oxygen bucket was then moved into closer contact with the solid nitrogen as shown in figure 19c. Solid oxygen could be readily formed with this arrangement, but the quantity was relatively small and problems arose in removing the oxygen from the copper bucket. Small wire forms inserted in the solid oxygen aided in lifting the solid oxygen.

The configuration which was found most suitable is that shown in figure 19d, in which a glass oxygen bucket was used. A mixture of molecular sieve and lead shot was added to the liquid nitrogen to improve its operation by helping to maintain good thermal contact with the oxygen bucket. This system worked satisfactorily and solid oxygen could be readily formed in the glass bucket for transport studies. The complete final test system is shown in figures 20, 21, and 22.

#### Test Operations

Several methods of mechanically moving the solid oxygen were attempted with this equipment. These involved picking up the solid oxygen with a magnet and with hooks.

The use of a magnet for moving the solid oxygen has merit in that on-and-off control can be obtained if the magnet is an electromagnet. The initial attempts to lift solid oxygen using its paramagnetic properties, discussed previously in the preliminary study section, were inconclusive. Further tests were tried using the new apparatus but with the same results. The solid oxygen could be lifted with a magnet, but the ability to do so was so marginal that freezing of the oxygen on the magnet probably was the primary mode of adhesion. However, lifting the solid oxygen by using its paramagnetic properties is not ruled out by these preliminary experiments. The experiments did show that the problem is complex. Stronger magnets and better contact of the surfaces between the oxygen and the magnet may be required.

The solid oxygen could be lifted with a magnet indirectly by placing a small steel-wire coil in the oxygen prior to its freezing; the solid oxygen was easily lifted with the magnet in a similar manner so that proposed for the paramagnetic oxygen method.

The solid oxygen was also lifted as shown in figure 19c by using a fishhook in conjunction with a looped wire in the solid oxygen. This method posed no problem manually but might be difficult to set up for automatic operation.

The final method tried was to use a wire hook arrangement submerged in the oxygen during the solidification phase. The full amount of solid oxygen formed in the vessel could be readily lifted out of the glass tube by this method. Solid oxygen was lifted through an air lock valve by this method, as shown in figure 23. When the air lock

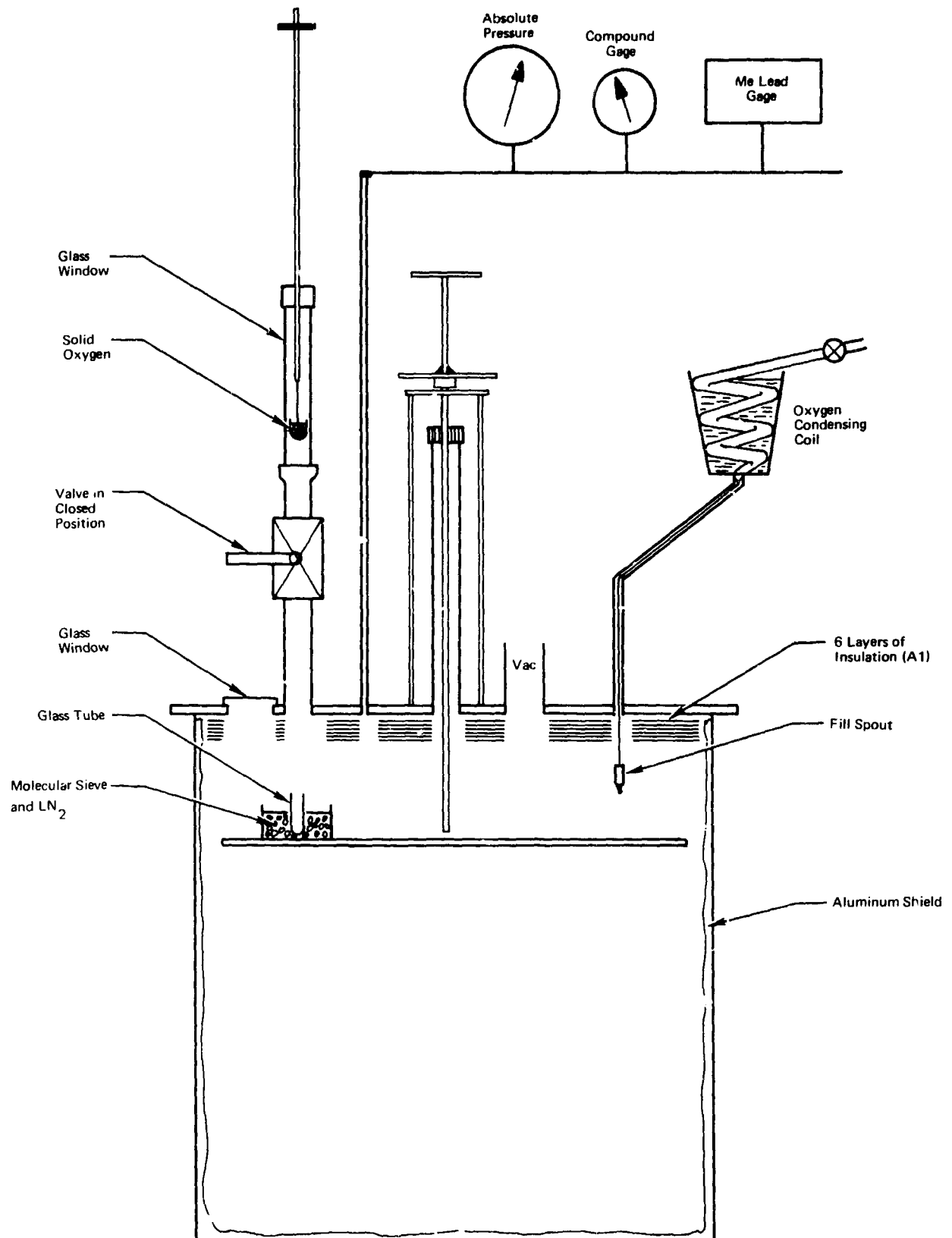


Figure 20. Final Test Arrangement – Solid Oxygen Mechanical Transports



Figure 21. Internal Arrangement of Solid Oxygen  
Mechanical Transport Test System

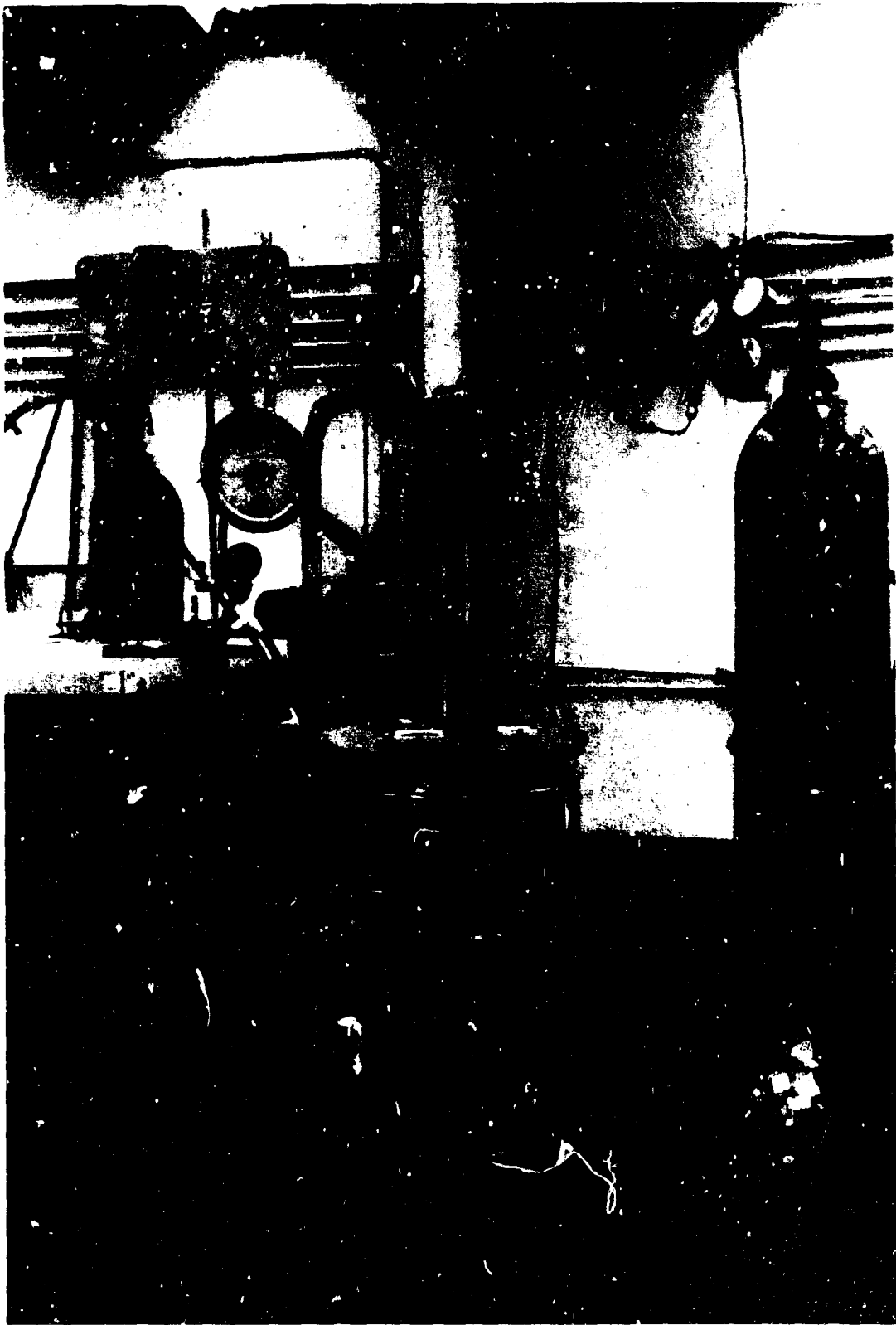


Figure 22. Overall View of Solid Oxygen Mechanical Transport Test System

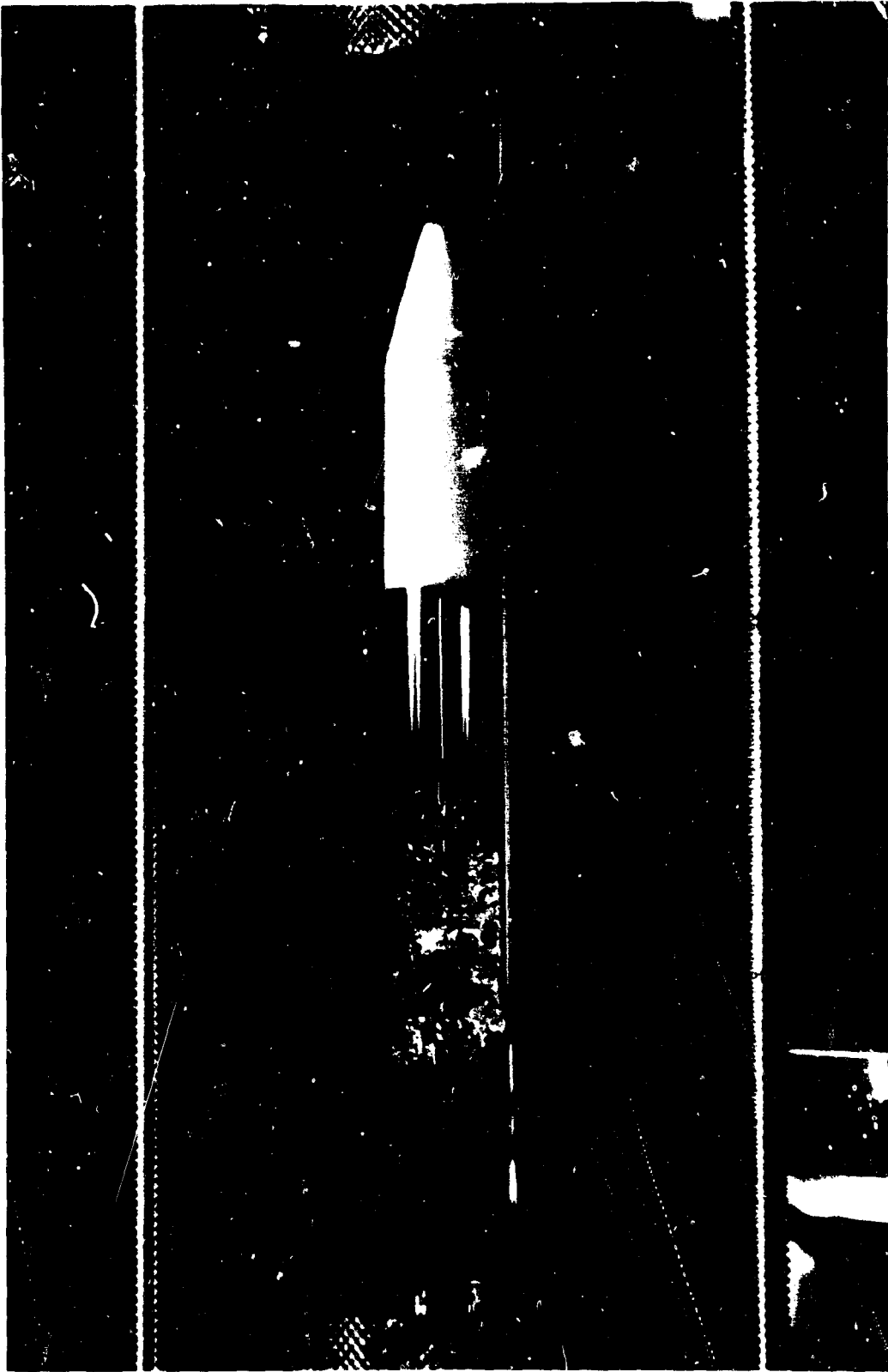


Figure 23. Solid Oxygen in Pressure Chamber

valve is closed, the oxygen melts, evaporates, and is ready for breathing under the pressure conditions existing in the area above the air lock valve.

### Discussion of Test Results

Various methods of preparing and mechanically transporting solid oxygen were studied. For economy, the preparation of solid oxygen was restricted to using solid nitrogen as a coolant, although the use of liquid helium or neon would be much more suitable in a practical system. Mechanical methods could readily move the solid oxygen by using a wire-hook lifting device with or without a wire coil in the solid oxygen. The solid oxygen could be lifted with a magnet if a steel wire coil was located in the solid oxygen. Direct lifting of solid oxygen using the paramagnetic characteristics of solid oxygen was not conclusively demonstrated, and further study would be required in this area. The practical application of these methods or similar methods of mechanically moving solid oxygen, must consider the overall requirements of the oxygen supply system.

### Evaluation and Application of Results

The experiments demonstrated that solid oxygen can be transported from a vacuum storage space to a chamber where it can be converted into a breathable condition. The solid oxygen mass was moved through an air-lock valve and then isolated from the vacuum storage volume. This method of oxygen transport appears completely realistic, and the application of the method should entail no major problems.

In the experimental test, the solid oxygen was moved through the air-lock valve by manually lifting the oxygen solidified around a wire hook. An electromagnet can be used to transport the oxygen mechanically if a wire coil is frozen into the oxygen when it is prepared. For automatic operation with multiple transfers, the basic method tested would be modified depending on the specific application requirements. For example, ice-cube trays of solid oxygen cubes could be prepared with wire coils frozen into each cube. An electromagnet pickup could then attach itself to a cube when turned on, and the oxygen cube moved through the air-lock valve. After the solid oxygen cube is in place, the electromagnet is turned off releasing the cube and the cycle repeated as required. The actual method selected for a given application would be the result of a study for the specific requirements of the application.

### DISCUSSION OF EXPERIMENTAL RESULTS

The experimental work has demonstrated the feasibility of transporting oxygen from the solid state to a condition suitable for breathing by two methods, the cryosorption pump method and the mechanical transport method. Data was also obtained on the adsorption of oxygen on molecular sieves for use in determining the size of cryosorption pumps required for a practical system.

The transport of oxygen involved no major problems. The greatest difficulty in the experimental work was encountered in preparing the solid oxygen using solid nitrogen as the coolant. This problem would not exist in any practical system since the oxygen could be solidified with liquid helium or neon.

The practicality of these two methods for oxygen transport in any given system will have to be developed. The major factor determining the practicality of the adsorbent transport system for any given application will be the size and weight of the system. In addition, the modification of the basic system to achieve fast cool-down rates will further increase its weight and size. The major factor determining the practicality of the mechanical transport method will be the capability to develop a mechanical system which can operate reliably and which can provide oxygen at a rate to meet the demand requirements.

The mechanical oxygen transfer system has the advantage of being more versatile as well as being potentially simpler. Since the oxygen is transferred as a solid, the volume being handled in the transfer is small and small transfer passages can be designed into the system. The adsorbent transfer method, on the other hand, requires large flow areas because of the low gas pressure, and a practical system design using the adsorbent method could be a problem for many requirements. The solid transfer system could be used for space cabin oxygen, for supplying oxygen for extra-vehicular activity, and for quick oxygen supply from a long-term storage container in an emergency.

The mechanical transfer system is therefore considered to be the most promising of the two transfer methods examined. The design and operation of a breadboard test system involving this concept would be the next step in the experimental evaluation of oxygen transport from the storage state to a breathable state.

## SECTION IV

### ANALYTICAL STUDY

#### OBJECTIVE

The objective of the analytical portion of the study was to perform a parametric analysis of the storage of oxygen for breathing purposes in space. Oxygen stored as solid, subcritical liquid, and supercritical fluid was studied for comparing various storage performance parameters.

By starting with solidified oxygen, instead of the saturated liquid for either the subcritical or supercritical storage systems, advantage can be taken of the sensible heat capacity, heat of fusion, and increased density of the solid to increase its storage life. This can be done for the subcritical storage system by launching it as a solid and then allowing it to liquefy after launch. Similarly to increase the storage life of oxygen in a supercritical system, the storage Dewar would be initially filled with solid oxygen which would first be allowed to liquefy after which it would be allowed to change to the supercritical state.

In lieu of transforming the oxygen, it can be maintained by subliming it to space in the solid state, from which condition it is transported to a breathable condition. A combination of the two methods investigated in the experimental study (transport by adsorbents and by mechanical manipulation) could be used to achieve maximum usage of the solidified oxygen. An example would be the case in which a portion of the solid oxygen is sublimed to space prior to liquefaction. Instead of wasting that part of the oxygen which would be lost to space, it could be sublimed to adsorbents that would be used to raise its pressure to a breathable level.

Appendices I through V formulate the weights, heat transfer, usage rates, and mission length in terms of the storage container geometry, number of men, space cabin leakage, support loading, and the oxygen phase being stored. The formulations were programmed for the IBM 360 digital computer and parametric data were developed for the following range of input parameters:

- Number of men are 1 to 10, each using 1.15 kilogram/day
- Space cabin leakage is 0 to 1 kilograms of oxygen per day

- Extra-vehicular activities consider an airlock of 1.5 cubic meters opened once per day for 0 to 100% of the mission days. A cabin oxygen partial or total pressure of 150 to 250 torr will be considered.
- Dynamic load placed upon titanium supports in storage Dewar, during launch phase, varied from 10 G in one direction and 50 G in three directions. Titanium supports were loaded with safety factor of 1.67 of the yield strength.
- Oxygen container radius of 5 to 125 centimeters.
- Insulation thickness of 0.5 to 10 centimeters for the flexible multilayer insulation.
- Number of shields from 0 to 5 for the rigid radiation shield insulation.

#### BACKGROUND TECHNICAL DATA

Several important physical and thermodynamic properties of oxygen must be determined to conduct the solid oxygen storage analytical study. The required properties are the density of the various oxygen states, heat of sublimation of the solid, heat of vaporization of liquid, and the specific internal energy of the various states.

Stewart (1966) describes the thermodynamic properties of liquid and gaseous oxygen for the temperature range of 65 K to 298 K and for a pressure range of 0.02 to 340 atmospheres. Density, enthalpy, and internal energy data are also presented and heat of vaporization of the liquid phase can be calculated by the difference in enthalpy of the gas and liquid at saturated conditions.

The density of various solid oxygen phases is reported by Mullins, et al, (1965) and is reproduced in table II of this report. Solid phase I (43.8 K to the triple point) has a density of 1.300 gm/cc, solid phase II (23.8 to 43.8 K) has a density of 1.397 gm/cc, and solid phase III (0 to 23.8 K) has a density of 1.461 gm/cc. There is a 7.5% increase in density from phase I to II and a 12.4% increase in density from phase II to III for the solid. From Stewart (1966), the density of liquid oxygen at the normal boiling point (90.18 K) is 1.1407 gm/cc. Thus in cooling a fixed mass of liquid oxygen to a solid at the triple point, the mass increases in density by 13.9%. Cooling the liquid to a solid at 30 K results in an increase in density of 22.4%, and cooling to a solid at 20 K, an increase of 24.1% is realized.

Heat of sublimation of solid oxygen and heat of vaporization of liquid oxygen for a temperature range of 20 to 100 K were taken from the work of Mullins, et al, (1965), and compared with similar data initially calculated for this study from the data given by Stewart (1966) at the lowest temperature, 65 K, and heat capacity data presented by Scott (1959) and reproduced in table III of this report. The two sets of data agree within 0.35% which is within the presented accuracies of experimental data used in the work of Mullins, et al (1965).

TABLE II

MOLAL VOLUMES AND DENSITIES OF SOLID OXYGEN

<u>Temperature range</u> K	<u>Molal volume</u> cc/gm-mol	<u>Density</u> gm/cc	<u>Phase</u>
0 to 5	21.9	1.4612	$\alpha$ or III
5 to 8	21.9	1.4612	$\alpha$ or III
8 to 23.781	21.9	1.4612	$\alpha$ or III
23.781 to 43.772	22.9	1.3974	$\beta$ or II
43.772 to 54.352	24.62	1.2998	$\gamma$ or I

Data from: U. E. Gross et al (1962, pp. 126 - 134)

TABLE III

HEATS OF SUBLIMATION AND VAPORIZATION FOR OXYGEN

<u>Temperature</u> <u>K</u>	<u>Latent heat<sup>(a)</sup></u>		<u>Latent heat</u>
	<u>Cal/g-mol</u>	<u><math>\frac{\text{W-sec}}{g}</math></u>	<u><math>\frac{\text{J}}{g}</math></u>
100	1551.02	202.76	202.4 (b)
90.18(N.B.P.)			213.3 (b)
90	1631.25	213.25	213.5 (b)
80	1700.77	222.33	223.0 (b)
70	1763.44	230.53	230.8 (b)
60	1822.50	238.25	
54.352(a)	1855.20	242.52	241.50 (b)
54.352(a)	1961.50	256.4	255.50 (b)
52	1971.19	257.67	
46	1995.58	260.87	
43.772(a)	2004.70	262.06	261.21 (c)
43.772(a)	2182.30	285.28	284.43
40	2196.12	287.09	
34	2207.94	288.53	
30	2209.28	288.80	
28	2208.22	288.67	
23.781(a)	2202.56	287.93	287.15 (c)
23.781(a)	2224.98	290.86	290.08 (c)
20	2214.50	289.49	

(a) Gross et al (1964, pp 126-134)

(b) Stewart (1966)

(c) Calculated from data in Scott (1959) and (b)

The latent heat of sublimation and vaporization are plotted in figure 24 as a function of temperature. Liquid data is from Stewart (1966) and solid data is from Mullins, et al (1965) along with the calculated data for this study. The heat of sublimation reaches a maximum at 22.78K (Solid III) and decreases on further cooling. For the Solid II phase there is a maximum at approximately 30K, and cooling the solid below 43.77K (Solid II) results in only a small increase (2% maximum). However, the heat capacity (figure 3) from a low temperature, say 12K, to 43.77K is 20% of the total heat capacity from a solid at 12K to a liquid at the normal boiling point (90.18K).

#### STORAGE SYSTEM DESIGN FOR THE ANALYTICAL STUDY

A relatively simple Dewar configuration was selected for the analytical study. A cut-away view of the oxygen storage container is presented in figure 25. The basic components of the storage container considered in this study are:

- . Inner container (spherical)
- . Insulation (two vacuum types; multilayer and radiation shields)
- . Outer container (vacuum jacket)
- . Wire supports

With the vacuum region at approximately  $10^{-7}$  torr or lower, the outer container must support an external collapsing pressure, and the inner container will always support a net positive internal pressure except when the solid oxygen is stored below a temperature of 30K. However, both liquid and solid oxygen containers must be strong enough to withstand an internal pressure of one atmosphere. For this study, the inner container for the supercritical storage must be able to withstand a maximum pressure of 55 atmospheres.

The two insulations selected for this study are of the high-performance type and require a high vacuum to fully develop their low heat-transfer properties. The flexible multilayer insulation consists of alternate layers of thin, aluminized mylar and a thin spacer material. The aluminized mylar can be coated on one or both side, making it a highly reflecting radiation shield. A shield configuration of 80 layers<sub>3</sub> (mylar and spacer) per inch with a density of approximately 0.0933 gm/cm<sup>3</sup> was used for this study. The thermal performance of this insulation is presented in Appendix I.

The second insulation selected for this study consists of rigid multiple radiation shields, coated with a highly reflective metallic material such as silver, aluminum, or gold on the shield base surface. The base surface can be metal sheets such as aluminum or magnesium or they can be formed sheets of impregnated Fiberglas. Vacuum-deposited gold (room temperature emissivity of 0.02) on both sides of 0.5 milli-

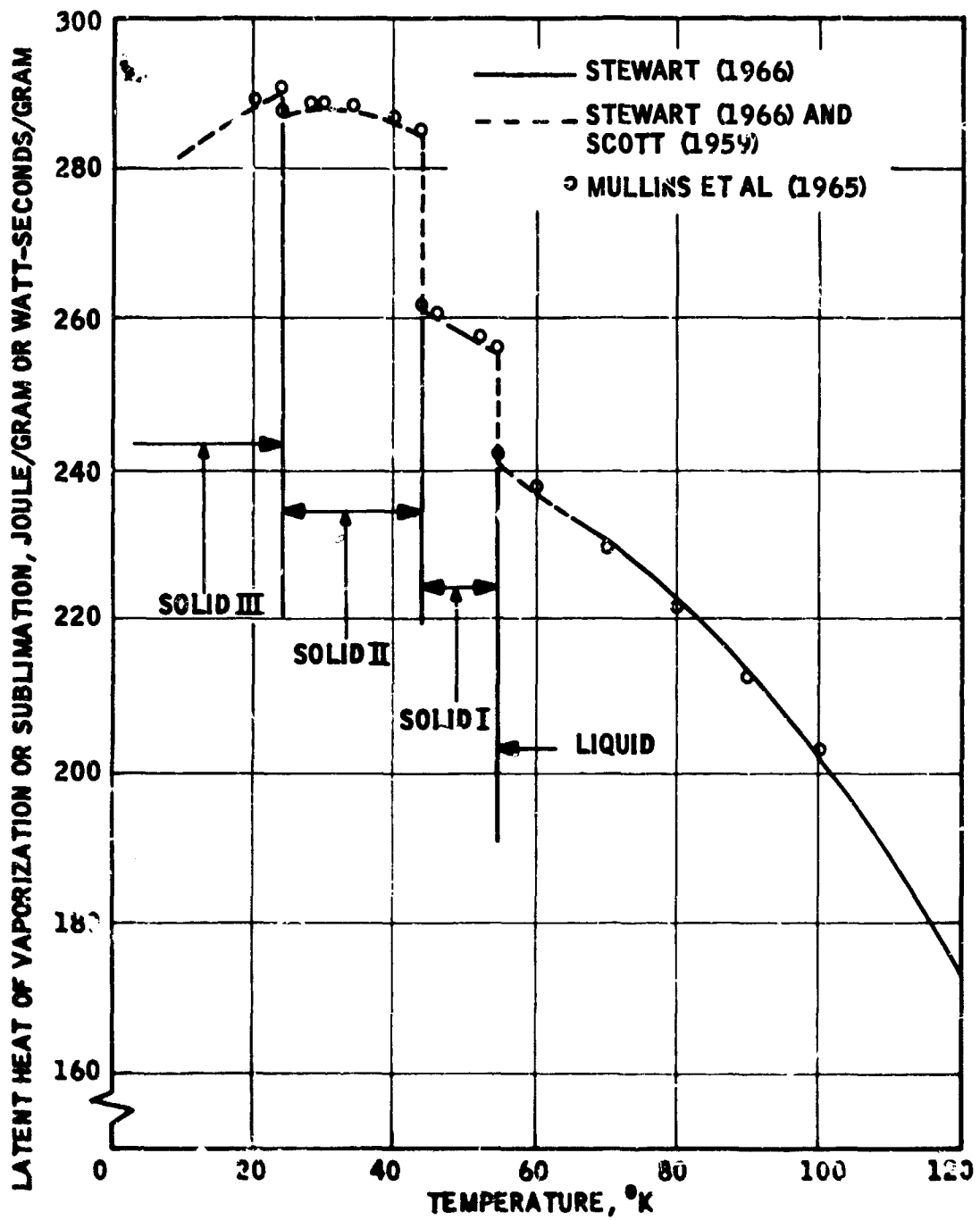


Figure 24. Latent Heat of Vaporization and Sublimation of Oxygen as a Function of Temperature

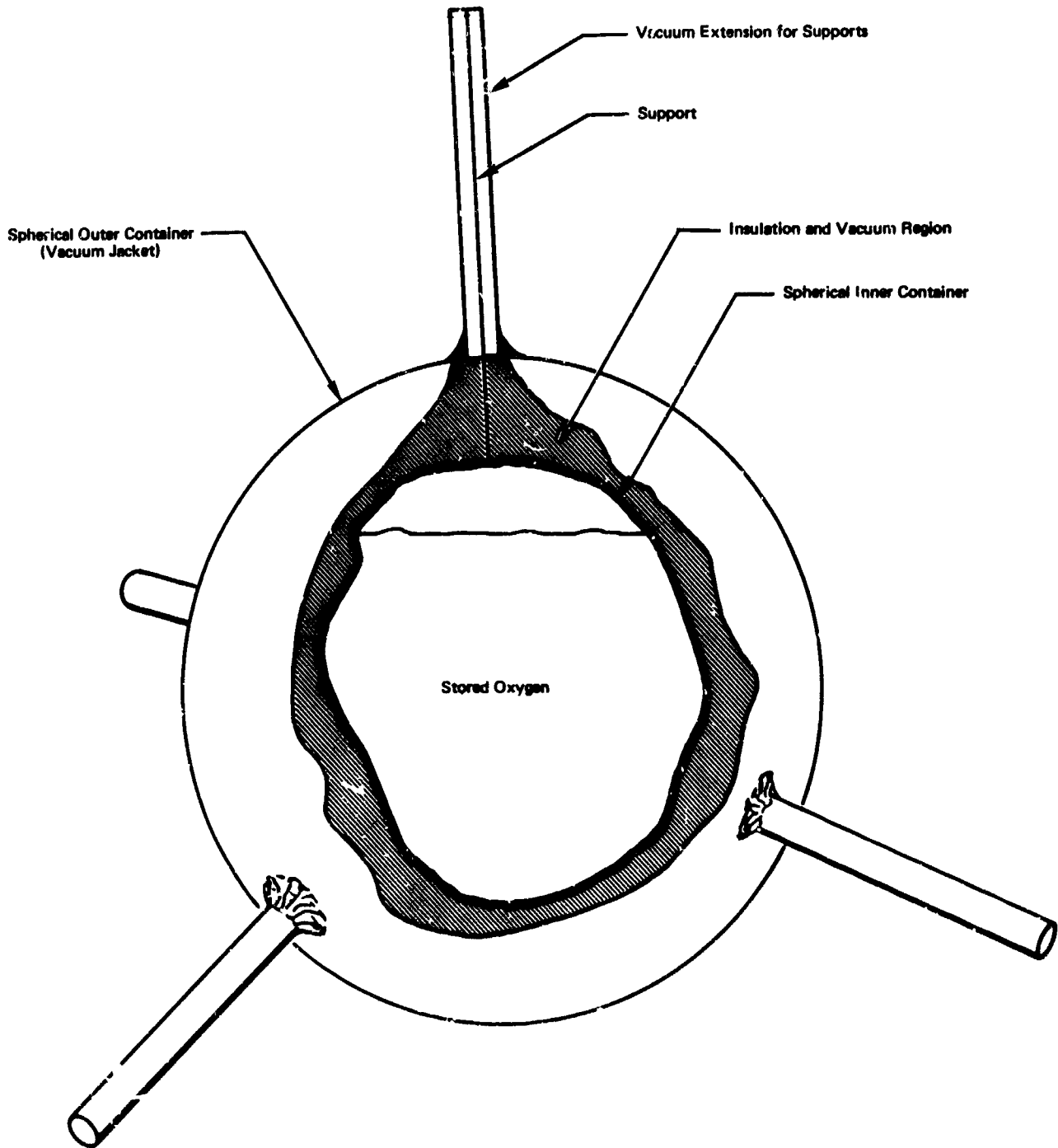


Figure 25. Cut-Away View of the Oxygen Storage Dewar-Analytical Study

meter thick aluminum shields was used for this study. The number of shields is a variable in the study and the shields are separated by a spacing of 0.5 centimeters. The container surfaces facing the shields were also considered to have a similar gold coating to further increase the insulation performance.

The supports for the inner container were selected for a combination of low heat conduction and high strength to withstand the effects of acceleration and shock loading during launch. Loadings on the oxygen (inner) container of from 10 G in one direction to 50 G in three directions were considered. The latter condition will give an 86.69 G-load on any single support wire that was the basis of the design analysis. These values are representative of what can be experienced by the inner container and include any amplification by the supports and container (loaded) acting as a "spring mass" system. Of course, with the greater G-loading, supports with larger cross-sectional area will be required which would consequently incur a higher heat conduction penalty.

The four supports are radial, high-strength, titanium alloy wires that extend from the inner container through the outer container to the corners of an imaginary tetrahedron which would circumscribe the outer container. Rigid tubes would extend the vacuum jacket from the container to the end of the supports and simultaneously act as legs for the whole container. It was necessary to make the supports long to reduce the heat transfer to the order of magnitude of that through the insulation. However, for some missions where the oxygen usage rate is high, shorter supports and higher heat loads can be tolerated. When the oxygen is to be stored for extended periods of time before usage, the minimum total heat load is required.

Several items associated with actual oxygen storage hardware were not considered in this analytical study. Some of these items with the type of storage are:

- . Heater (solid, liquid or supercritical)
- . Phase separator (liquid)
- . Pressure regulator (supercritical)
- . Heat exchanger for solidification (solid)

These items are low in weight compared to the overall storage system, and these weights are essentially the same for all systems. Therefore, neglecting these weights in the analysis does not introduce a significant error.

## STORAGE OF OXYGEN WITH NO USAGE

Many potential applications exist for future storage of oxygen for long periods of time without usage. Standby oxygen systems in manned space systems could provide a practical means of extending oxygen supply as well as serving as an emergency oxygen supply source. A standby oxygen supply on the lunar surface or in orbiting space stations would allow the manned shuttle vehicle or manned transport vehicle to carry with them only the oxygen necessary for the flight phase. The oxygen supply system for extra-vehicular activities can possibly be made more practical if it is separated from the main oxygen supply source serving the cabin atmosphere.

The various methods of storage of oxygen without usage have been analytically evaluated. The discussion of the analysis and the results of the analysis are presented in this section.

### Analytical Procedures

The basic procedure for analysis of the extended storage of oxygen was to assume an initial starting condition of the oxygen and then to determine the quantity and state of the fluid at various intervals of time. The analyses were made for liquid oxygen, initially at the triple point, and for solid oxygen at various initial temperatures.

The heat leak into the liquid oxygen containers was handled in two ways; in one case, oxygen was allowed to vent at one atmosphere pressure, and in the other case, the pressure was allowed to rise to supercritical pressure conditions, 55 atmospheres, before venting. The heat leak into the containers with solid oxygen was allowed to raise the temperature of the solid through its sensible heat, and to change the state of the oxygen through its transformation and melting phases. Sublimation occurred in some cases when the density decreased and a constant volume of oxygen is to be maintained.

The study was made with different size storage vessels which have supports to handle two different launch G-loads of 10 G and 86.6 G. The analyses also included the performance evaluation with a varying number of rigid radiation shields and with different thicknesses of multilayer insulation.

The equations that were used in this parametric analysis are developed in Appendices B, D, and E. These equations were programmed in FORTRAN IV for the IBM 360 computer, and cases were run over the range of the parameter.

### Results of the Analyses

The data from the computer runs were plotted in various ways to (a) provide working curves for determining storage time as a function

of tank size, insulation design, and support requirements, and (b) to compare the extended storage capabilities of oxygen when stored initially under different conditions.

The working curves are presented in figures 26 through 29 for solid oxygen stored at 54.36K (triple point) and at 43.8K (transition point between Phase I and Phase II). These curves show the storage time as a function of inner container radius and 2 G-loads. Figure 26 is for flexible multilayer insulation of various thicknesses and figure 27 is for different numbers of rigid radiation shields, both for the solid oxygen stored at the triple point. Figures 28 and 29 are the same curves as 26 and 27 respectively for solid oxygen stored at 43.8K.

The storage performance of these systems can best be compared by normalizing the oxygen in terms of the percentage of oxygen remaining in the container after a given period of time. Figures 30 through 37 show this comparison for selected tank sizes, insulations, and G-loads. All of the figures show the performance, or storage capability of saturated liquid oxygen for comparison. In addition, figures 30 and 31 show the storage capability of saturated liquid oxygen when it is allowed to self-pressurize to a supercritical pressure of 55 atmospheres before venting.

#### Discussion of Results

The increased storage capacity when using solid oxygen is clearly shown in these figures. For example, figure 31 shows that the percentage of oxygen remaining after 250 days of storage (in the same size tanks with equal insulation and G-loads) is as follows:

<u>Initial Oxygen Condition</u>	<u>Relative Weight of Oxygen Remaining after 250 days Storage</u> *
Solid oxygen @ 12K	100%
Solid oxygen @ 43.8K	86%
Solid oxygen @ 54.36K (triple point)	58%
Saturated liquid oxygen @ 90.18K (vented at 1 atm)	14%
Saturated liquid oxygen @ 90.8K (vented at 55 atm)	7%

\* Reference weight is saturated liquid oxygen at 90.18K, 95% full.

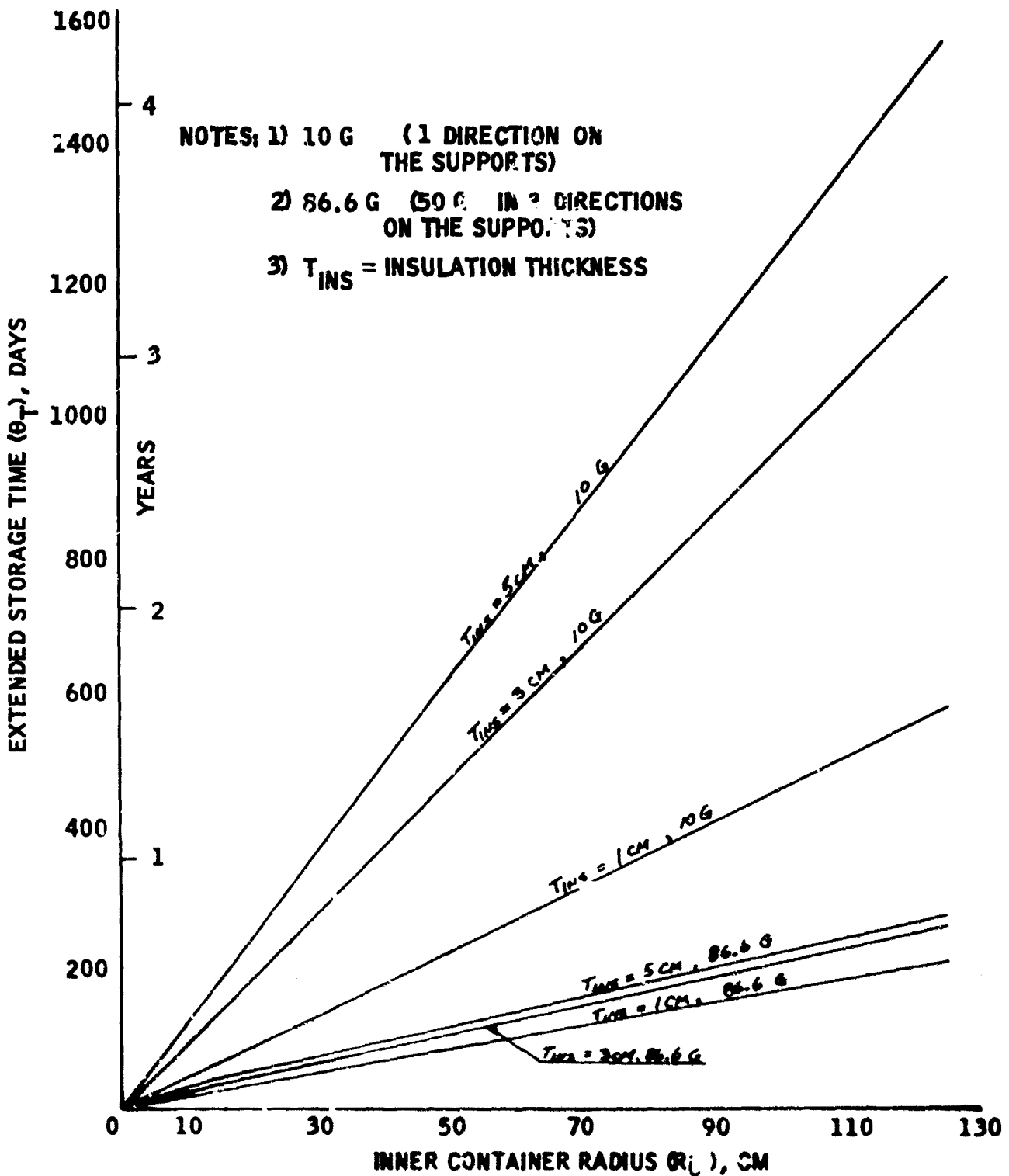


Figure 26. Extended Storage Time of Liquid Oxygen by Subliming and Melting Solid Oxygen as a Function of Inner Container Radius (Solid Oxygen Storage 54.36K, Flexible Multilayer Insulation)

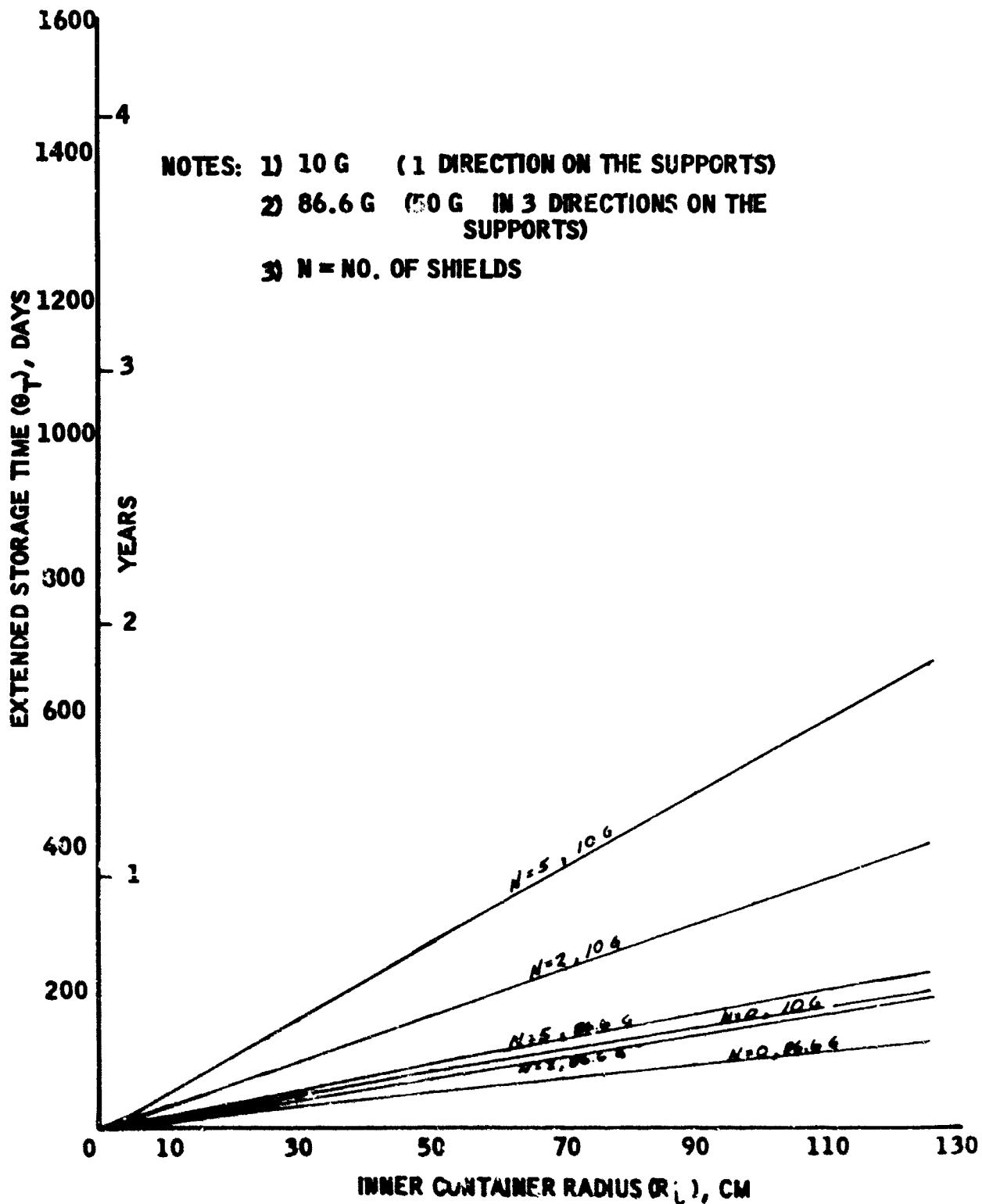


Figure 27. Extended Storage Time of Liquid Oxygen by Subliming and Melting Solid Oxygen as a Function of Inner Container Radius (Solid Oxygen Storage at 54.3K, Rigid Shield Insulation)

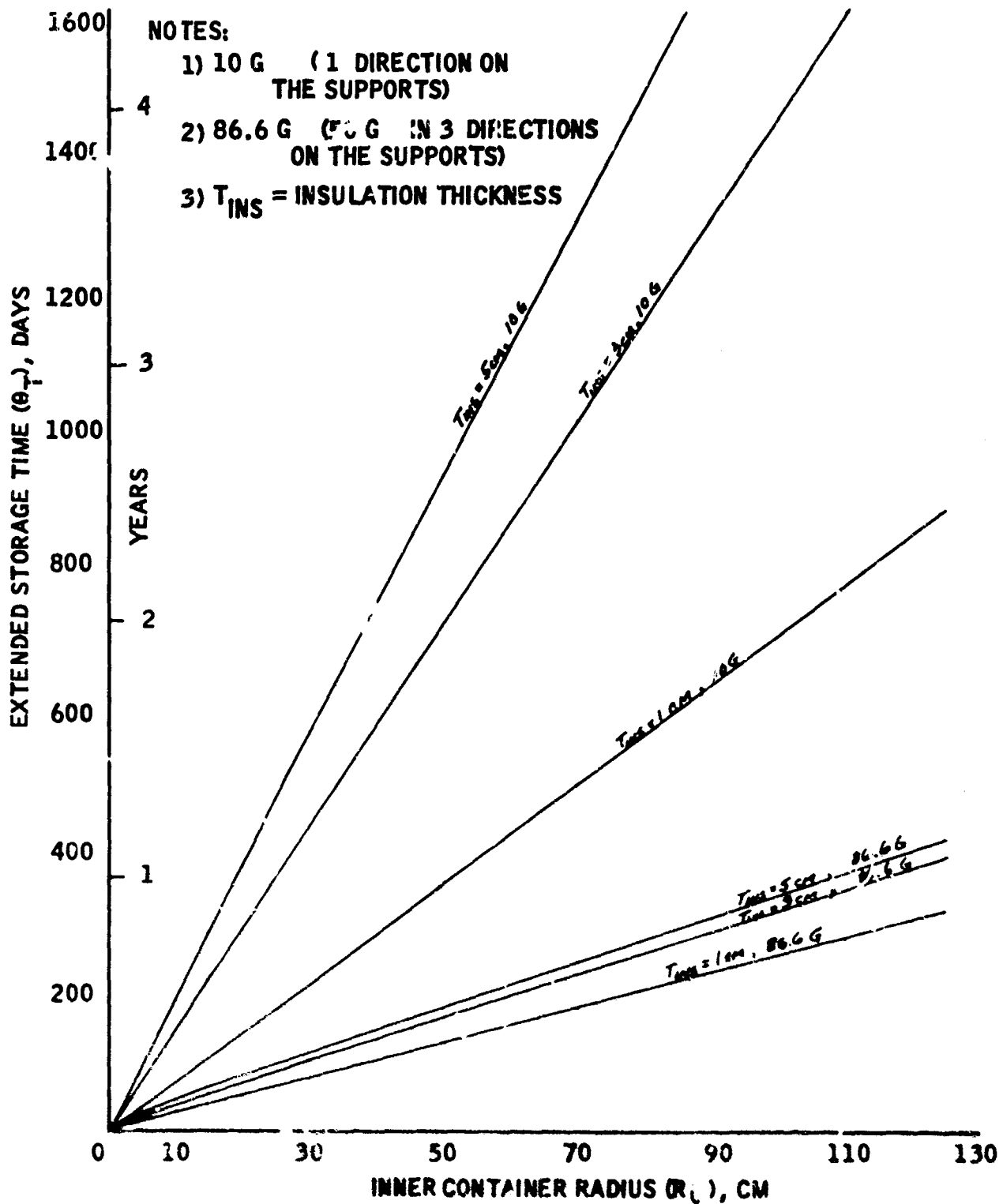


Figure 28. Extended Storage Time of Liquid Oxygen by Subliming and Melting Solid Oxygen as a Function of Inner Container Radius (Solid Oxygen Storage at 43.8K, Flexible Multilayer Insulation)

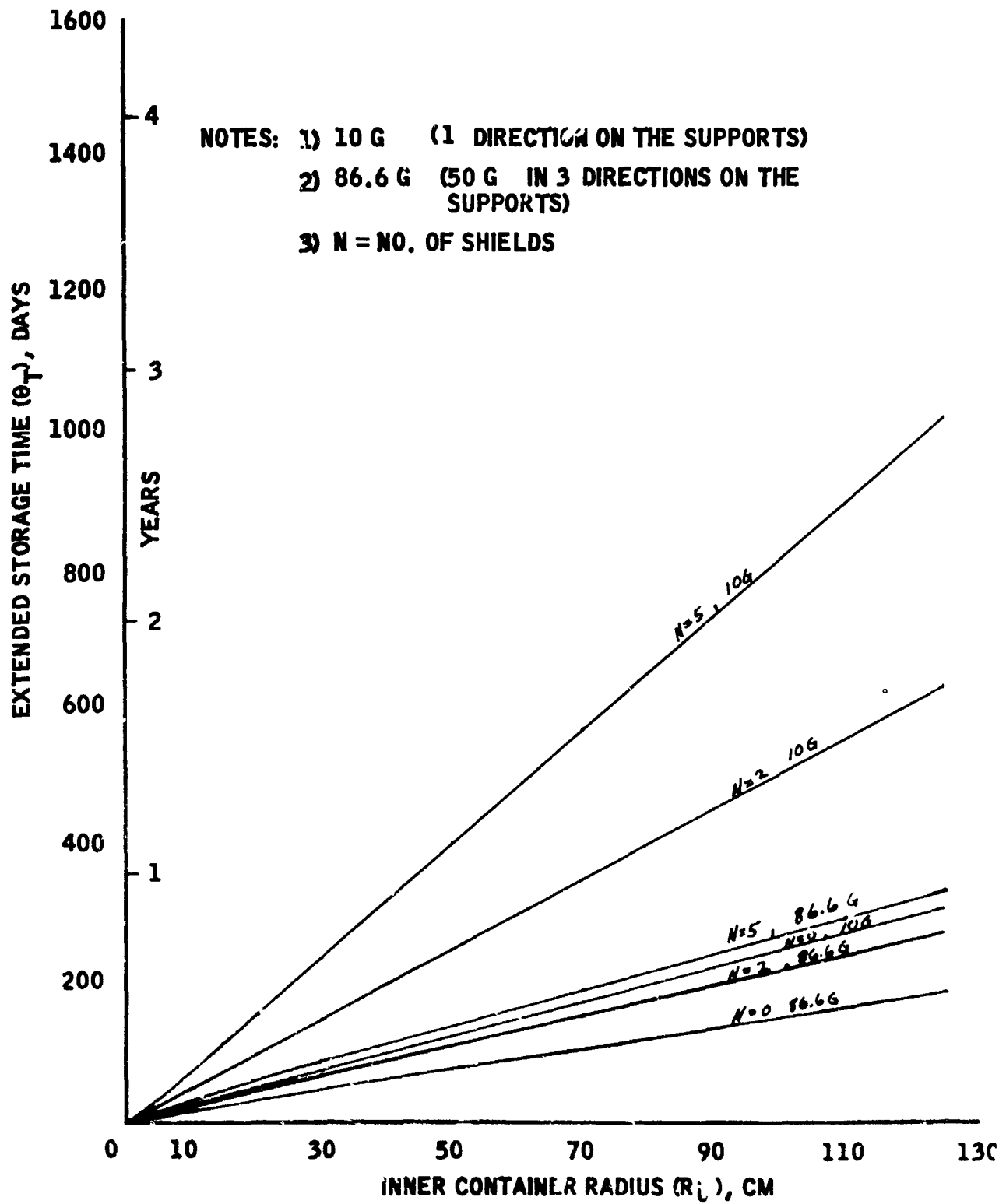


Figure 29. Extended Storage Time of Liquid Oxygen by Subliming and Melting Solid Oxygen as a Function of Inner Container Radius (Solid Oxygen Storage at 43.6K, Rigid Shield Insulation)

$R_i = 30 \text{ CM}$ ,  $T_{INS} = 1.0 \text{ CM}$ ,  $86.6 \text{ G}$  LOADING ON THE SUPPORTS  
 FLEXIBLE MULTILAYER INSULATION

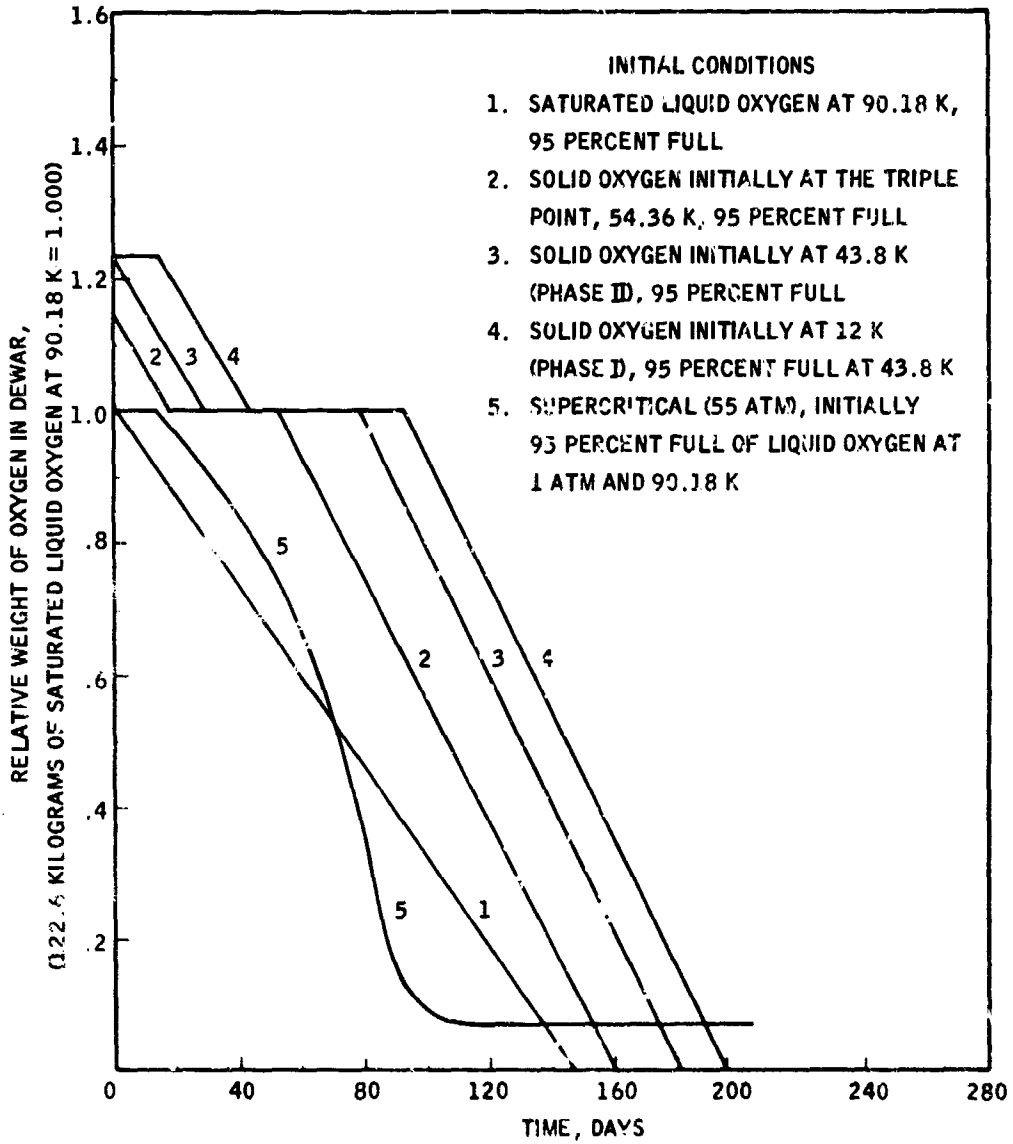


Figure 30. Comparison of Solid as a Function of Liquid Oxygen Storage Times, Flexible Multilayer Insulation  
 $R_i = 30 \text{ CM}$ ,  $T_{INS} = 1.0 \text{ CM}$ ,  $86.6 \text{ G}$ 's

$R_1 = 30 \text{ CM}$ ,  $T_{INS} = 1.0 \text{ CM}$ ,  $10.0 \text{ G}$  LOADING ON THE SUPPORTS

FLEXIBLE MULTILAYER INSULATION

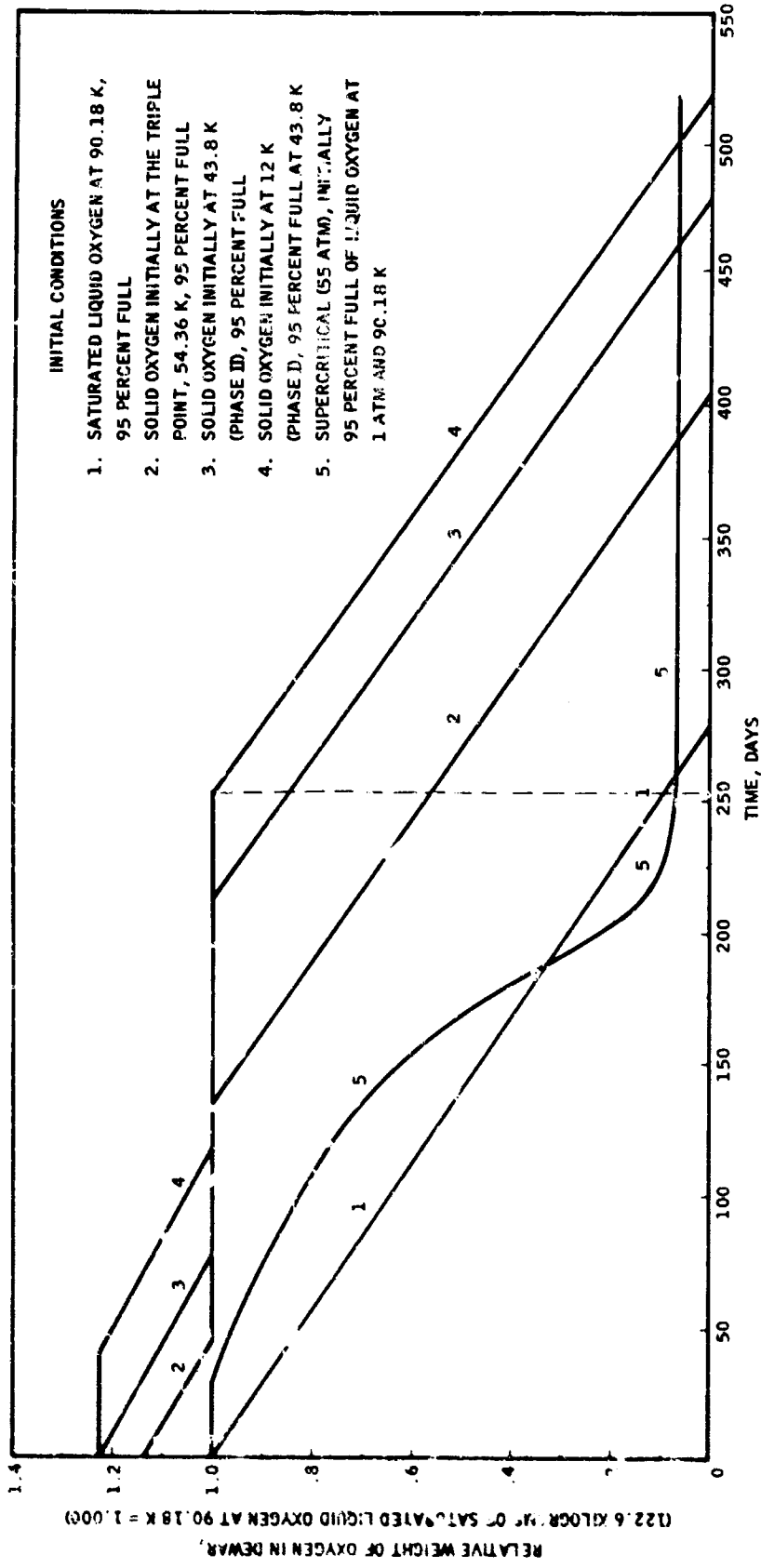


Figure 31. Comparison of Solid as a Function of Liquid Oxygen Storage Times, Flexible Multilayer Insulation  
 $R_1 = 30 \text{ CM}$ ,  $T_{INS} = 1.0 \text{ CM}$ ,  $10.0 \text{ G's}$

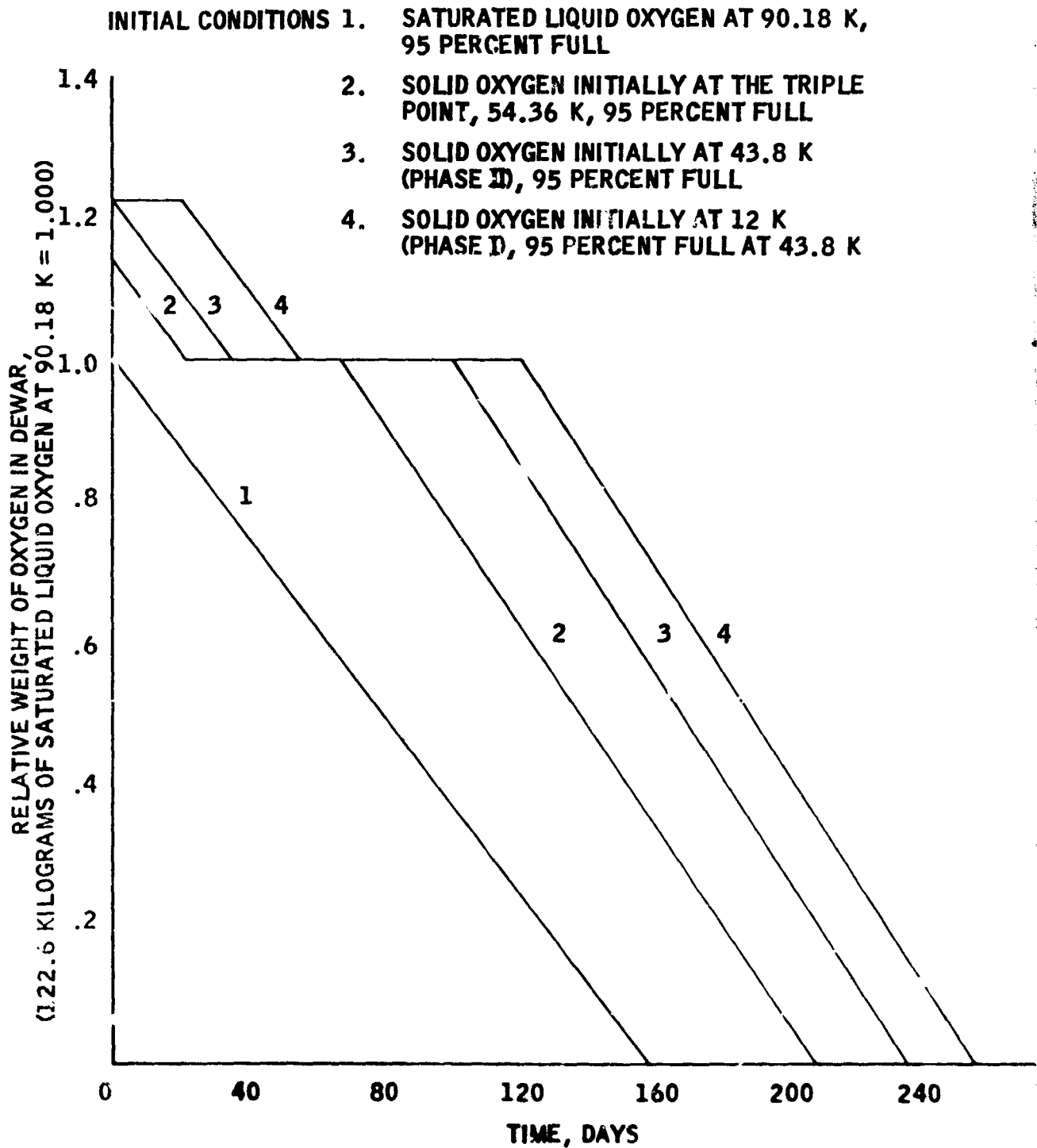
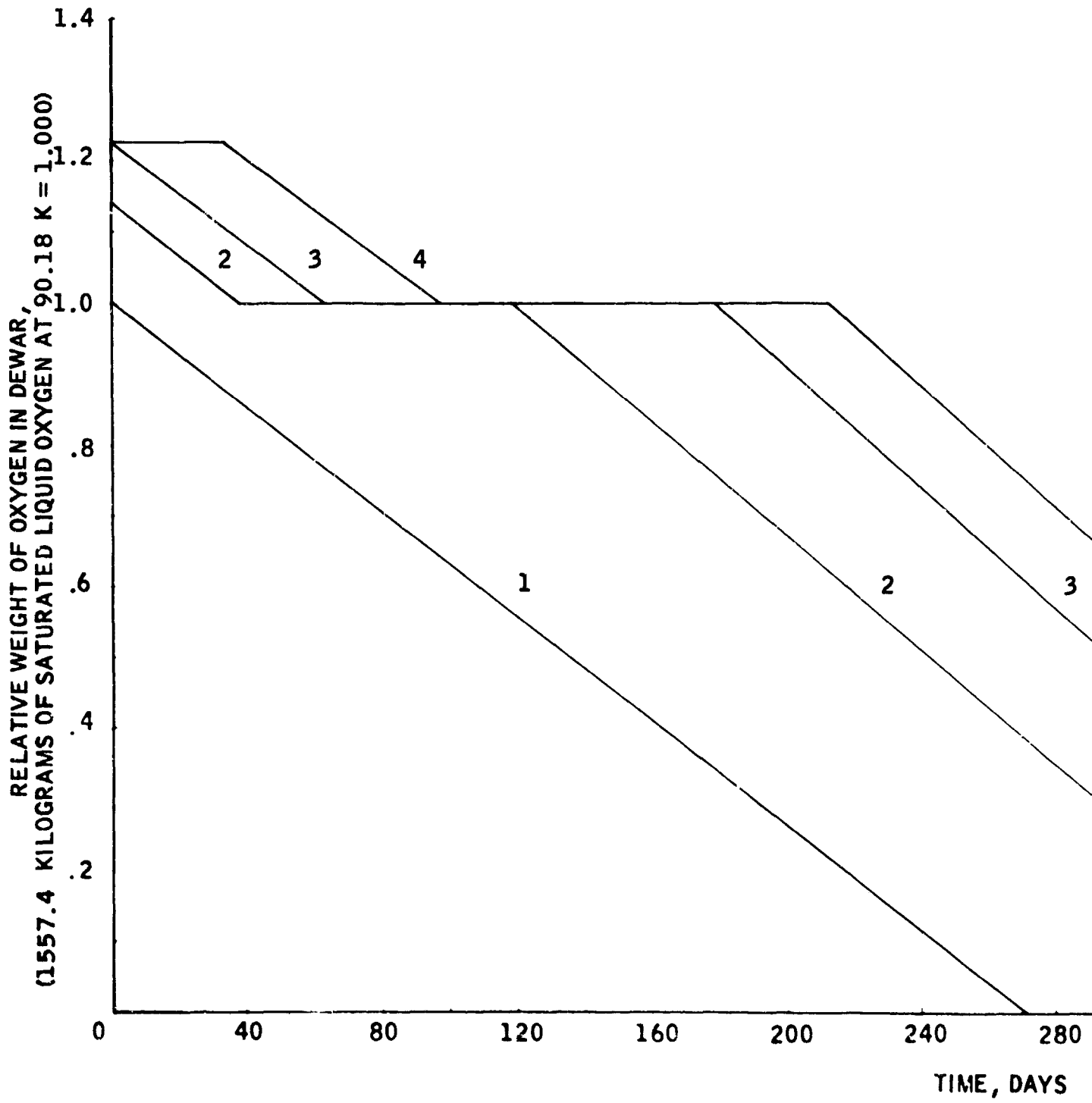


Figure 32. Comparison of Solid as a Function of Liquid Oxygen Storage Times, Flexible Multilayer Insulation  
 $R_j = 30 \text{ CM}$ ,  $T_{INS} = 1.0 \text{ CM}$ , 86.6 G's



A

### INITIAL CONDITIONS

1. SATURATED LIQUID OXYGEN AT 90.18 K, 95 PERCENT FULL
2. SOLID OXYGEN INITIALLY AT THE TRIPLE POINT, 54.36 K, 95 PERCENT FULL
3. SOLID OXYGEN INITIALLY AT 43.8 K (PHASE III), 95 PERCENT FULL
4. SOLID OXYGEN INITIALLY AT 12 K (PHASE D), 95 PERCENT FULL AT 43.8 K

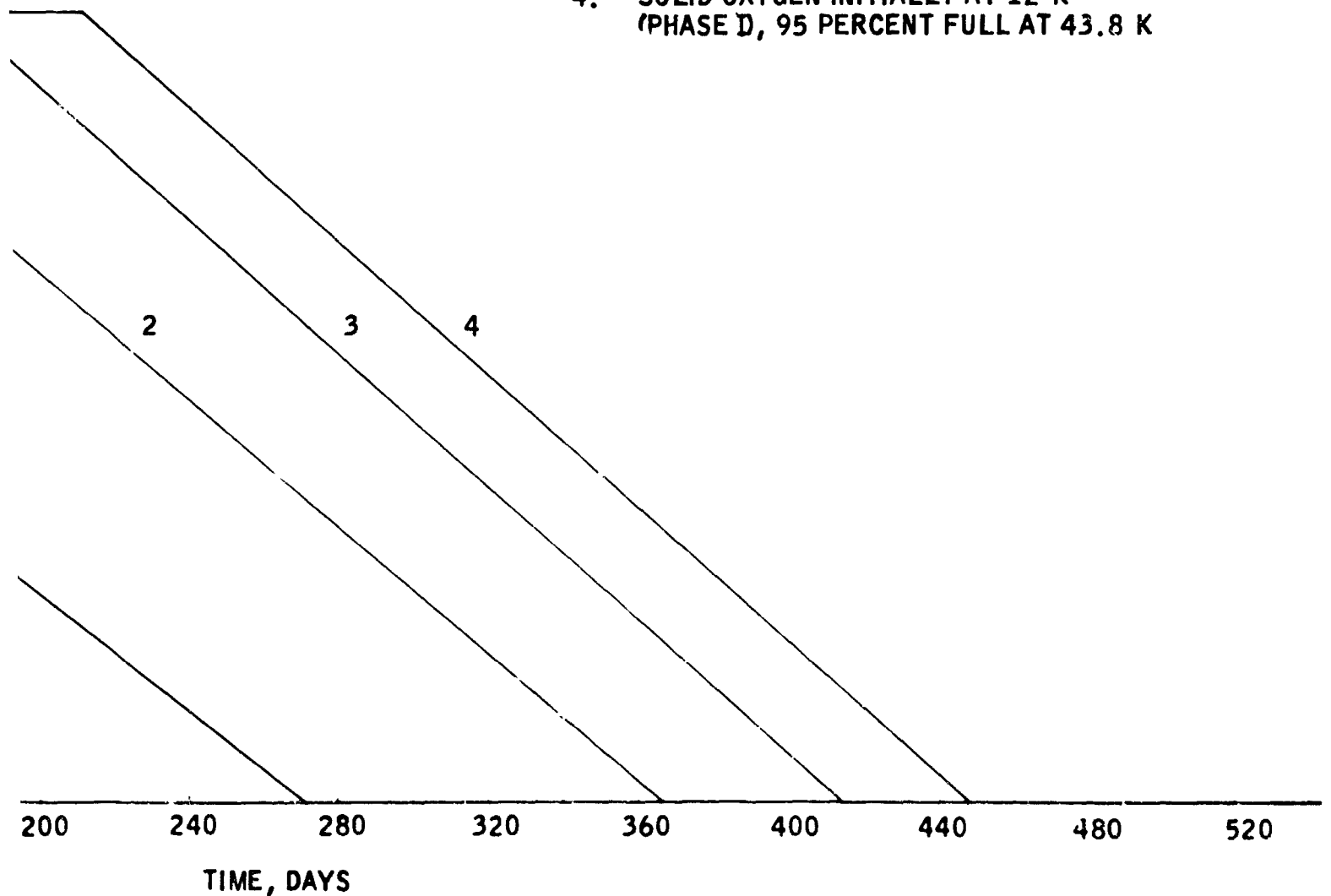


Figure 33. Comparison of Solid as a Function of Liquid Oxygen Storage Times, Flexible Multilayer Insulation  
 $R_j = 70 \text{ CM}$ ,  $T_{\text{INS}} = 1.0 \text{ CM}$ , 86.6 G's

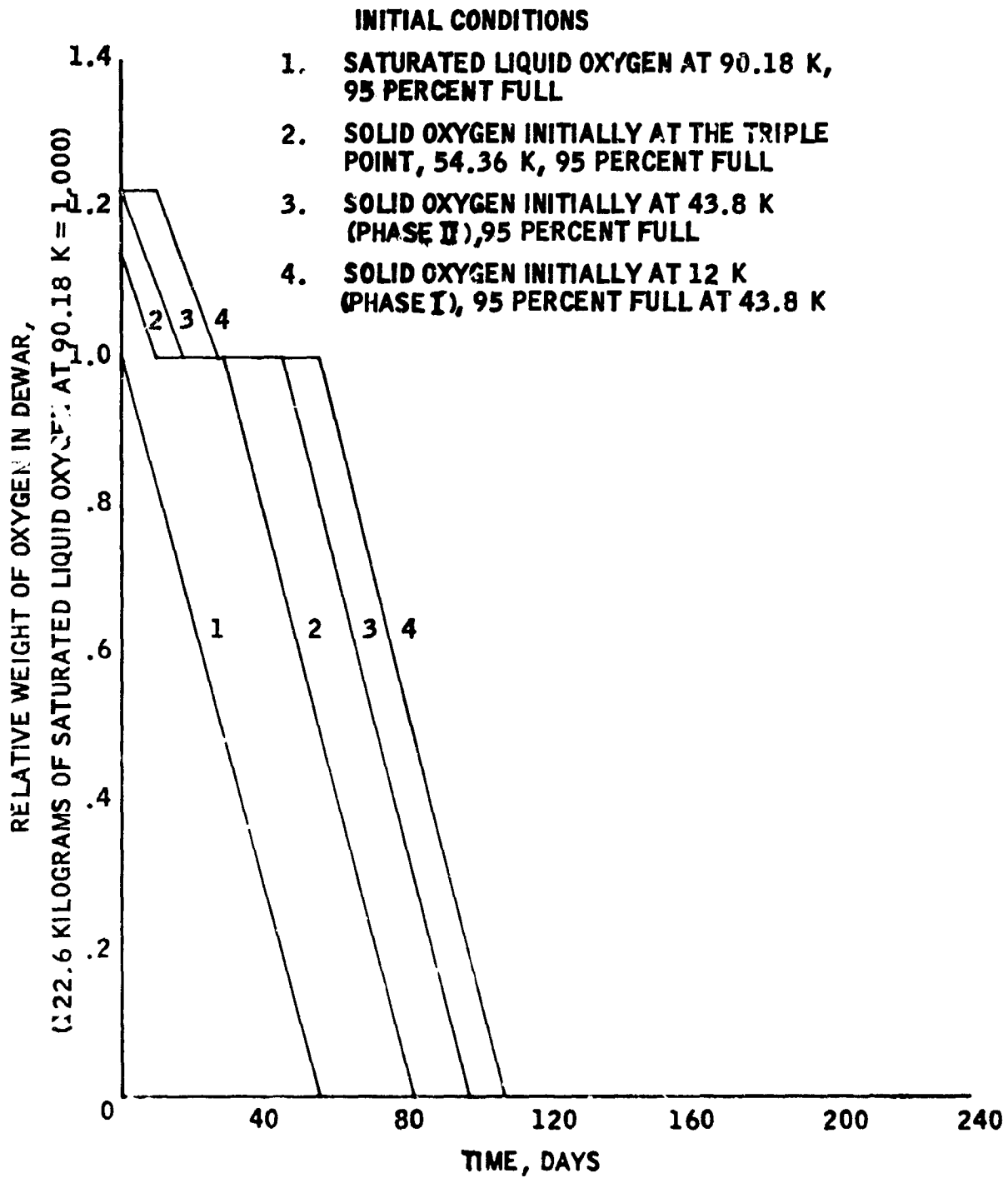


Figure 54. Comparison of Solid as a Function of Liquid Oxygen Storage Times, Rigid Shield Insulation  
 $R_j = 30 \text{ CM}$ ,  $N = 0$ ,  $86.6 \text{ G's}$

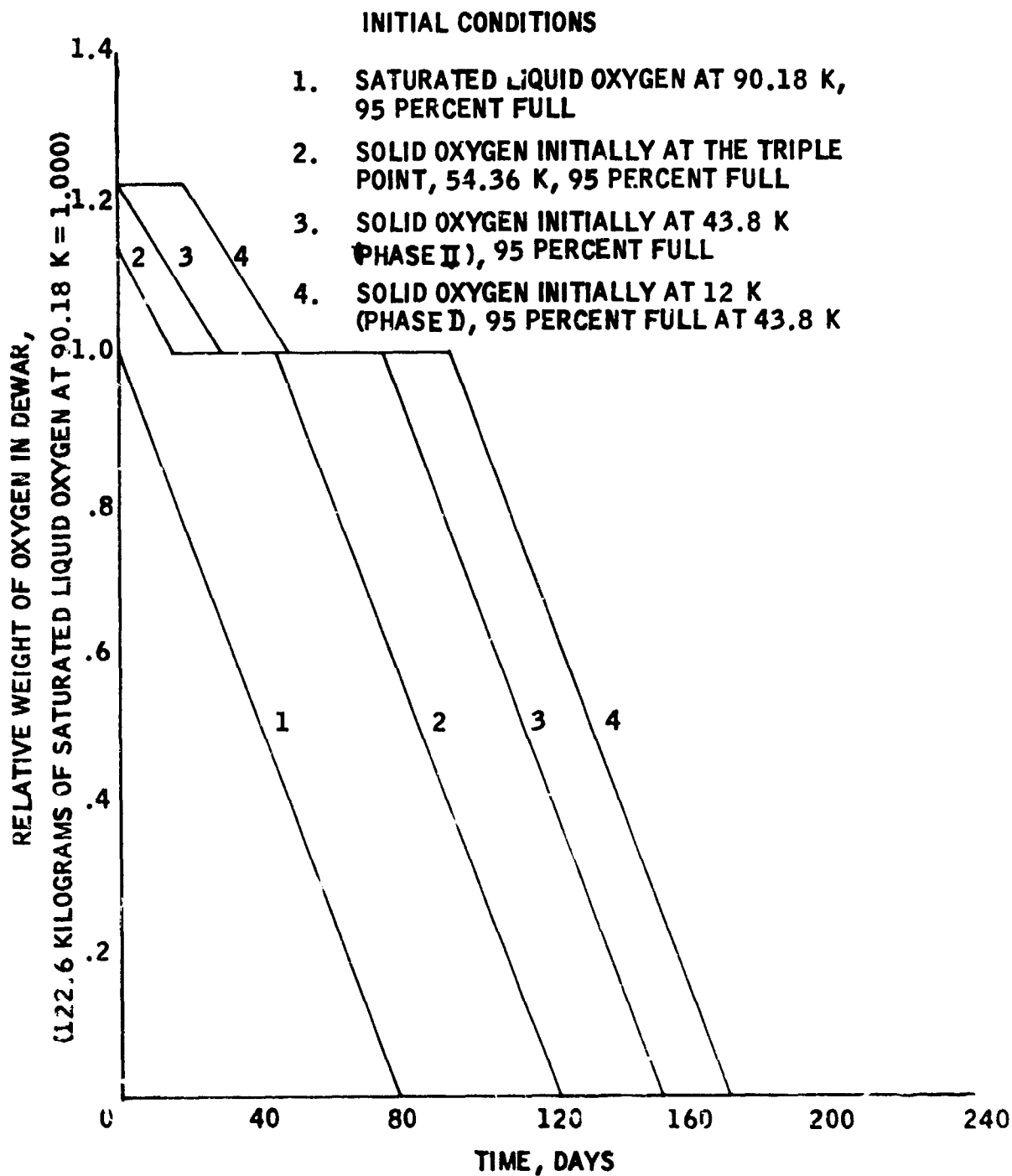


Figure 35. Comparison of Solid as a Function of Liquid Oxygen Storage Times, Rigid Shield Insulation  
 $R_j = 30 \text{ CM}$ ,  $N = 0$ ,  $10 \text{ G's}$

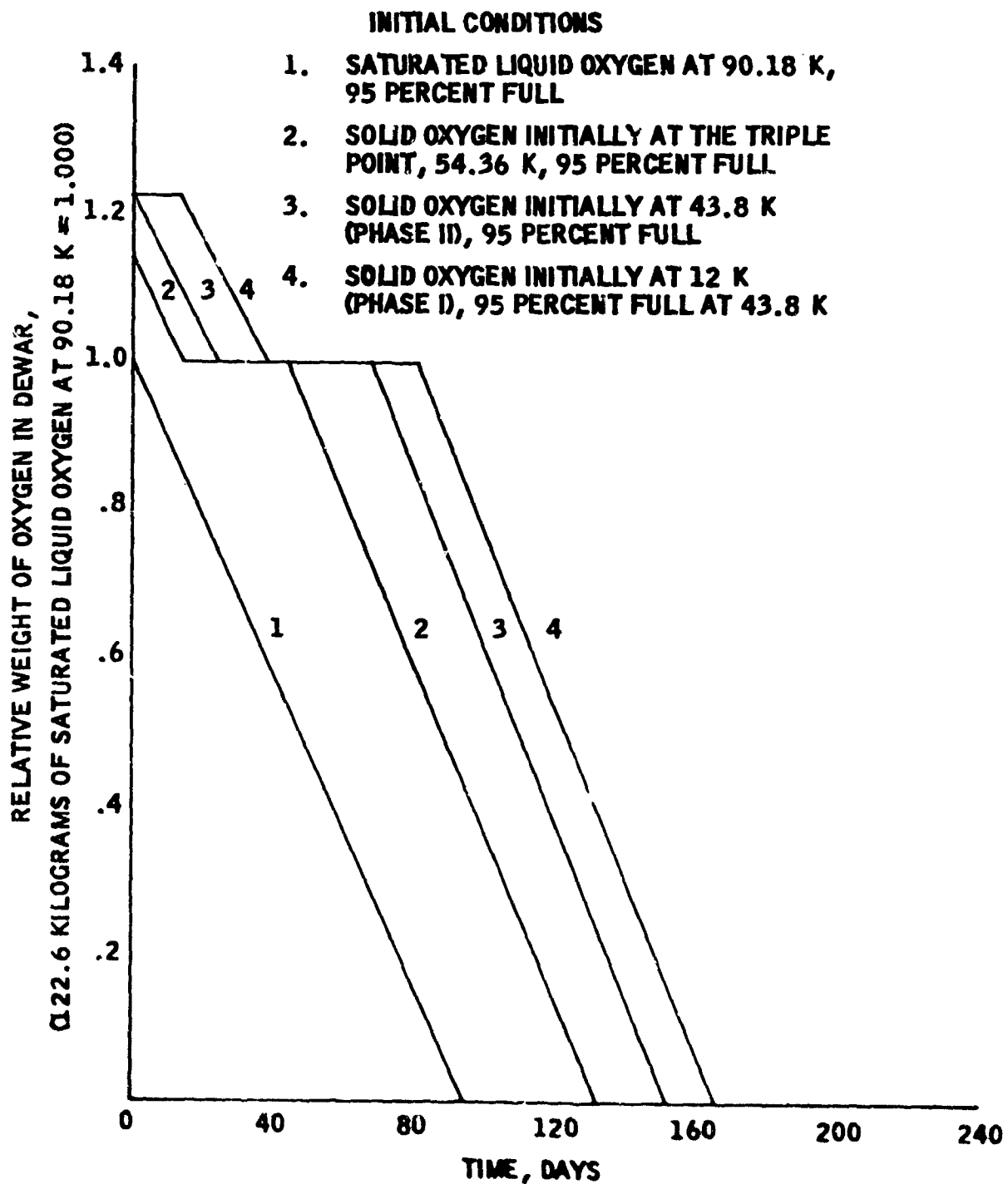
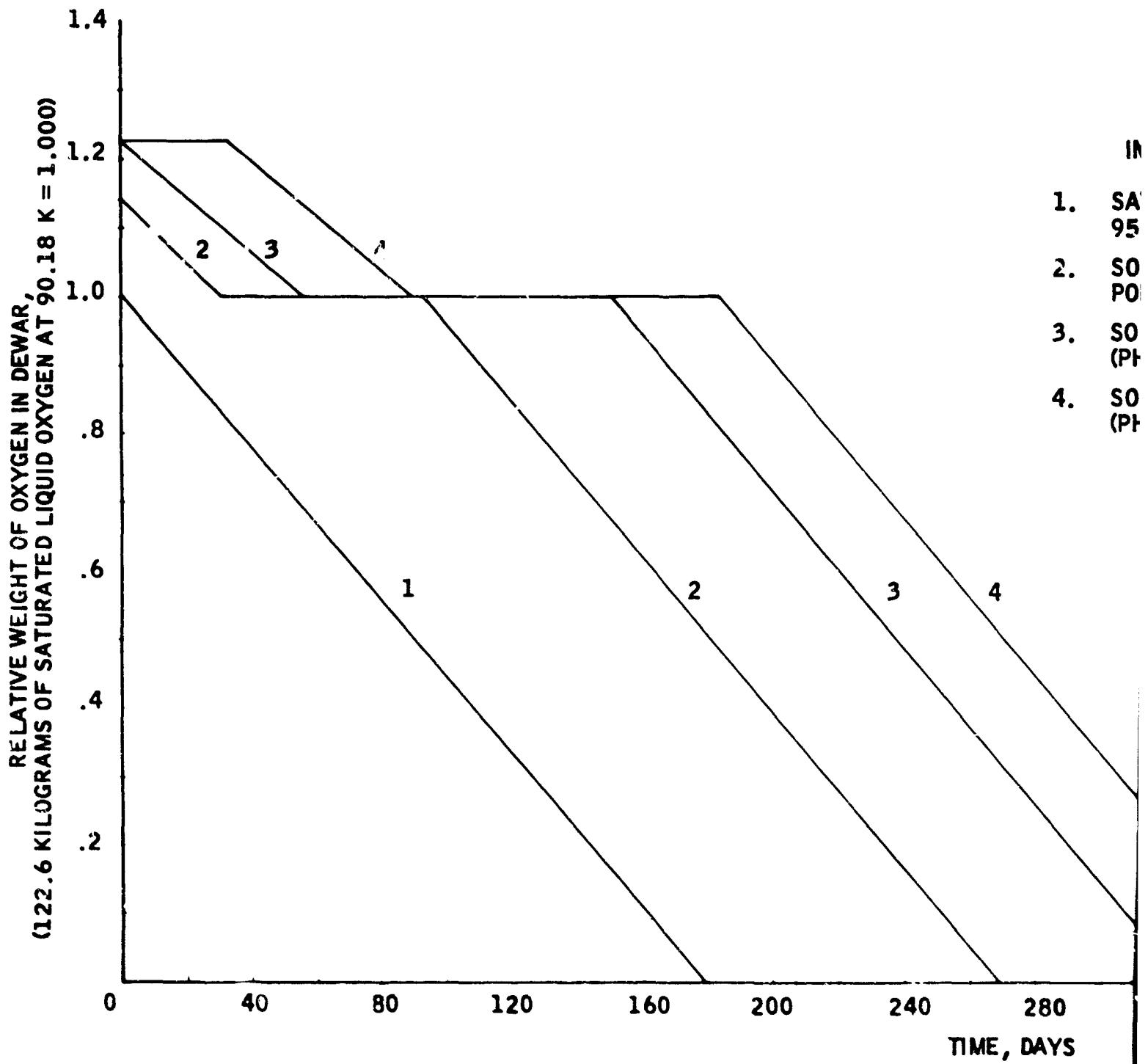


Figure 36. Comparison of Solid as a Function of Liquid Oxygen Storage Times, Rigid Shield Insulation  
 $R_j = 30 \text{ CM}$ ,  $N = 2$ ,  $86.6 \text{ G's}$



- IN
1. SA 95
  2. SO PO
  3. SO (Pt)
  4. SO (Pt)

Figure 2

A

### INITIAL CONDITIONS

1. SATURATED LIQUID OXYGEN AT 90.18 K, 95 PERCENT FULL
2. SOLID OXYGEN INITIALLY AT THE TRIPLE POINT, 54.36 K, 95 PERCENT FULL
3. SOLID OXYGEN INITIALLY AT 43.8 K (PHASE II), 95 PERCENT FULL
4. SOLID OXYGEN INITIALLY AT 12 K (PHASE I), 95 PERCENT FULL AT 43.8 K

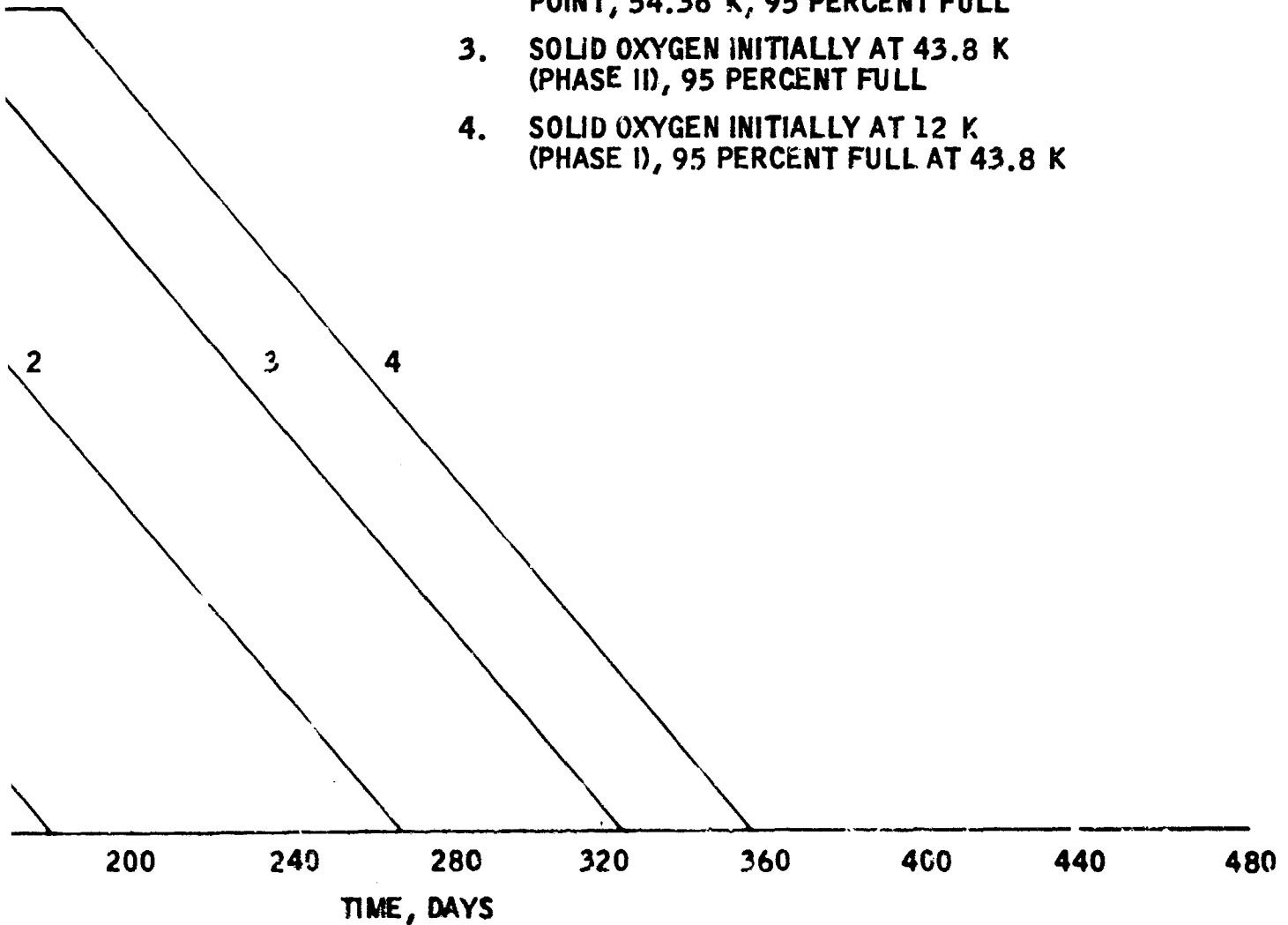


Figure 37. Comparison of Solid as a Function of Liquid Oxygen Storage Times, Rigid Shield Insulation  
 $r_j = 30$  CM,  $N = 2$ , 10 G's

This same ratio of percent of oxygen remaining holds generally for other tank sizes, insulation design, and load requirements at the maximum time where the solid oxygen stored at 12 K has 100% of its oxygen remaining.

The ratio of improvement in storage capacity can provide a guide for selection of the practical storage method for a given requirement. It is noted from figures 30 and 31 that the oxygen which is allowed to go to supercritical pressure (55 atmospheres) before venting has better storage life initially than for liquid oxygen vented at 1 atmosphere pressure, but as the time is extended, the storage capacity drops below that for the oxygen venting at atmospheric pressure. This is due to the varying thermodynamic properties of the supercritical oxygen, primarily the specific heat. The supercritical oxygen curves level out at a constant stored amount, which is the condition where a gas exists at 55 atmospheres under ambient temperature conditions and no further heat leak occurs.

Storage of oxygen initially as a solid at the triple point provides a major improvement when compared to storage of oxygen as a subcritical liquid. This is shown by figure 30 where the oxygen stored as a solid at the triple point can be stored for over 50 days without loss compared to twelve days for the supercritical liquid and zero days for the subcritical liquid (oxygen is vented immediately). The ground preparation of triple-point solid oxygen is not difficult using liquid helium or neon as a coolant.

Another major step in improving the storage capabilities can be achieved by cooling the solid oxygen to a temperature of 43.8 K. Consistent with the discussion above, solid oxygen stored at 43.8 K (below the Phase I/Phase II transition point) will remain for about 78 days compared to the 50 days for the triple-point solid. This is due to the fact that the latent heat of the transition from Phase I to Phase II of the solid is actually greater than the latent heat of fusion. The ground preparation of solid oxygen at 43.8 K should pose no major problem using liquid helium or neon as the coolant.

Storage life can be further improved by storing the solid at 12 K. This extends the storage life before loss of oxygen to about 92 days compared to the 78 days for the 43.8 K solid. This last gain, however, is obtained by reducing the solid temperature to 12 K which can be accomplished by using liquid helium to prepare the solid oxygen.

In summary, the length of oxygen storage life can be substantially improved by initially storing the oxygen as a solid. The lower the initial storage temperature of the solid oxygen, the longer the storage life will be. The most practical initial temperature for storage of solid oxygen is 43.8 K, just below the Phase I-Phase II transition. At this point, 85% of the potential storage capability of the solid is available. To achieve the remaining 15% storage capability requires cooling down to around 12 K, which would be more difficult than cooling to 43.8 K and which would require a more sophisticated internal heat exchanger and large quantities of liquid helium.

## STORAGE OF OXYGEN WITH USAGE

In lieu of transforming the solid oxygen to either the liquid state or the supercritical state, it can be maintained as a solid by subliming it to space. Upon demand, oxygen can be transported to a breathable condition by raising the pressure and temperature of the vapor which has been sublimed from the solid state. The pressure may be raised by the use of adsorbents such as used in experimental portion of this study, or discrete units of the solid oxygen can be mechanically moved to a place outside the storage container to allow controlled melting and vaporization. The subject of this section is the comparison of solid storage with liquid and supercritical storage where the solid is delivered to the breathable state by sublimation and raising the pressure by adsorbents.

The choice of method for using solid oxygen for respiration in space depends on the following independent parameters:

- Mission Length
- Number of Men
- Space Cabin Leakage
- Extra-Vehicular Activities

In addition, the following parameters, among others, must be considered: weight and size constraints, power limitations, and the launch environment to which the oxygen system shall be subjected. Ideally, the heat will transfer into the container at a rate just sufficient to supply the required oxygen for breathing, cabin leakage, etc., in order to minimize the power requirements. The cold oxygen vapor leaving the container (either solid, liquid or supercritical) can be raised to the cabin temperature by circulating through a heat exchanger with cabin air on the "hot" side of the exchanger. Since the cabin must be air-conditioned, this procedure also results in a power savings.

### Analytical Procedure

A heat transfer analysis was first made to develop the equations describing the heat leakage into the container configuration described in Section III, Subsection titled, "Oxygen Transport by Mechanical Manipulation". The heat transfer or "leakage" into the

container sublimates solid, vaporizes liquid, or drives off supercritical fluid in order to maintain a constant pressure. With a given initial weight of oxygen a mission length for the container can be computed and compared with the weight of oxygen required for a given number of men, mission length, leakage, etc., to determine if oxygen must be "dumped" (heat leak greater than usage requirements), or if external power is required (heat leak less than usage requirements). If the result is that oxygen must be "dumped," a better container with more insulation and lower-conducting supports should be designed for the mission. If the result is that power is required, the insulation thickness and/or support length may be reduced to increase the heat leak into the container.

### Results of Analysis

The parametric data developed for oxygen supply systems which yield a continuous flow of vapor are presented in figures 38 through 48. These figures show the storage system weight and oxygen weight as a function of mission length, the number of crew members, and the amount of insulation on the storage vessel. Because of the large number of variables involved in the analysis, curves are required for some secondary factors (such as heat leak as a function of insulation thickness and vessel radius) in order to fully develop the performance characteristics of the storage systems. These curves are presented in Appendix I.

Figures 38 through 40 present the weight of oxygen required for a given mission length with the number of men using 1.13 kilograms per day as a parameter. These figures also include one kilogram per day total leakage rate and no air lock usage. Superimposed upon these figures is the mission length versus the weight of oxygen when the heat supplied is equal to the heat transfer through the insulation and supports (launch loading of 86.8 G); curves for various insulation thicknesses are shown.

Figures 41 through 43 present similar results for a launch loading of 10 G. Figures 38 and 41 are for solid storage, figures 39 and 40 are for liquid storage, and figures 40 and 43 are for supercritical storage. The curves for the amount of the oxygen required per number of men are the same for the two figures because the same weight of oxygen should give the same mission length for the equal usage.

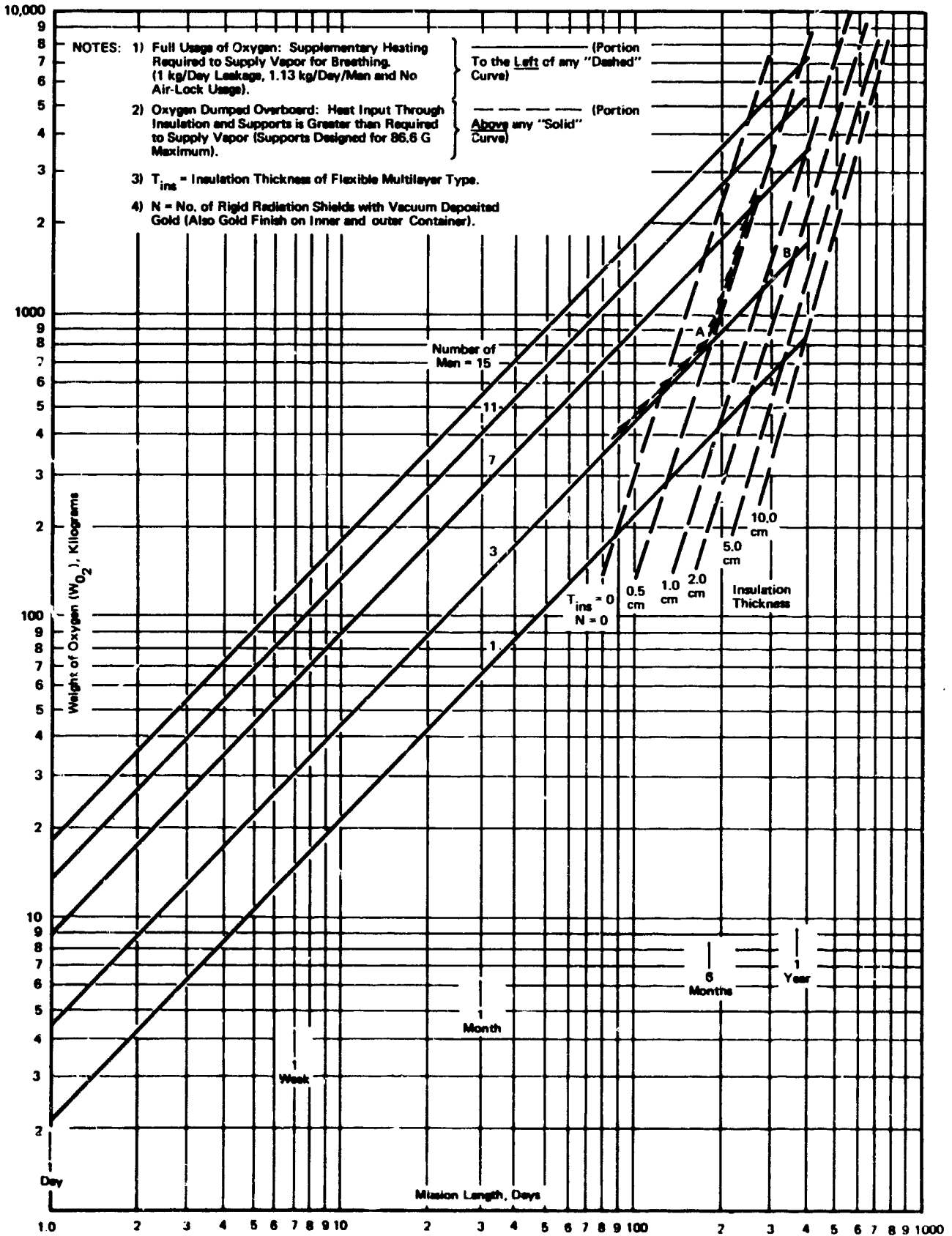


Figure 38. Required Initial Oxygen Weight as a Function of Mission Length and Number of Men and Heat Transfer into the Container for Solid Oxygen Storage

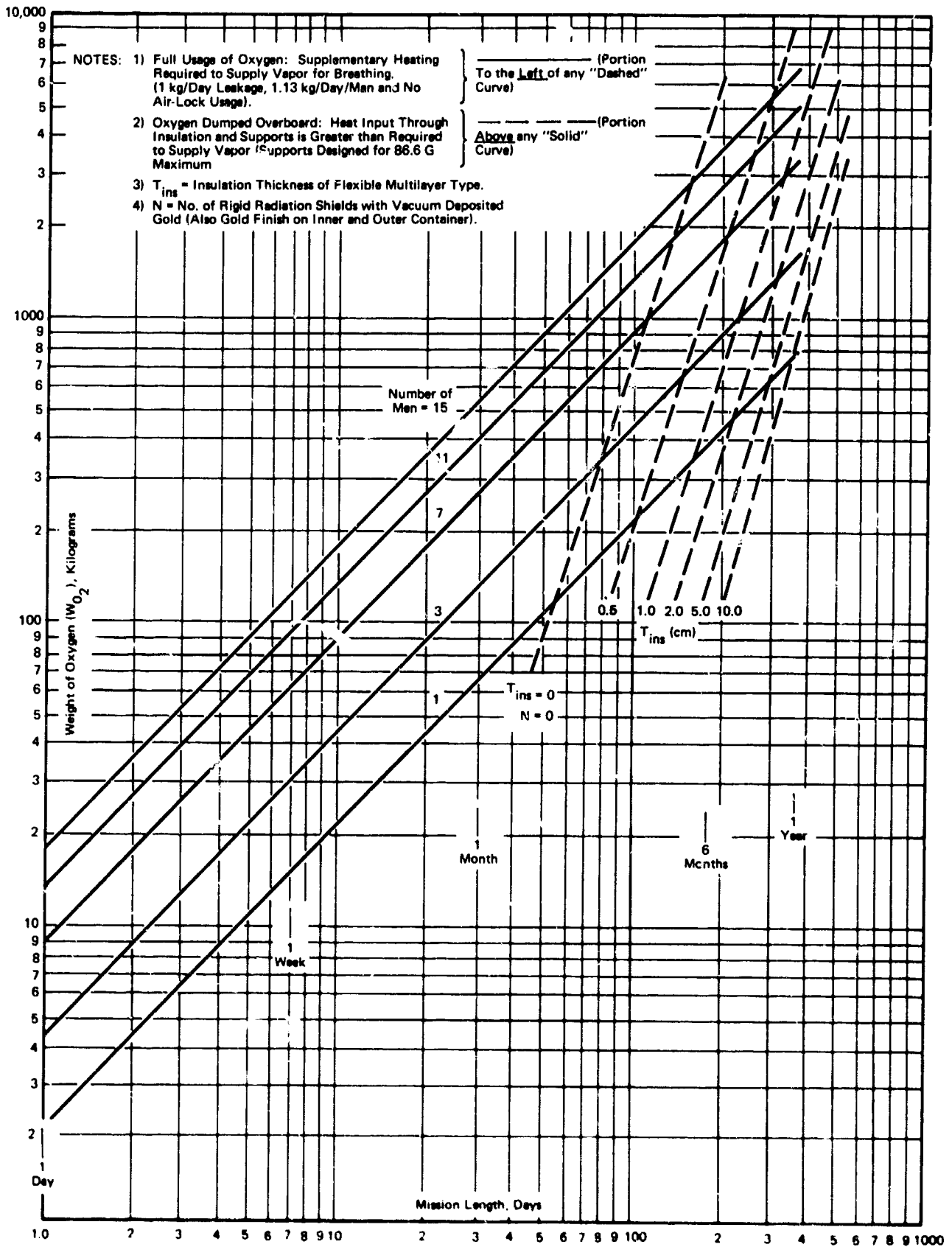


Figure 39. Required Initial Oxygen Weight as a Function of Mission Length and Number of Men and Heat Transfer into the Container for Liquid Oxygen Storage



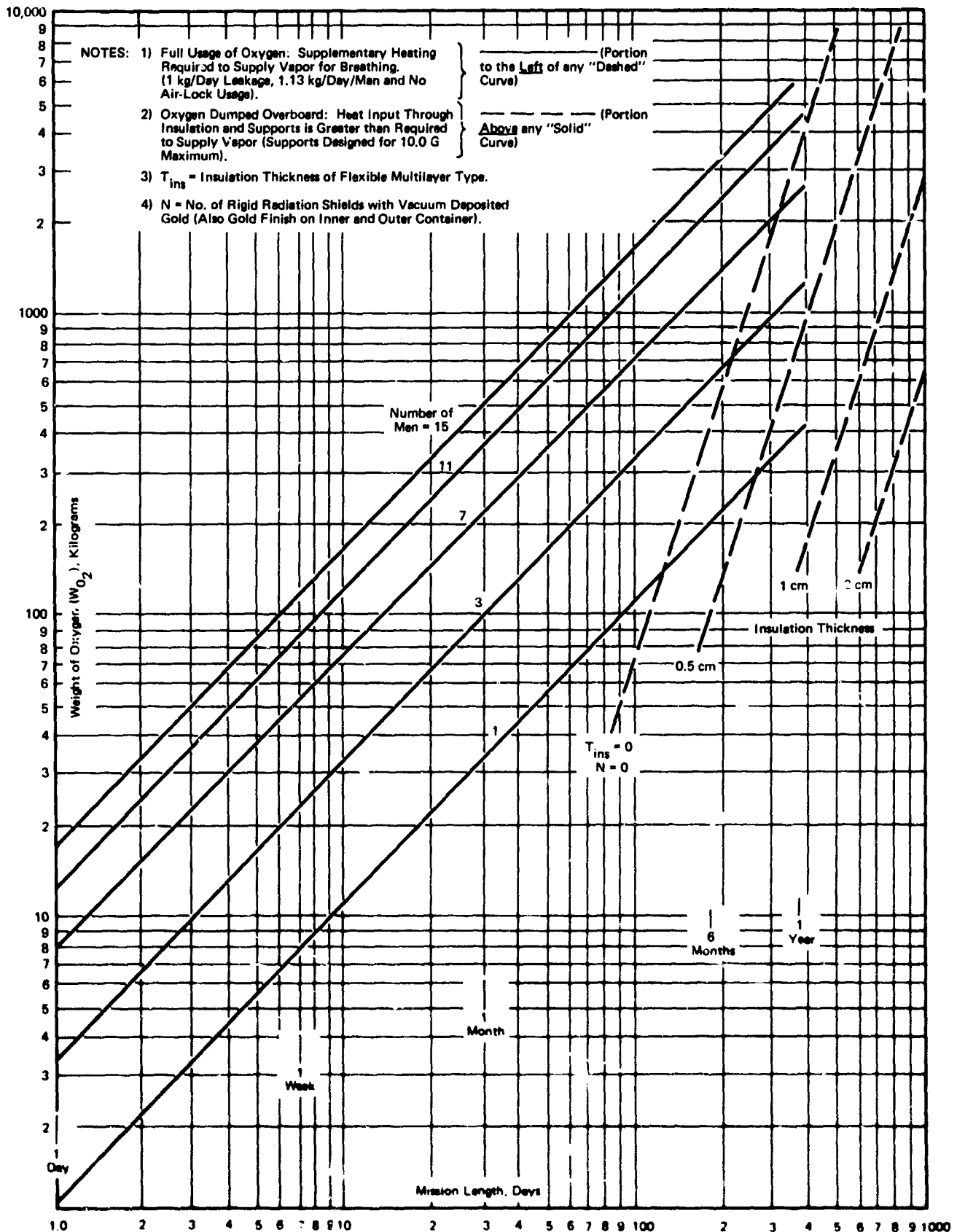


Figure 41. Required Initial Oxygen Weight as a Function of Mission Length and Number of Men; and Heat Transfer into the Container for Solid Oxygen Storage

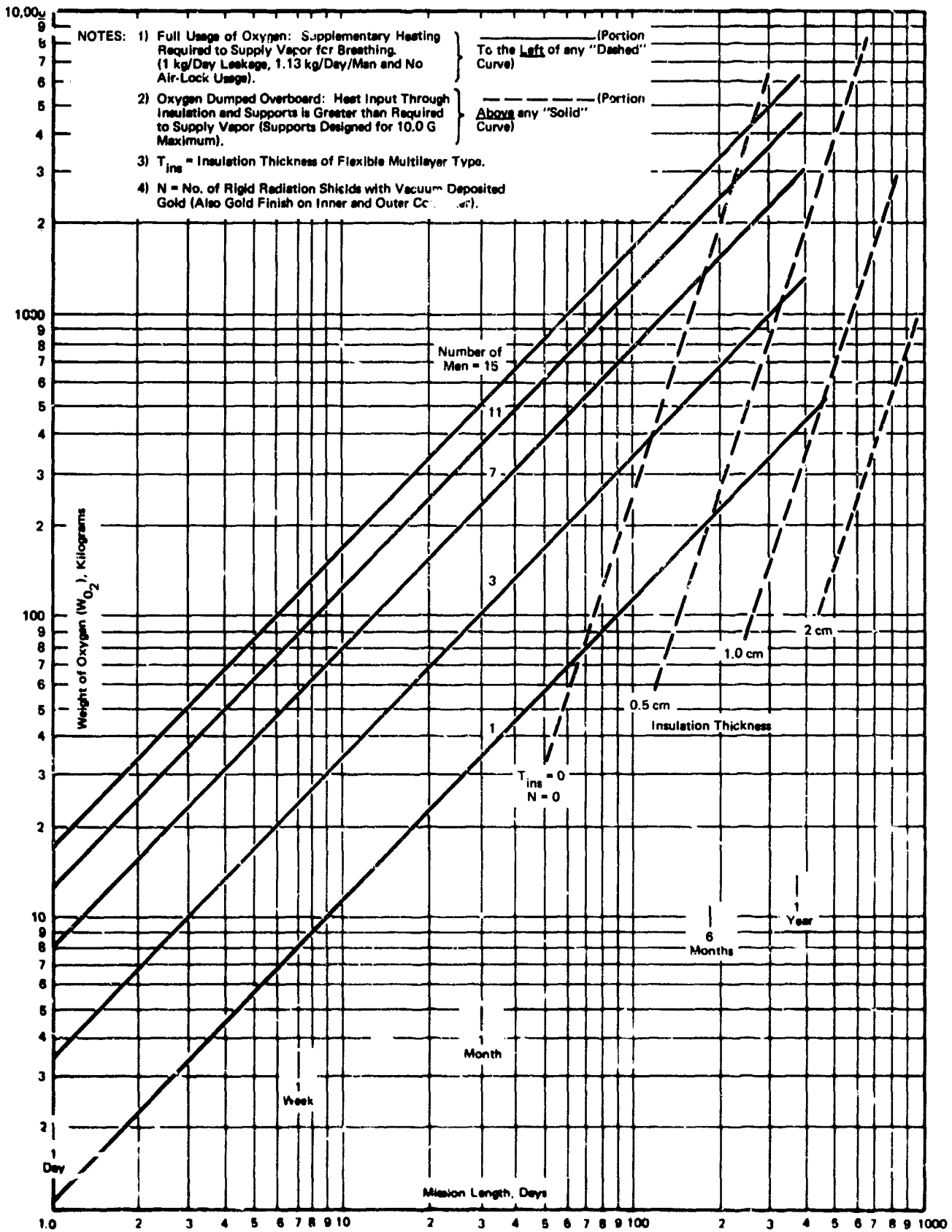


Figure 42. Required Initial Oxygen Weight as a Function of Mission Length and Number of Men and Heat Transfer into the Container for Liquid Oxygen Storage



NOTES: 1) USAGE RATE FOR ONE MAN AT 1.13 KG/DAY  
PLUS 1 KG/DAY LEAKAGE

2) 86.6 G MAXIMUM SUPPORT LOADING

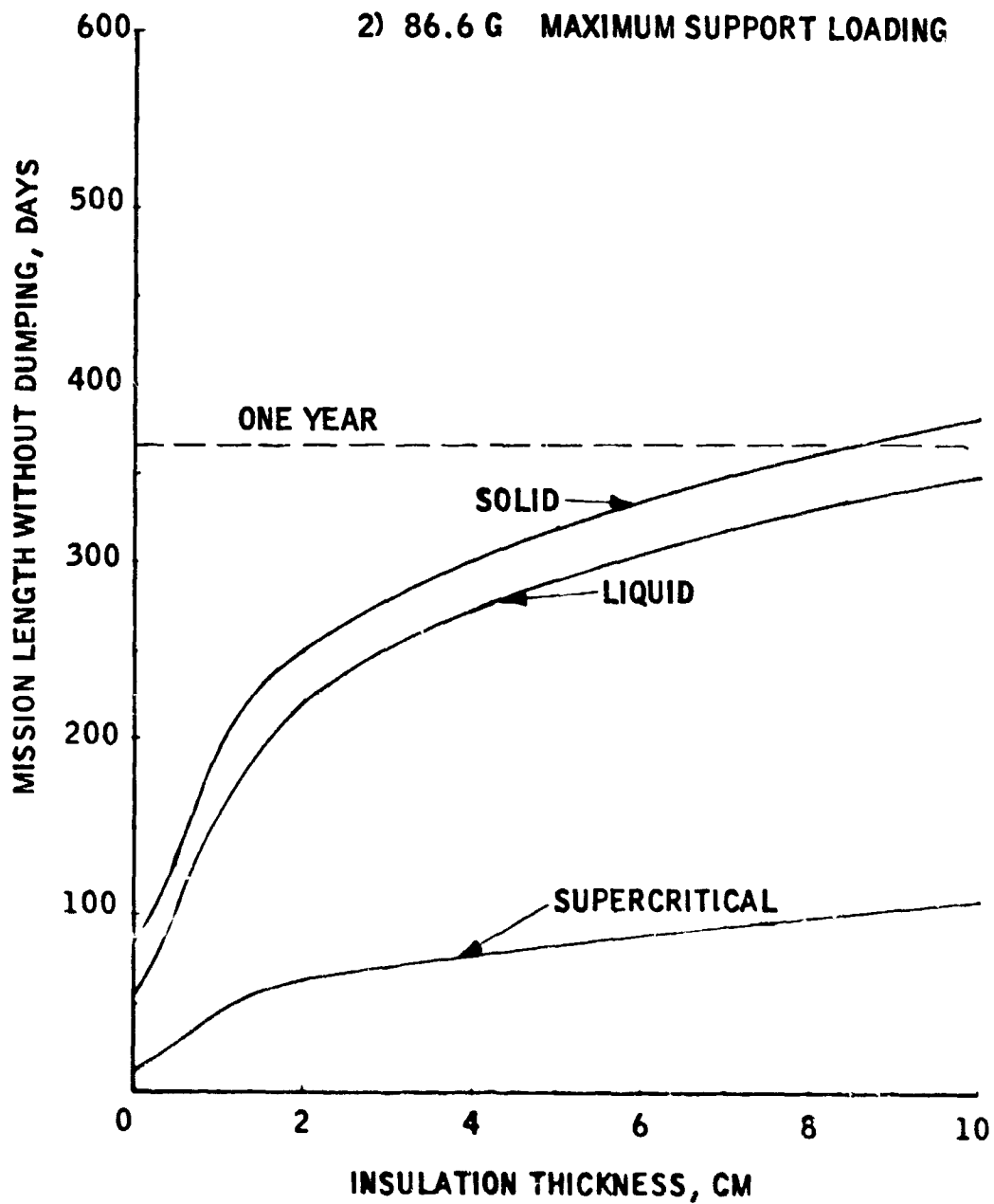


Figure 44. Mission Length Without Dumping Oxygen as a Function of Insulation Thickness (One Man Usage)

- NOTES: 1) USAGE RATE FOR THREE MEN AT 1.13 KG/DAY/MAN PLUS 1 KG/DAY LEAKAGE  
2) 86.6 G'S MAXIMUM SUPPORT LOADING  
3) "ZERO" INSULATION THICKNESS IS WITH A GOLD COATED VACUUM DEWAR

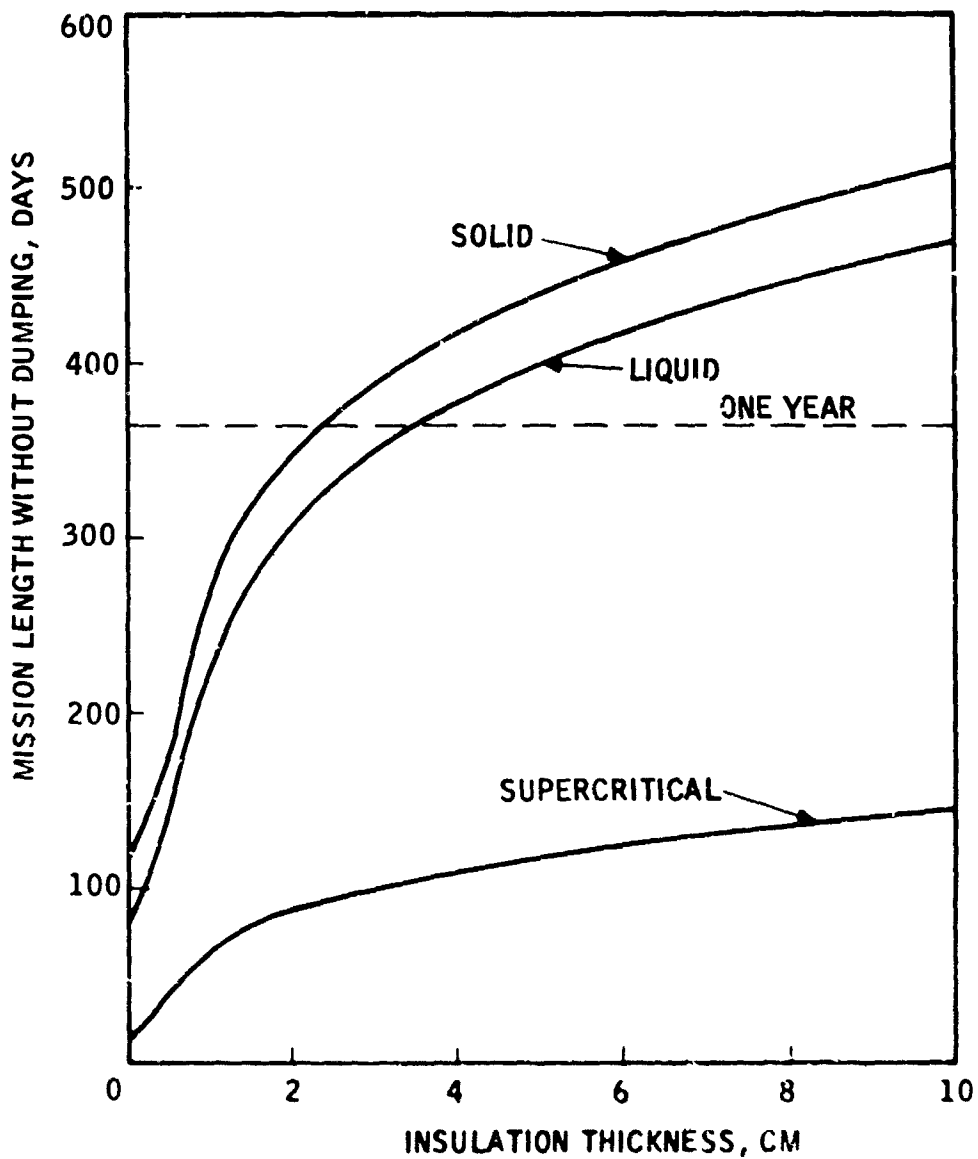


Figure 45. Mission Length Without Dumping Oxygen as a Function of Insulation Thickness (Three Men Usage)

NOTES: 1) USAGE RATE FOR SEVEN MEN AT 1.13 KG/DAY  
PLUS 1 KG/DAY LEAKAGE

2) 86.6 G MAXIMUM SUPPORT LOADING

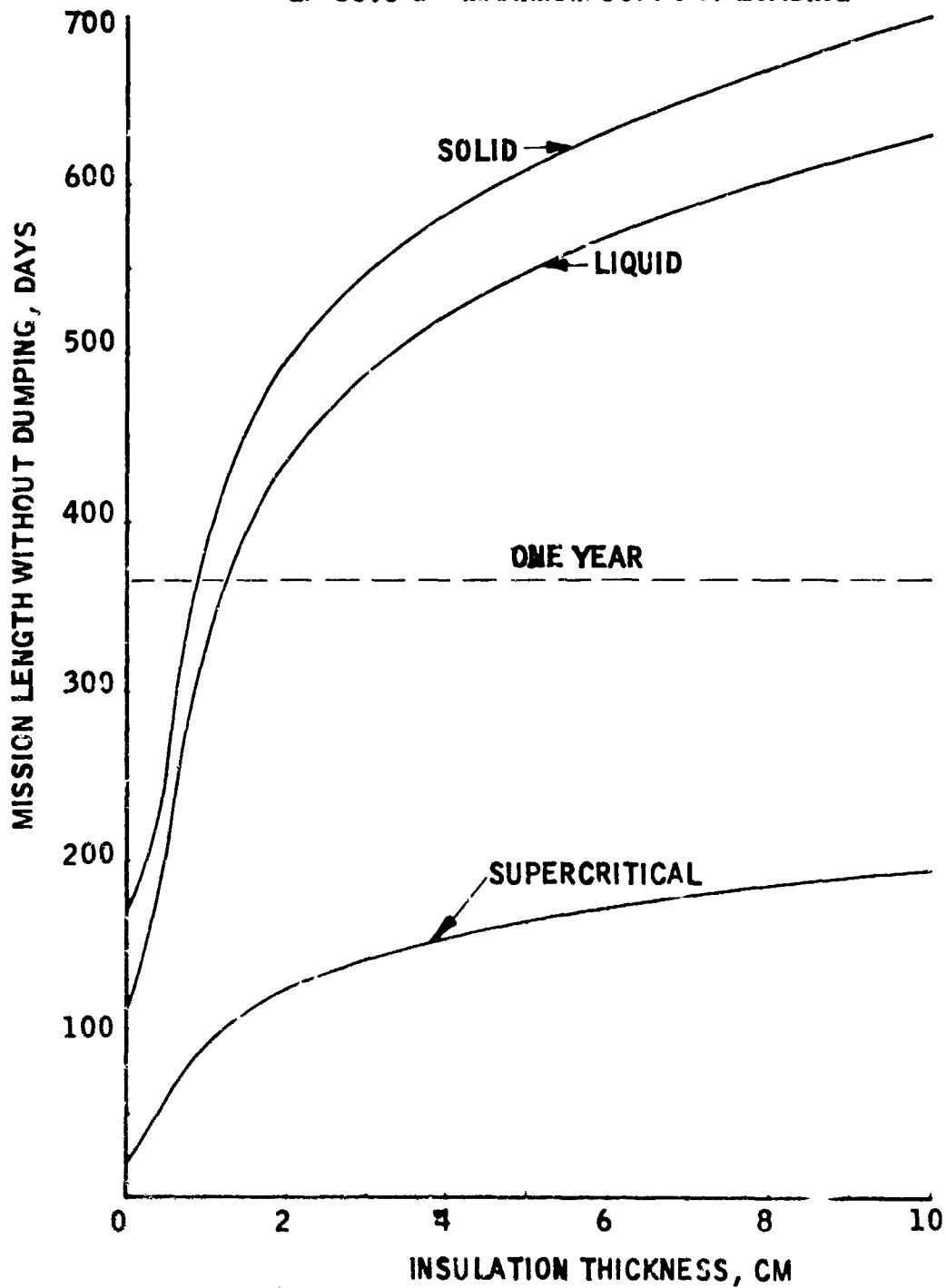


Figure 4b. Mission Length Without Dumping Oxygen as a Function of Insulation Thickness (Seven Men Usage)

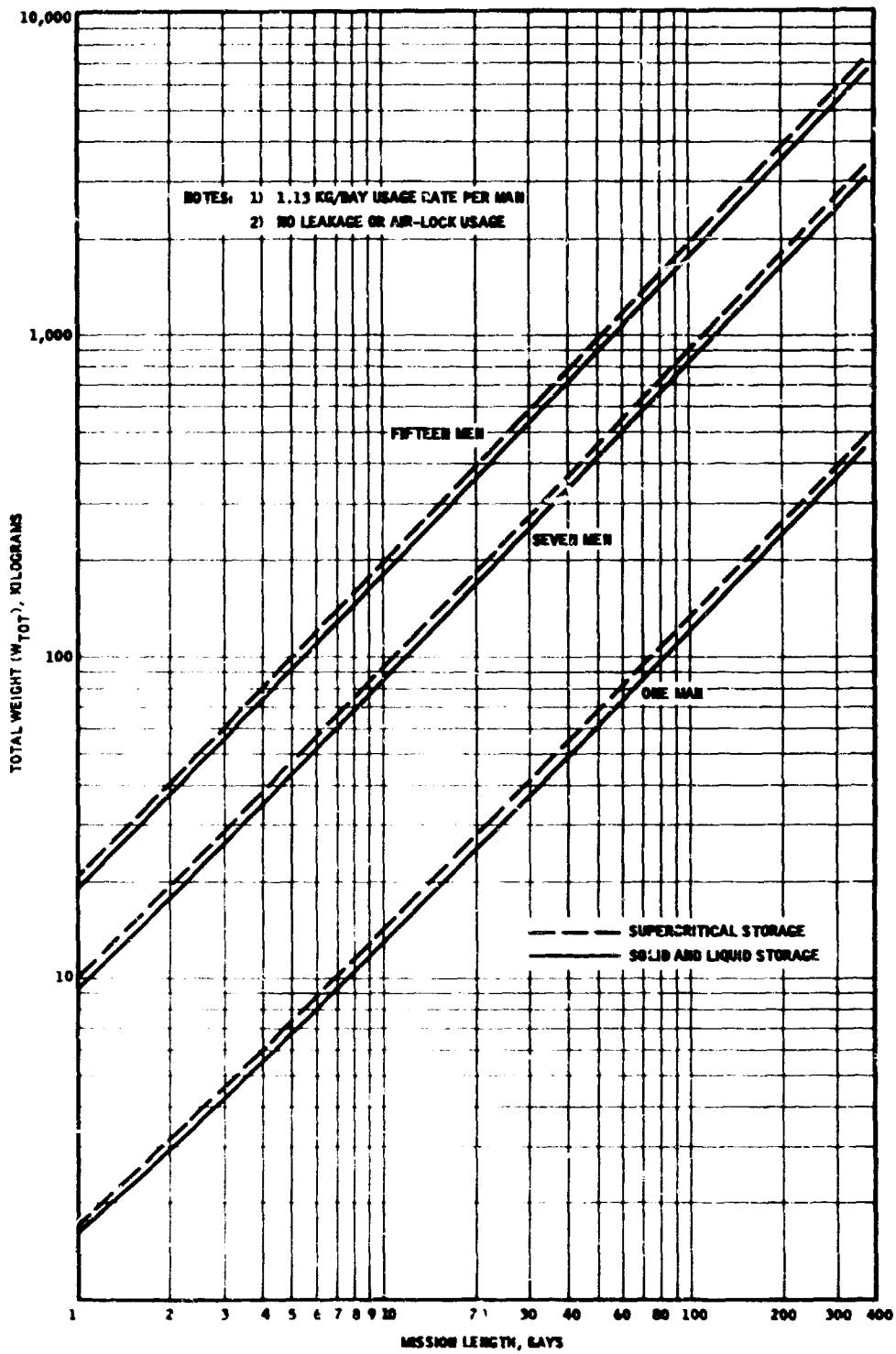


Figure 47. Total Weight as a Function of Mission Length and Number of Men (Insulation Thickness = 0.5 Centimeters, Flexible Multilayer Type)

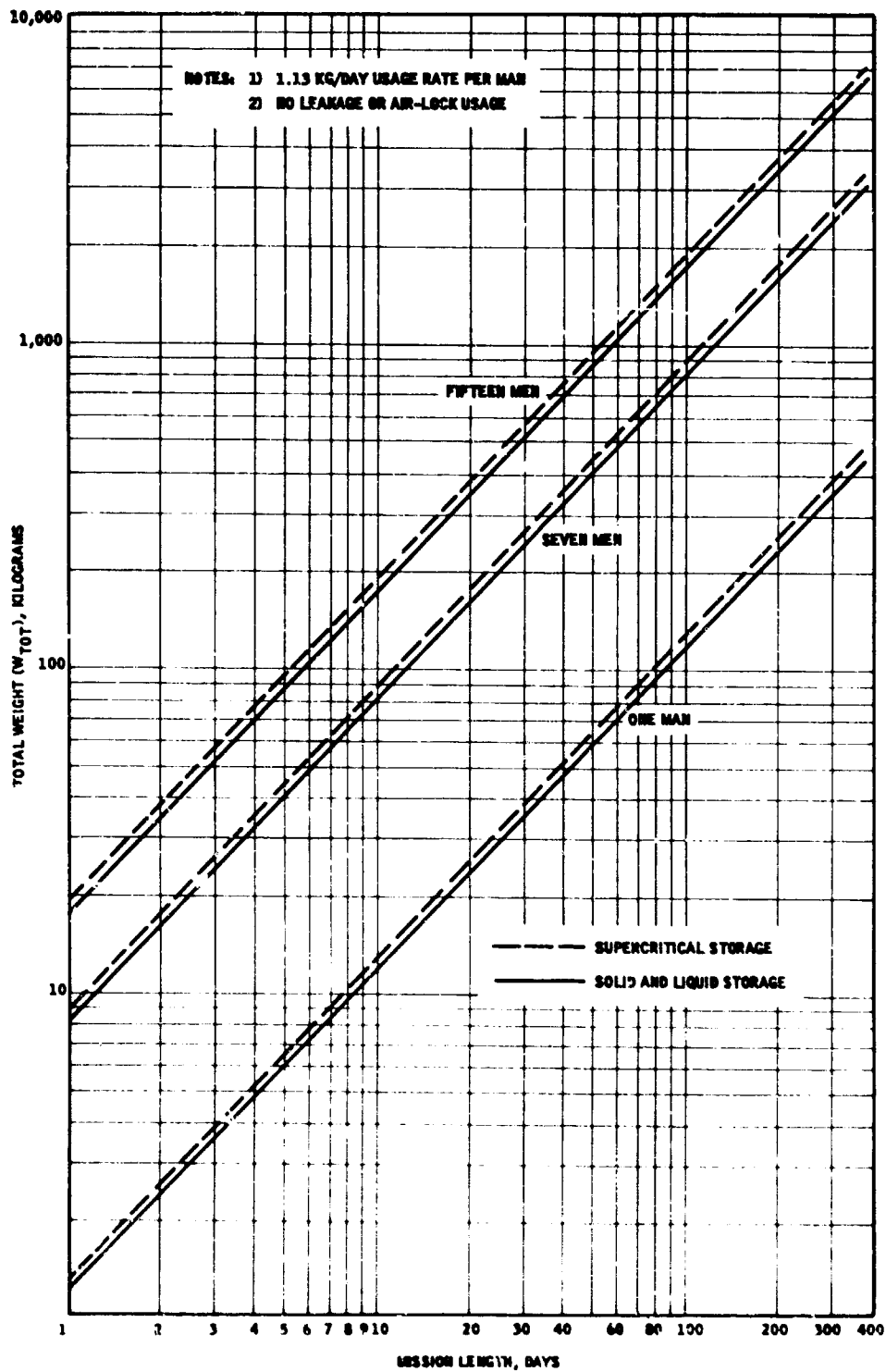


Figure 48. Total Weight as a Function of Mission Length and Number of Men (Insulation Thickness = 5.0 Centimeters, Flexible Multilayer Type)

For supercritical oxygen storage (figures 40 and 43), the "dashed" curves actually vary with time during the mission. This variation is caused by two factors: (1) the oxygen temperature increases continuously during supercritical storage due to the decreasing density (see figure 61 in Appendix II). The "dashed" curves of figures 40 and 43 are for the minimum ( $q/\dot{m}$ ) parameter of 73 watts per gram per second at 32.5 percent weight remaining in the Dewar and where the oxygen temperature is 158 K. The "dashed" curves should then represent an approximate minimum mission length without having to dump oxygen overboard because the heat transfer is greater than that required to supply oxygen.

A comparison of the performance curves for supercritical, liquid and solid storage shows that the supercritical storage method requires more insulation than the liquid or solid storage methods to provide the same mission length for the longer missions. Likewise, the liquid storage method requires more insulation than the solid storage method. Figures 44, 45, and 46 present this comparison for the case where the support loading is designed for 86.6 G and for missions for one-, three-, and seven-man crews, respectively. These figures were drawn from the intersections of the "dashed" and continuous curves of figures 38 through 40. Similar comparison curves can be drawn for other crew sizes, leakages, and support loading by using figures 38 through 43 as working curves.

Figures 47 and 48 present the total system weight including insulation and structure versus mission length comparing solid, liquid, and supercritical oxygen storage, with the number of men (1, 7, 15) as a parameter. This type of data has been evaluated for different insulation thicknesses ranging between 0.5 and 10 cm, as well as for rigid shield insulation. The comparisons are shown for insulation thicknesses of 0.5 cm and 5 cm as representative of the results for total container weights.

#### Discussion of Results

The results presented in figures 38 through 43 show the regions where heat must be added to supply oxygen (to the left of the dotted curves), and where heat transfer would be greater than required, and, consequently, oxygen would have to be dumped overboard to maintain cabin pressure (along dotted curves above any given solid curve). For instance, for three men, the solid curve to the left of Point A on figure 38 represents mission lengths where heat must be added to supply oxygen when the insulation thickness is equal to 0.5 cm. For an insulation thickness of 0.5 cm, the weight of oxygen required to supply a given mission length in excess of 133 days is given by values on the dashed curve above Point A. More oxygen is required in this case because oxygen usage does not keep pace

with the oxygen generation rate and the excess must be dumped overboard. For instance, a mission length of 200 days would indicate a requirement for 1030 kilograms of oxygen when utilizing 0.5 cm of insulation. In order to keep from dumping oxygen overboard for a given mission, the insulation thickness must be increased, for instance, to Point B with 2 cm of insulation would yield approximately 350 days without dumping oxygen. For the example of a 200 day mission, only 880 kilograms of oxygen are required for 2.0 cm of insulation as compared to 1030 kilograms for 0.5 cm. Similar comparisons of the effect on insulations can be drawn for liquid and supercritical storage presented in figures 39 and 40 and for missions with the lower loading of 10 G on the supports.

A comparison of mission length without having to dump oxygen as a function of insulation thickness, storage method and the number of men in the crew is presented in figures 44, 45, and 46. The results for zero insulation thickness is also for no shields and the inner and outer containers coated with vacuum deposited gold. Several facts are shown by these curves. First, as the total usage rate is increased (one man, three men, and seven men) for a given required mission length, say, one year, the required insulation thickness decreases significantly. For instance, with the solid storage on the three curves:

- one man requires 8.3-cm thick insulation
- three men require 2.4-cm thick insulation
- seven men require 0.9-cm thick insulation

The reason for this is that for the same mission length, a larger container is required for larger usage rates and for spherical containers, the weight of oxygen increases as the cube of the radius, and the heat transfer increases only as the radius squared. Thus, for larger usage rates, the insulation thickness can be decreased to provide the required increase in heat transfer.

Second, solid oxygen provides a longer mission than either liquid or supercritical storage in all regions of parameters considered. The relative performance of the three storage phases does not change. This is due primarily to solid oxygen's large latent heat of sublimation. By the same token, solid oxygen requires more external power than the liquid if the container heat transfer is lower than for the required usage rate.

The comparison of storage container total weight (with oxygen) is presented in figures 47 and 48 for insulation thicknesses of 0.5 cm and 5.0 cm, respectively. There is negligible difference in liquid and solid oxygen total storage container weight for the same mission length. Also, the loaded supercritical storage container is heavier than both the solid and liquid containers.

The results of the analyses are significant in three respects:

1. A slight saving in total weight of less than 1% is gained by using solid oxygen instead of liquid oxygen. This result does not include the weight attributable to the peripheral equipment required to maintain a low pressure over the solid.
2. There is, however, a significant reduction in the volume of oxygen (14%) when utilizing a solid instead of a liquid.
3. The advantages of a solid oxygen continuous supply system over a liquid system are outweighed by the consideration that additional weight is required for pumps to maintain a low pressure over the solid.

#### SOLID OXYGEN STORAGE AND SUPPLY SYSTEMS

The analytical and experimental work described previously has shown distinct advantages for considering the solid phase of oxygen for storage and supply systems. A preliminary evaluation of potential storage and supply systems can be made from the data. In this section, three potential systems are described using the information generated in the study.

##### Systems for Space Cabin Oxygen Supply

The analytical data presented in Section II provides the information for selection of the oxygen storage system design as a function of the number of crew members and the length of the mission. The comparison curves of figures 44, 45, and 46 show that the solid oxygen supply system has no real advantage over the liquid oxygen system once oxygen is being used by crew members. If solid oxygen is initially used at launch or during space transport to a space station, then it could be supplied to crew members either by transporting the solid sublimating vapors or by melting the solid and using the vapors which are evaporated for the liquid.

The supply of oxygen to the crew compartment from a subliming solid would require the 3-pump systems shown in figure 49. To use this system, an improvement in the cooldown rate of the cryosorption pumps is required as noted in the discussion of the experimental study. The weight of the cryosorption pump material is given in figure 13, for example a 10-man crew would require a 14-kilogram pump, and for three pumps, this would mean 42 kilograms for the total molecular sieve weight in the system. Other system limitations must be considered in this application such as the maximum rate of sublimation from the solid oxygen surface shown in figure 50. From this curve the surface area requirements for solid oxygen sublimation at the triple point and for lower solid oxygen temperatures can be evaluated for a given application. This minimum surface area requirement can be a serious limitation to the use of the solid subliming system for large number of crew members and short mission durations (small supply tanks) when solid temperatures are much below the triple point. The other potential problem in the system design for this oxygen transport method is the flow area requirements between the subliming solid and the cryosorption pumps. Figure 51 shows that large flow areas are required even for short lengths, especially for the lower temperature solid where vapor pressures are very low. (See Dushman, 1962)

The liquid oxygen supply would be a conventional system and would be usable as soon as the solid oxygen in the tanks (if used for launch and transport) is melted.

The solid oxygen supply system for crew cabin oxygen supply has several serious limitations due to maximum sublimation rates and low conductance. Only triple-point oxygen should be considered for the cryosorption transfer method since no advantage is gained with lower temperature solid during use by crew members. Since no real performance advantage is gained in using the solid oxygen over the liquid oxygen during crew use (except for elimination of two-phase problems of the liquid), solid oxygen should only be considered for special cases. One possible case is where only intermittent use of oxygen from storage will occur, and good storage characteristics are required between these phases of use.

#### Systems for Long-Term Storage

The analytical study indicated a major advantage of solid oxygen over subcritical and supercritical oxygen for long-term storage without usage. This is due to the heats of fusion and transition of the solid as well as the sensible heat.

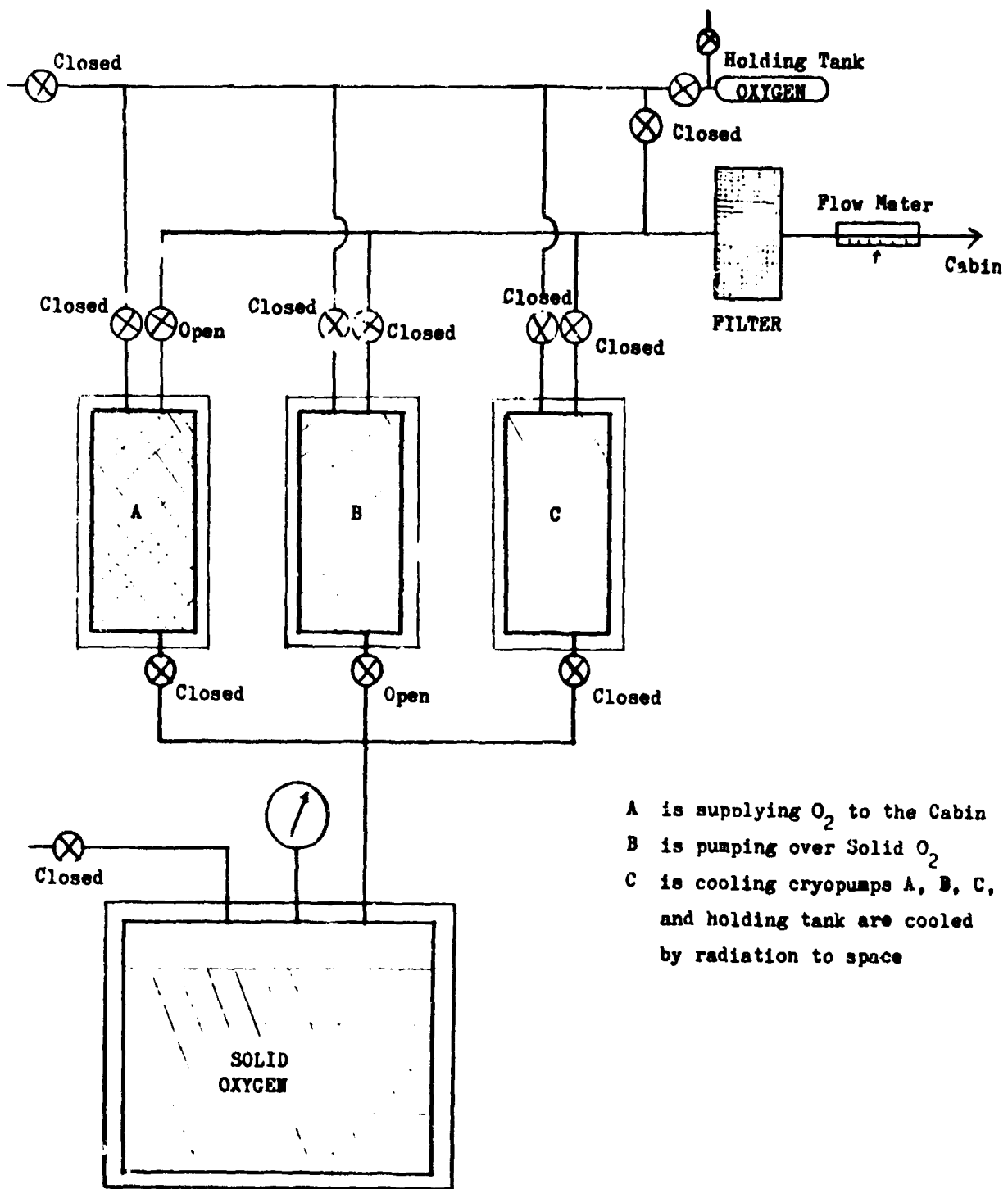


Figure 49. Three Cryosorption Pump Transfer System

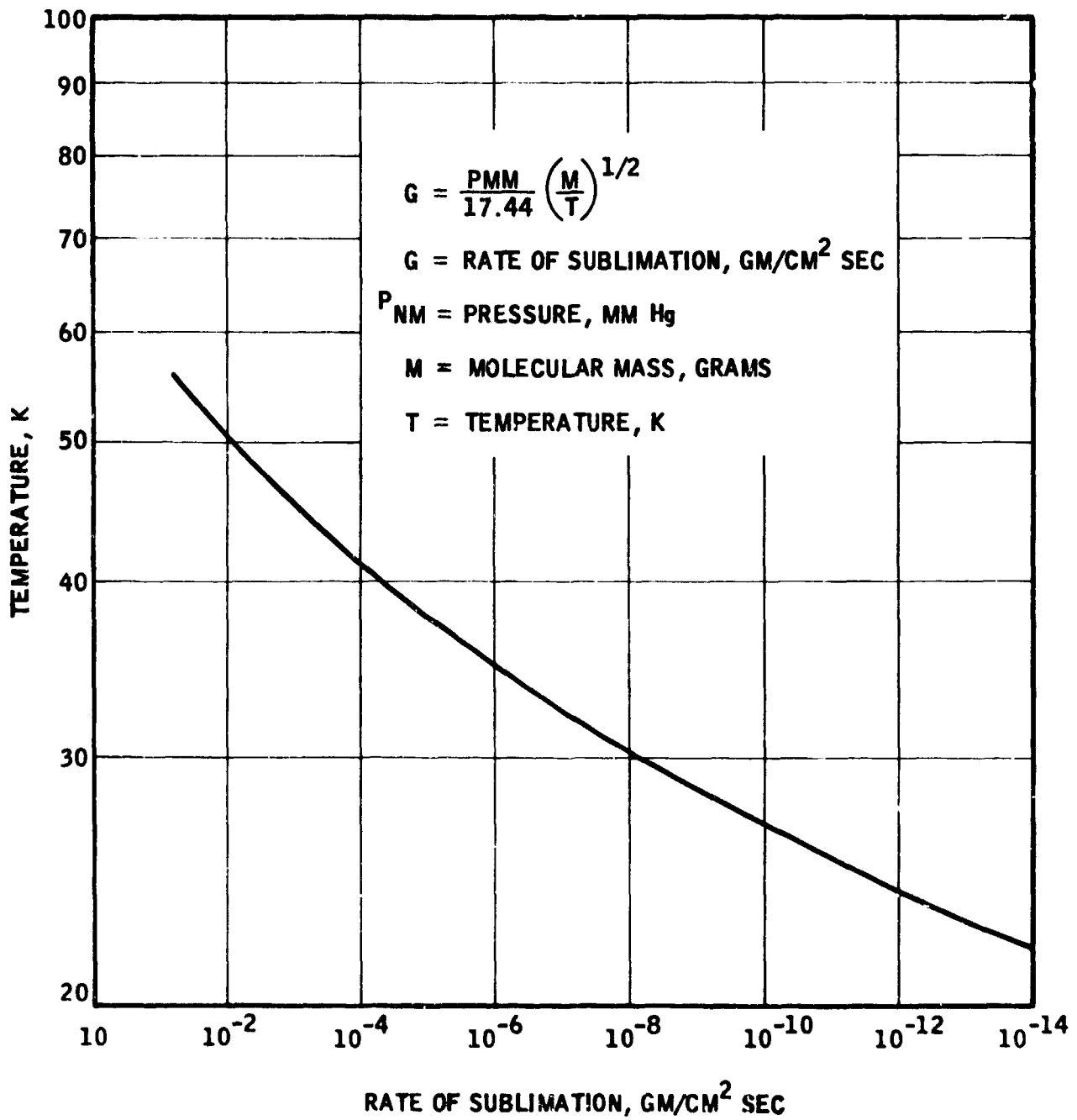


Figure 50. Maximum Rate of Sublimation of Oxygen

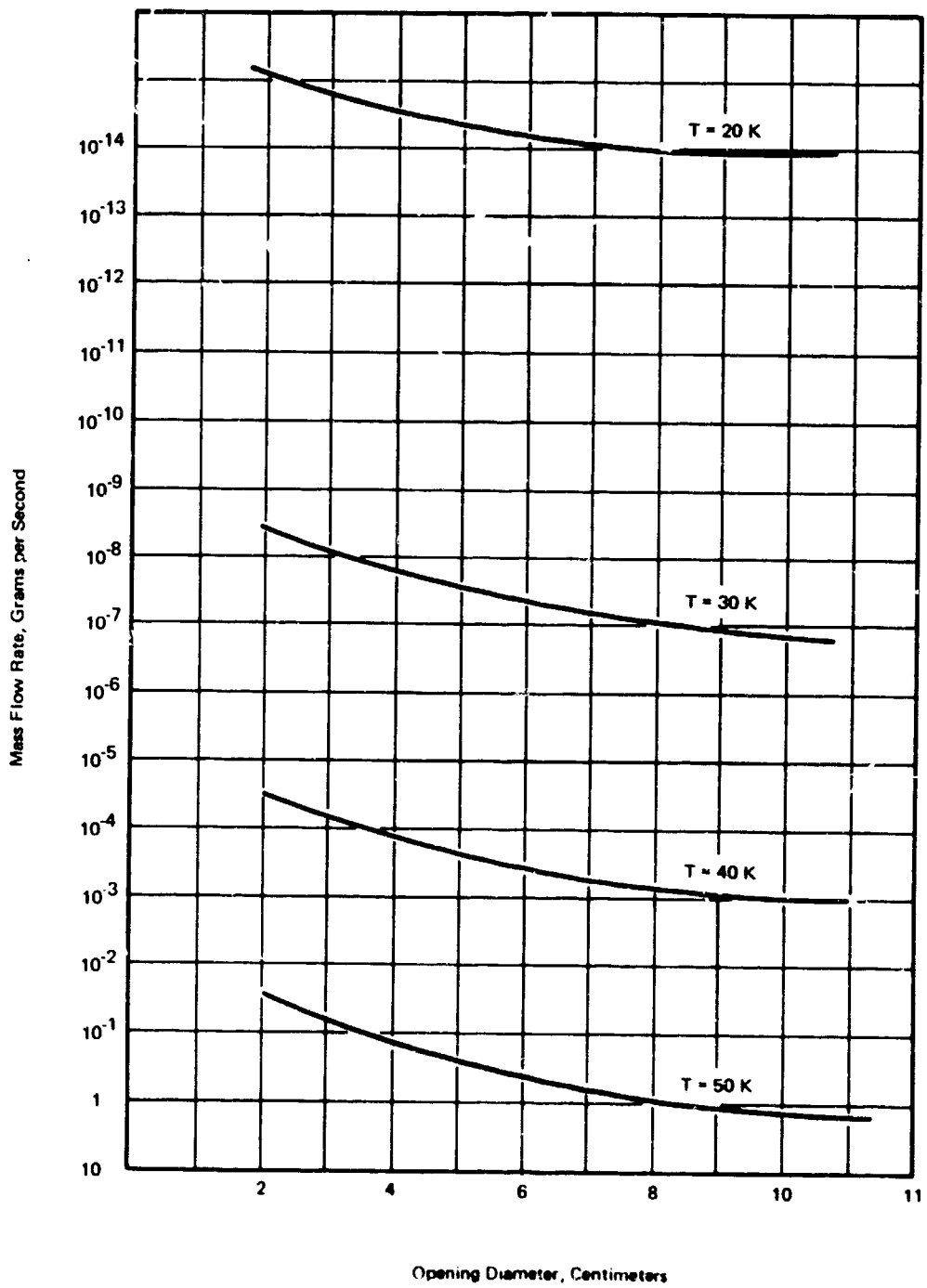


Figure 51. Flow Conductance of Subliming Oxygen Vapor, Zero Flow Length Assumed (Orifice)

During the phase transitions and melting of the solid, no loss of mass occurs. Since the solid has a greater density than liquid, some oxygen must be vented off before the oxygen is melted. For greatest storage effectiveness, this oxygen should be subliming to absorb heat leak thermal energy rather than allow it to be lost as a liquid. Therefore, sublimation will occur to some extent during long-term storage. The rate of sublimation in this case is only dictated by the heat leakage into the storage vessel, and generally, the rate will be very small. For example, the rate of oxygen sublimation from a 60-cm radius spherical storage tank with 6 cm of superinsulation at a solid temperature of 40 K will be 65 grams per day and will require 75 cm<sup>2</sup> of oxygen surface area. The surface area of the solid in this tank when 95% full is over 1000 cm<sup>2</sup>, and therefore the surface sublimation limitation will not apply. However, the flow conductance of the low-vapor-pressure vapor can be a limiting factor if the gas is to flow a long distance (see Dushman, 1962). If the subliming vapor is to be collected for use, then the vapor must be routed to a cryosorption pump; otherwise, it would be rejected directly to space. An indication of this flow resistance for subliming oxygen vapor is shown in figure 51. The conductance must be critically examined for any specific system design to assure satisfactory system operation during sublimation.

Long-term storage of oxygen can best be accomplished by starting with solid oxygen. The lower the initial temperature of the solid oxygen, the longer the storage life will be. The system design for long-term storage of oxygen will be simple, except where subliming vapors are to be recovered and in some cases where subliming vapors are rejected to space. The complications are encountered due to the low vapor pressures where the restrictions to sublimation and removal of the subliming vapors from the storage tank can become major factors in the system design, an alternate, though less effective, method can be used in which less solid oxygen is initially stored in the vessel and no sublimation of the solid occurs. In this case, all the heat leak into the vessel is absorbed as sensible heat, transition heat, and melting of the solid.

#### Systems for Extra-Vehicular Activity Supply

Certain future applications will require that a long-term storage system for oxygen be available and designed so that a certain mass of the oxygen can be removed for individual use for short periods of time. Extra-vehicular activity from space stations and search activities on the lunar surface are two possible applications. For these requirements, a solid storage system with a mechanical transport system would be of interest.

The oxygen stored in solid form under vacuum will provide long-term storage capability. If the oxygen is in the form of blocks, mechanical removal of blocks of oxygen from the vacuum storage system can be readily accomplished. This was demonstrated in the experimental work conducted in this program. The blocks of oxygen can be removed through an air-lock valve into capsules where they can be liquidified for breathing purposes.

The system for solid oxygen removal by mechanical methods will require a development study to determine the most effective way of accomplishing the task. The experimental work in this program demonstrated that this could be done simply by lifting the solid oxygen through an air-lock valve in a one-G field. Operation of the system under zero-G and during maneuvering of the vehicle will require a different approach. In any case, the air-lock valve is required to maintain vacuum conditions in the solid storage system during transfer.

The system of oxygen storage and transfer for extra-vehicular activity will consist of a simple storage system having an air-lock transfer system. The specific design of the heat transfer system can be established in a design and development program.

## SECTION V

### CONCLUSIONS

The analysis has shown that solid oxygen can substantially extend the storage time beyond that obtained under the subcritical and supercritical storage conditions. The benefits are great enough to seriously consider the use of solid oxygen storage for all space oxygen supply systems where long-term storage of oxygen is a requirement.

The use of solid oxygen in systems where the oxygen is continuously being used by crew members has only a small advantage over the use of subcritical oxygen. Some complications are added to the oxygen transfer system when solid oxygen is used since the oxygen vapor pressure must be raised to cabin pressure either by a cryosorption pump with vapor transport or by use of an airlock with solid mechanical transport. The benefit to be gained by solid oxygen in terms of longer mission duration does not appear to warrant the added complexity of the transfer system.

The benefit in extended storage time of solid can be of major importance in standby emergency systems or systems for extra-vehicular activity. The solid extended storage system combined with a mechanical transfer system to bring oxygen blocks through an airlock would provide a practical system for these requirements.

The following specific conclusions can also be made.

- . Solid oxygen transfer through an airlock to a high-pressure area can be accomplished with a mechanical transport system.
- . Transport of subliming oxygen vapors by cryosorption pump to a high-pressure area can be accomplished, but vapor flow restrictions can seriously limit the application to some systems.
- . Moving solid oxygen with a magnet using the paramagnetic properties of oxygen does not appear practical from the preliminary work done in this study.
- . The preparation of solid oxygen by using the cooling effect of solid nitrogen can only be done on a small scale by having good heat transfer between the nitrogen and the oxygen, low heat leak into the oxygen, and a good vacuum pump to reduce the vapor pressure over the oxygen to around 1 torr.

## SECTION VI

### RECOMMENDATIONS

On the basis of the work conducted in this program the following recommendations can be made:

- The long-term storage of solid oxygen is substantially better than for subcritical and supercritical liquid storage, and experimental tests should be conducted on a prototype storage system to substantiate the storage capabilities and to evaluate the system design requirements.

- Transport of solid oxygen from the vacuum storage area to a breathable state by mechanically transferring oxygen blocks through an air lock should be developed for future EVA and emergency oxygen supply requirements.

- Before consideration is given to the use of subliming oxygen vapor transport by cryosorption pumps, system studies should be made to assure that the low pressures of sublimation do not cause problems in system design to achieve adequate flow conductance. In addition, the cool-down characteristics of molecular sieve material must be improved to develop a practical cycle of operation.

- Design study of specific application requirements should be made to further define the suitability and benefits of using solid oxygen in the specific application in place of liquid oxygen.

## APPENDIX I

### ANALYSIS OF HEAT TRANSFER TO THE STORED OXYGEN

#### HEAT TRANSFER THROUGH THE INSULATION

The heat transfer through the insulation will be calculated assuming the temperatures and their gradients are steady (i.e., assuming that the temperature changes are slow). For the solid and subcritical storage methods, this assumption is valid; however, for the supercritical storage method, the fluid temperature in the container increases during the thermal pressurization. The  $C \frac{dT}{d\theta}$  (heat capacity) of the inner container and insulation for the supercritical storage method will be neglected. The magnitude of this term can be checked once a usage rate (number of men) has been established for a given size container.

The temperature of the inner container,  $T_i$ , will be assumed to be equal to the temperature of the stored oxygen. The temperature of the outer container,  $T_o$ , will be assumed to be equal to the ambient temperature, 298K.

#### Flexible Multilayer Type of Insulation

The heat transfer through a layer of insulation in the form of a spherical shell is given by

$$Q_{INS} = \frac{4\pi k_{ins} (T_o - T_i)}{\frac{1}{r_i + t} - \frac{1}{r_o}} \quad (1)$$

where

$Q_{INS}$  = Heat transfer into the oxygen by way of the flexible multilayer insulation, watts

$k_{ins}$  = Thermal conductivity of the insulation, w/cm K

$r_i$  = Inside radius of the inner container, cm

$t$  = Wall thickness of the inner container, cm

- $r_o$  = Inside radius of the outer container, cm  
 $T_i$  = Temperature of the inner container, K  
 $T_o$  = Temperature of the outer container, K

Figure 52 shows the geometry used in defining the parameters of equation (1).

The inner container wall thickness is given by

$$t = \frac{f P_i r_i}{2 S_y} \quad (2)$$

where

- $f$  = Safety factor  
 $P_i$  = Internal pressure  
 $S_y$  = Yield stress

for the solid  $O_2$  and subcritical  $O_2$  storage and by

$$t = r_i \left[ \sqrt{1 + \frac{f P_i}{S} - 1} \right] \quad (3)$$

for the supercritical  $O_2$  (higher pressure) storage. (see Appendix IV, Analysis of Weights for Oxygen Storage Systems).

The insulation thermal conductivity is a function of the temperature on each side. The ambient temperature will be assumed to be 298 K, which will also be  $T_o$ . The oxygen temperature (and  $T_i$ ) will depend upon the method of oxygen storage.

Solid  $O_2$ : 12 K to 54.36 K

Subcritical  $O_2$ : 90.18 K (1 atm)

Supercritical  $O_2$ : 104.2 K (55 atm; initially 95% full of liquid at 1 atm) initially and increasing with time (or amount of fluid remaining as shown in Appendix IV)

The laboratory measured thermal conductivity on flat samples is approximately  $0.173 \times 10^{-6}$  w/cm-K for temperatures at 77 K and 300 K. For the insulation applied to a spherical container with overlapping and penetrations, the value is approximately twice that of the laboratory value:  $0.35 \times 10^{-6}$  w/cm-K. Using a temperature variation for the thermal conductivity given by Wang (1961), the relation to be used for this analysis is

$$\bar{k}(T_1, T_2) = \left[ 0.0374 \left( \frac{T_1 + T_2}{100} \right) + 0.0059 \left( \frac{T_1 + T_2}{100} \right) \left( \frac{T_1^2 + T_2^2}{100^2} \right) \right] \times 10^{-6} \text{ w/cm-K} \quad (4)$$

For  $T_1 = 77$  K and  $T_2 = 298$  K,

$$\frac{T_1 + T_2}{100} = 3.75; \quad \left( \frac{T_1}{100} \right)^2 + \left( \frac{T_2}{100} \right)^2 = 9.475$$

$$\bar{k}(77, 298) = 10^{-6} (0.1403 + 0.2097) = 0.35 \times 10^{-6} \text{ w/cm-K}$$

At  $T_1 = T_2 = 298$  K

$$\frac{T_1 + T_2}{100} = 5.96; \quad \left( \frac{T_1}{100} \right)^2 + \left( \frac{T_2}{100} \right)^2 = 17.764$$

$$\bar{k}(298, 298) = 10^{-6} (0.223 + 0.625) = 0.848 \times 10^{-6} \text{ w/cm-K}$$

Multiplying Equation (4) by  $(T_1 - T_2)$  gives

$$\bar{k} \Delta T = \left\{ 0.0374 \left[ \left( \frac{T_1}{100} \right)^2 - \left( \frac{T_2}{100} \right)^2 \right] + 0.0059 \left[ \left( \frac{T_1}{100} \right)^4 - \left( \frac{T_2}{100} \right)^4 \right] \right\} \times 10^{-4} \text{ (w/cm)} \quad (5)$$

For  $T_1 = 298$  K

$$(T_1/100)^2 = 8.8804 \text{ K}^2$$

$$(T_1/100)^4 = 78.8615 \text{ K}^4$$

So that

$$\bar{k}(T, 298)(298-T) = \left[ 7.9741 - 0.374 \left( \frac{T}{100} \right)^2 - 0.059 \left( \frac{T}{100} \right)^4 \right] x \cdot 10^{-5} \text{ w/cm} \quad (6)$$

The results of equation (6) for T from 0 K to 298 K are shown plotted in figure 53. The parameter

$$(298 - T) \bar{k}(T, 298)$$

will be used in place of  $k_{ins} (T_o - T_i)$  in equation (1) for computing the heat transfer through the insulation.

#### Rigid-Radiation-Shield Insulation

The rigid radiation shields (shown in figure 52) will have a spacing of  $x$  cm. Each shield will be made of aluminum which is vacuum-deposited with gold. Thus, each surface will have a low emittance and high reflection. The use of "vapor-cooled" shields\* will not be considered in this study. Since the temperature range under consideration in this analysis is from ambient (298 K) down to cryogenic temperatures (100 K and lower) and the emissivity of vacuum-deposited gold varies considerably with temperature (see figure 54), the radiation exchange factor for two closely spaced surfaces (shields)

$$F_{ij} = \frac{1}{\frac{1}{\epsilon_i} + \frac{1}{\epsilon_j} - 1} \quad (7)$$

---

\*Vapor-cooled shields are where the vent tubing for the cryogen vapors is coiled around each shield and the exhaust vapors cool part of the incoming heat.

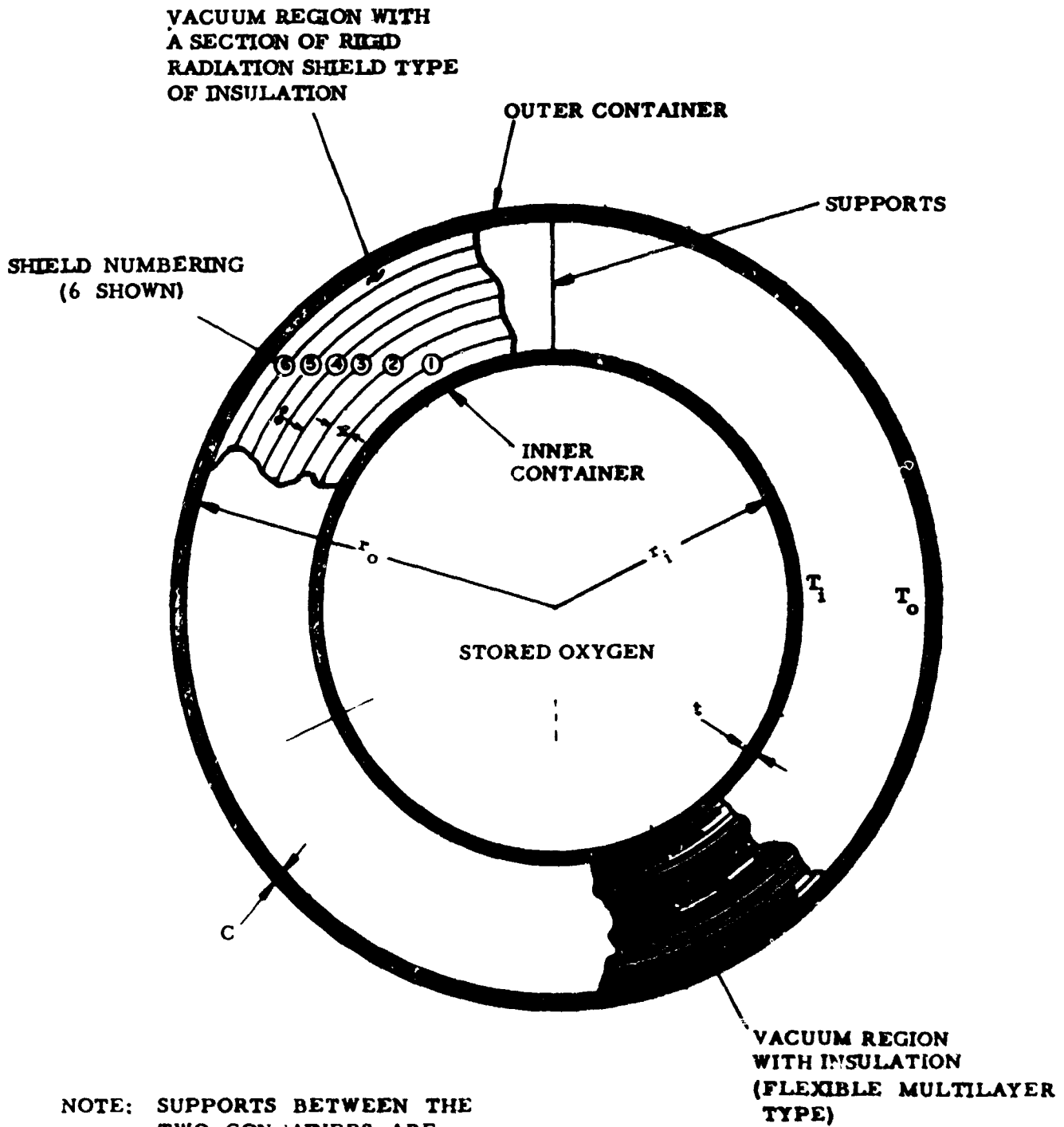


Figure 52. Cross-Section View of Oxygen Container Illustrating Insulation Shielding Geometry

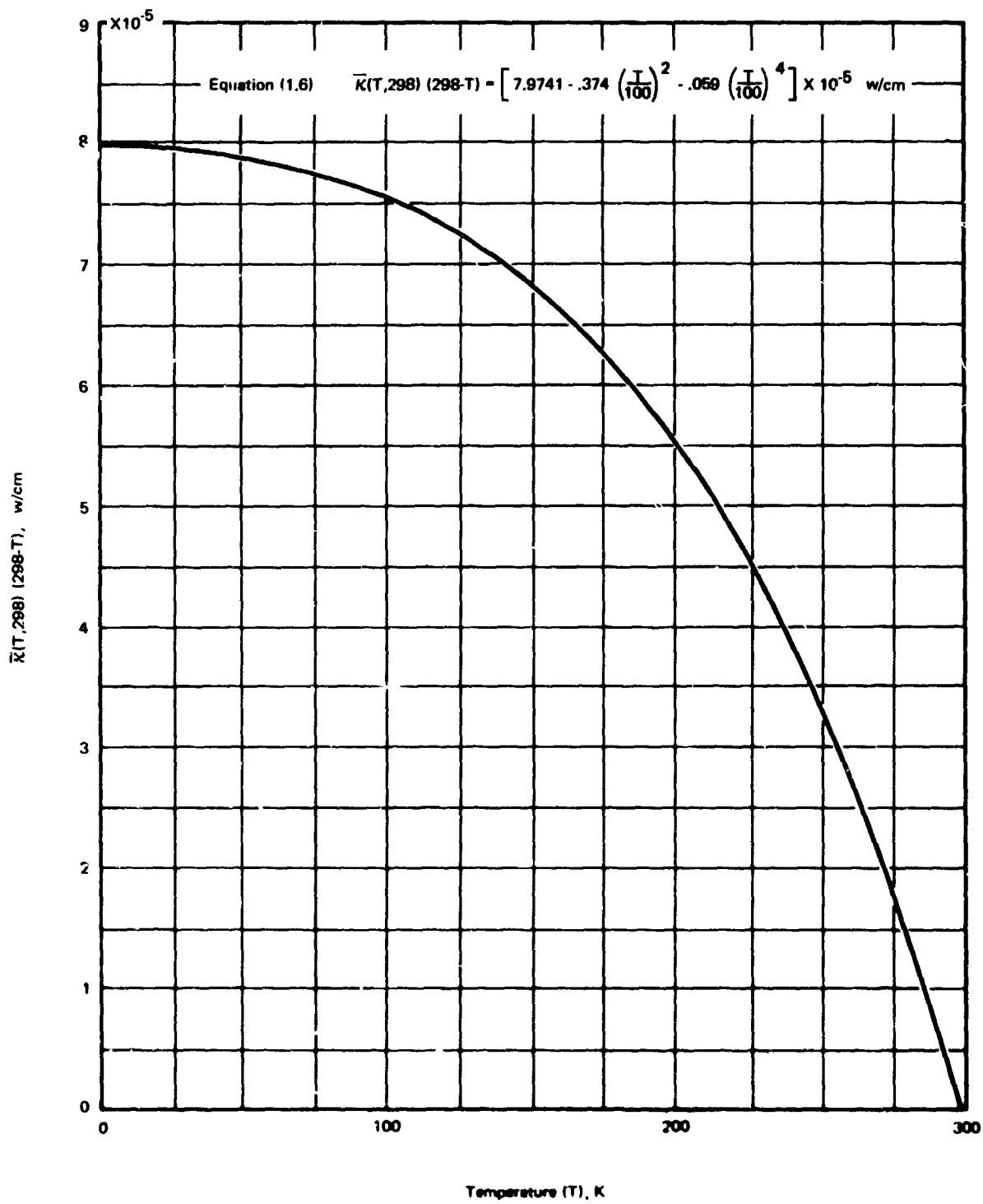


Figure 53. Flexible Multilayer Thermal Conduction Parameter  $\bar{\kappa}(T, 298) (298-T)$

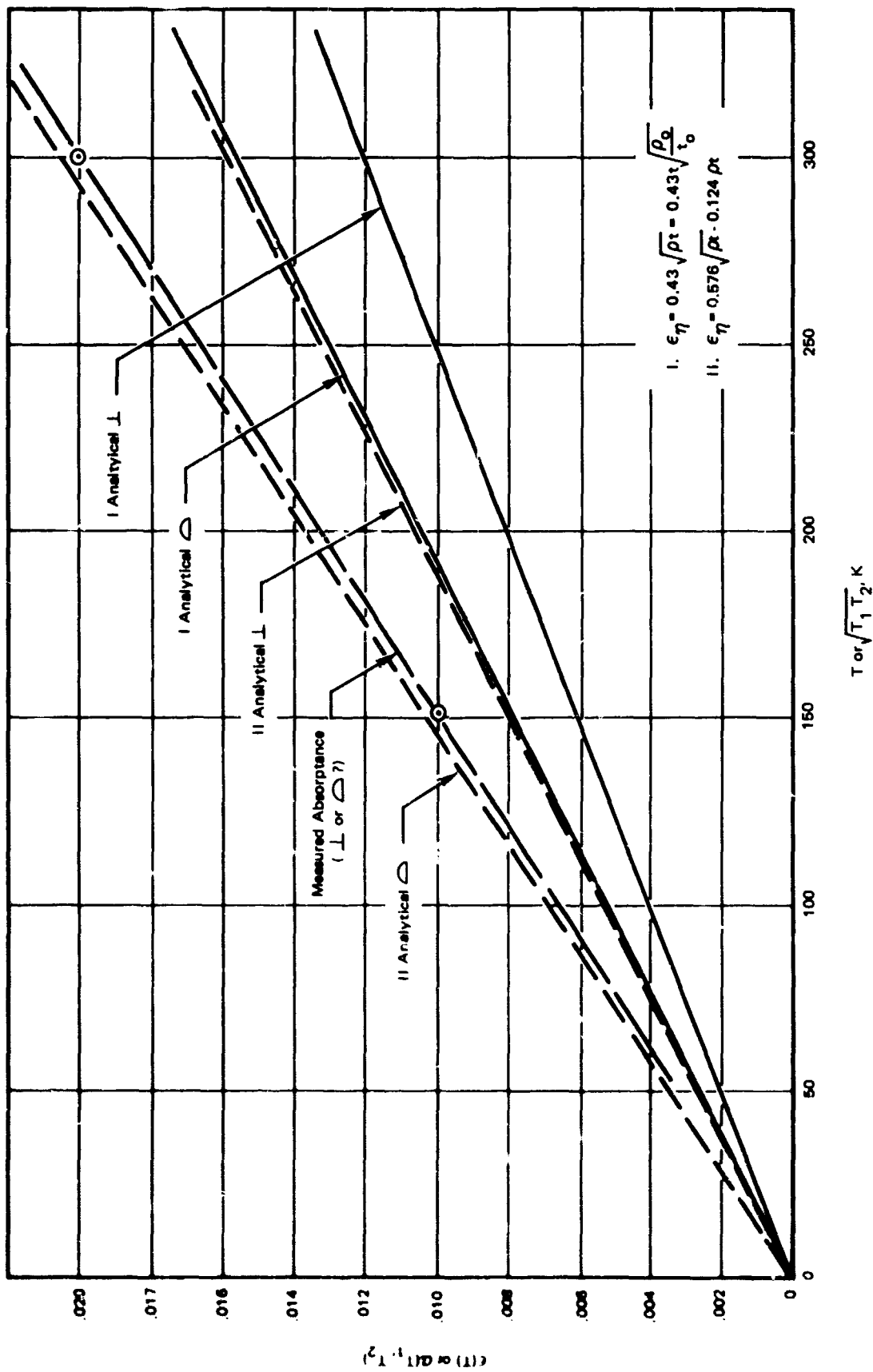


Figure 54. Hemispherical and Normal Emittance and Absorbance of Gold  
(Multiply by 1.3 to Obtain Hemispherical Values)

is not strictly valid (in this equation,  $\epsilon_i$  and  $\epsilon_j$  represent the emissivity of surfaces i and j respectively). However, for energy at any wavelength  $\lambda$ , the relation holds (see Eckert and Drake, 1959, pp. 403-404) such that

$$q_\lambda = \frac{E_{b\lambda i} - E_{b\lambda j}}{\frac{1}{\epsilon_{\lambda i}} + \frac{1}{\epsilon_{\lambda j}} - 1} \quad (8)$$

where

$q_\lambda$  = Heat flux transferred from surface i to surface j per unit increment of wavelength,  $w/cm^2 - \mu$   
 $E_{b\lambda i}, E_{b\lambda j}$  = Planck's blackbody radiation function with temperatures of surfaces i and j, respectively

$$E_{b\lambda i} = \frac{c_1 \lambda^{-5}}{e^{\frac{c_2}{\lambda T_i}} - 1} \quad (9)$$

$\epsilon_{\lambda i}$  = Emissivity of surface i at the wavelength  $\lambda$   
 $\epsilon_{\lambda j}$  = Emissivity of surface j at the wavelength  $\lambda$

The total heat transfer ( $q_T$ ) per unit surface area is given by summing equation (8) over all wavelengths as indicated below:

$$q_T = \int_0^\infty q_\lambda d\lambda$$

or

$$q_T = \int_0^\infty \frac{E_{b\lambda i} - E_{b\lambda j}}{\frac{1}{\epsilon_{\lambda i}} + \frac{1}{\epsilon_{\lambda j}} - 1} d\lambda \quad (10)$$

Multiplying the right side of equation (10) by  $\epsilon_{\lambda i} \epsilon_{\lambda j} / \epsilon_{\lambda i} \epsilon_{\lambda j} = 1$  gives

$$q_T = \int_0^{\infty} \frac{\epsilon_{\lambda i} \epsilon_{\lambda j}}{\epsilon_{\lambda i} + \epsilon_{\lambda j} - \epsilon_{\lambda i} \epsilon_{\lambda j}} (E_{b \lambda i} - E_{b \lambda j}) d\lambda \quad (11)$$

as a general relation.

In the problem with the vacuum deposited gold shields,  $\epsilon_{\lambda} \ll 1$  ( $\epsilon_{\lambda} \approx 0.02$ ), and  $\epsilon_{\lambda i} \epsilon_{\lambda j}$  can be neglected in comparison with  $\epsilon_{\lambda i} + \epsilon_{\lambda j}$ . Also with the gold finish, a type Hagen-Rubens equation (Dunkle, 1963) which is modified to give the total hemispherical emissivity and fit experimental data of figure 54.

$$\epsilon_{\lambda i} = k_r \left( \frac{\rho_i}{\lambda} \right)^{\frac{1}{2}} \quad (12a)$$

$$\epsilon_{\lambda j} = k_r \left( \frac{\rho_j}{\lambda} \right)^{\frac{1}{2}} \quad (12b)$$

where

$$k_r = \text{A constant, } 62.8 (\mu)^{\frac{1}{2}} \text{-ohm}^{\frac{1}{2}} \text{-cm}^{\frac{1}{2}}$$

$$\rho_i = \text{Electrical resistivity of surface } i$$

$$\rho_j = \text{Electrical resistivity of surface } j$$

$$\lambda = \text{Wavelength}$$

Then substituting equations (12a) and (12b) into equation (11) and defining  $\mathcal{F}_{\lambda}$ :

$$\mathcal{F}_{\lambda} = \frac{\epsilon_{\lambda i} \epsilon_{\lambda j}}{\epsilon_{\lambda i} + \epsilon_{\lambda j}} = \frac{k_r \sqrt{\rho_i \rho_j} \lambda^{-\frac{1}{2}}}{\sqrt{\rho_i} + \sqrt{\rho_j}} \quad (\text{approximate, small } \epsilon_{\lambda}) \quad (13)$$

and defining  $\bar{F}_i$  and  $F_j$ :

$$\bar{F}_i = \frac{1}{\sigma_{T_j^4}} \int_0^{\infty} F_{\lambda} E_{b\lambda_i} d\lambda$$

and

$$\bar{F}_j = \frac{1}{\sigma_{T_j^4}} \int_0^{\infty} F_{\lambda} E_{b\lambda_j} d\lambda$$

gives

$$q_T = \bar{F}_i E_{bi} - \bar{F}_j E_{bj}$$

For the approximate  $F_{\lambda}$  in equation (13)

$$\bar{F}_i = \frac{k T_i^{\frac{1}{2}} \sqrt{\rho_i \rho_j}}{\sqrt{\rho_i} + \sqrt{\rho_j}} \int_0^{\infty} \frac{(T_i \lambda)^{-2}}{\sigma} \frac{c_1 (\lambda T_i)^{-5} d\lambda T_i}{e^{\frac{c_2}{\lambda T_i} - 1}}$$

$$\bar{F}_i = \frac{k_r T_i^{\frac{1}{2}} \sqrt{\rho_i \rho_j}}{\sqrt{\rho_i} + \sqrt{\rho_j}} \quad (14)$$

where

$$k_r = c_1 \frac{k_r}{\sigma} \int_0^{\infty} (\lambda T_i)^{-\frac{11}{2}} \frac{d\lambda T_i}{e^{\frac{c_2}{\lambda T_i} - 1}} = 0.740 \left\{ \begin{array}{l} \text{hemispherical} \\ \text{measurement} \\ \text{corrected for} \\ \text{gold} \end{array} \right.$$

For gold (and most pure metals) below approximately 300 to 400 K, the electrical resistivity is linear with temperature.

$$\rho = \frac{\rho_0}{T_0} T \begin{cases} \rho_0 \text{ in ohm-cm} \\ T \text{ in K} \end{cases}$$

Using this relation in equation (14) gives

$$\begin{aligned} \bar{F} &= \frac{K_r \sqrt{T_i} \sqrt{T_i T_j} \left( \frac{\rho_0}{T_0} \right)}{\sqrt{\frac{\rho_0}{T_c}} (\sqrt{T_i} + \sqrt{T_j})} \\ &= 0.74 \sqrt{\frac{\rho_c}{T_c}} \frac{\sqrt{T_i T_i T_j}}{\sqrt{T_i} + \sqrt{T_j}} \end{aligned}$$

Then for both i and j

$$\bar{F}_i = 0.74 \sqrt{\frac{\rho_0}{T_0}} \left[ \frac{T_i}{-\sqrt{\frac{T_i}{T_j} + 1}} \right]; \quad \bar{F}_j = 0.74 \sqrt{\frac{\rho_0}{T_0}} \left[ \frac{T_j}{\sqrt{\frac{T_j}{T_i} + 1}} \right]$$

Note that

$$F_j = \frac{\sqrt{T_j}}{\sqrt{T_i}} F_i \quad \text{or} \quad \frac{F_j}{\sqrt{T_j}} = \frac{F_i}{\sqrt{T_i}}$$

Then

$$q_T = 0.74 \sqrt{\frac{\rho_0}{T_0}} \frac{T_i T_j}{\sqrt{T_i} \sqrt{T_j}} \left[ \sqrt{T_i} (\sigma T_i^4) - \sqrt{T_j} (\sigma T_j^4) \right] \quad (15)$$

Equation (15) can be written as

$$q_T = \frac{\alpha_{ij}}{\sqrt{T_i} + \sqrt{T_j}} \left[ \sqrt{T_i} (\sigma T_i^4) - \sqrt{T_j} (\sigma T_j^4) \right] \quad (16)$$

where  $\alpha_{ij}$  is the absorptivity of a surface at temperature  $T_i$  of energy from a radiating source at temperature  $T_j$  (or vice versa). Both surfaces radiate according to the Hagen-Rubens's Equation and  $\rho = \frac{\rho_0}{T_0} T$ . Using Kirchhoff's law and equation (12a)

$$\alpha_{\lambda ij} = \epsilon_{\lambda i} = k_r \left[ \frac{\rho_i}{\lambda} \right]^{\frac{1}{2}}$$

where  $\alpha_{\lambda ij}$  is the spectral variation of  $\alpha_{ij}$ . By definition,

$$\begin{aligned} \alpha_{ij} &= \int_0^{\infty} \alpha_{\lambda ij} \epsilon_{\lambda j} d\lambda = \int_0^{\infty} \frac{k_r}{\sigma} \left( \frac{\rho_i}{\lambda} \right)^{\frac{1}{2}} \frac{c_1 (\lambda T_j)^{-5}}{e^{c_2/\lambda T_j - 1}} d\lambda T_j \\ &= \frac{k_r}{\sigma} \sqrt{\frac{\rho_0}{T_0}} \sqrt{T_i T_j} \int_0^{\infty} (\lambda T_j)^{-1\frac{1}{2}} \frac{d\lambda T_j}{e^{c_2/\lambda T_j - 1}} \end{aligned}$$

or

$$\alpha_{ij} = k_r \sqrt{\frac{\rho_0}{T_0}} \sqrt{T_i T_j} = 0.74 \sqrt{\frac{\rho_0}{T_0}} \sqrt{T_i T_j}$$

A similar analysis shows  $\epsilon_i = 0.74 \sqrt{\rho_0/T_0} T_i$ . . . Thus, when  $T_i = T_j$ ,  $\epsilon_i = \alpha_{ij}$  satisfying Kirchhoff's law for equilibrium.

Several sources of emissivity and absorptivity data for gold are plotted as a function of temperature from 0 to 300 K in figure 54. The data for the measured absorptance was used in equation (16) for the solution of the shield temperatures and the heat transfer by radiation through the shields to the oxygen.

$$\alpha_{ij} = \left( \frac{0.02}{300} \right) \sqrt{T_i T_j} = 0.667 \cdot 10^{-4} \sqrt{T_i T_j}$$

Equation (16) applies to any two adjacent shields and  $q_T$  must be the same between each pair of adjacent shields. Likewise, the same must be true between either container (also assumed to be gold coated) to its adjacent shield. This condition is true for the assumption of negligible heat conduction through insulation stand-offs as in the present analysis.

$$q_{ij} = q_T \quad (17)$$

and equation (16) with  $\alpha_{ij} = 0.667 \cdot 10^{-4} \sqrt{T_i T_j}$  becomes

$$q_{ij} = 0.667 \cdot 10^{-4} \frac{\sqrt{T_i T_j}}{\sqrt{T_i} + \sqrt{T_j}} \left[ \sigma_{T_i}^{4.5} - \sigma_{T_j}^{4.5} \right] \quad (18)$$

$$Q_{ij} = A_j q_{ij}, \quad A_j = 4\pi R_j^2 \quad (19)$$

where  $Q_{ij}$  is the heat transfer through the total area of the  $j^{\text{th}}$  shield, watts

$A_j$  is the area of the  $j^{\text{th}}$  shield,  $\text{cm}^2$

$R_j$  is the radius of the  $j^{\text{th}}$  shield, cm

and  $R_j$  is given by

$$R_j = r_i + t + jx$$

where

$r_1$  = the inside radius of the inner container, cm

$t$  = the thickness of the inner container, cm

$j$  = the  $j^{\text{th}}$  shield from the inner container

$x$  = the shield spacing, cm

Equations (17), (18), and (19) were programmed on the IBM 360 digital computer for numerical solution by successive iterations on the shield temperatures with the inner container temperature equal to the stored oxygen temperature and the outer container temperature fixed at the ambient temperature of 298 K. Once the temperatures have converged (in the computer program), the program compares the radiant heat transfer through the shields. Solutions were run for 0, 1, 2, 3, 4, and 5 shields (N) and varying  $r_1$  from 5 cm to 125 cm. The case of  $N = 0$ , iteration is not necessary, and the heat transfer can be calculated immediately from equation (16) similar to the following:

In equation (16) with  $i = 1$  and  $j = 2$

$$q_{12} = \frac{\alpha_{12}}{\sqrt{T_1} + \sqrt{T_2}} \left[ T_1^{4.5} - T_2^{4.5} \right]$$

Use  $T_1 = 300$  K, then  $T_1^4 = 0.0459$  w/cm<sup>2</sup>

and  $T_2 = 77$  K, then  $T_2^4 = 0.0002$  w/cm<sup>2</sup>

$$\sqrt{T_1 T_2} = 152 \text{ K}$$

$$\alpha_{12} = 0.667(10^{-4}) \sqrt{T_1 T_2}$$

or from data on figure 54

$$\alpha_{1,2} = 0.010$$

$$\frac{\sqrt{T_1}}{\sqrt{T_1} + \sqrt{T_2}} = \frac{17.32}{17.32 + 8.95} = \frac{17.32}{26.27} = 0.659$$

$$\frac{\sqrt{T_2}}{\sqrt{T_1} + \sqrt{T_2}} = \frac{8.95}{17.32 + 8.95} = \frac{8.95}{26.27} = 0.330$$

$$q_T = 0.0100 \left[ 0.659(0.0459) - 0.330(0.0002) \right] = 2.93 \times 10^{-4} \text{ w/cm}^2$$

The results of this analysis, equations (15) or (16) are very similar to and are substantiated by work presented by Rolling and Tien (1967) and Tien and Gravalho (1967) on thermal radiation between non-gray metallic surfaces at low temperatures.

#### HEAT TRANSFER THROUGH THE SUPPORTS

The heat conducted to the stored oxygen through the supports between the inner and outer containers is a function of the number of supports (four), cross-sectional area of the supports (Appendix IV) length of each support, and the thermal conductivity of the support material.

The support material will be a titanium alloy such as Type 4Al-4Mn. The thermal conductivity of this type of titanium is shown in figure 55 as a function temperature. The heat conducted through the four supports is

$$q_S = 4 \frac{A_S}{L_S} \int_{T_1}^{T_0} k(T) dT \quad (20)$$

where  $L_S$  and  $A_S$  are the support length and cross-section area, respectively. Defining the average thermal conductivity as

$$\bar{k}(T_i, T_o) = \frac{1}{T_o - T_i} \int_{T_i}^{T_o} k(T) dT \quad (21)$$

where  $k(T)$  is the thermal conductivity at temperature  $T$ ,

$$q_S = 4 \frac{A_S (T_o - T_i)}{L_S} \bar{k}(T_i, T_o) \quad (22)$$

For all the different oxygen storage methods,  $T_o$  will be 298 K;  $T_i$  will vary with the type of storage.

The support cross-section area is, from Appendix IV, equation (99),

$$A_S = \frac{f W_T a}{S_y} \quad (23)$$

where

$W_T$  = Initial total support weight (mass), grams

$a$  = G-loading (10 to 50  $\sqrt{3}$ ), G

$S_y$  = Titanium yield strength, grams/cm<sup>2</sup>

$f$  = Safety factor

The four supports shown in figure 52 are radial, high-strength, titanium alloy wires which extend from the inner container through the outer container to the corners of an imaginary tetrahedron circumscribing the outer container. Rigid tubes would extend the vacuum jacket from the container to the end of the supports and simultaneously act as legs for the whole container. It was necessary to make the supports long in order to reduce the heat transfer to the order of magnitude of that through the insulation. However, for some missions where the oxygen usage rate is high, shorter supports and higher heat loads can be tolerated. When the oxygen is to be stored for extended periods of time before usage, a minimum total heat load is required. For the support configuration selected, the supports extend outside the outer container a distance of  $2r_o$ ; thus the total support length is given by

$$L_S = 3r_o - r_i - t \quad (24)$$

where

$r_o$  = Inside radius of the outer container, cm

$r_i$  = Inside radius of the inner container, cm

$t$  = Wall thickness of the inner container, cm

The total weight is

$$W_T = W_{O_2} + W_{IC} + W_{INS} \quad (25)$$

where

$W_{O_2}$  = Stored oxygen weight, grams

$W_{IC}$  = Inner container weight, grams

$W_{INS}$  = Insulation weight, grams

For subcritical storage, the weight of the phase separator must also be included in equation (25).

The thermal conductivity and average thermal conductivity between a variable low temperature and 300 K upper temperature are shown plotted in figure 55. The dashed curve  $\bar{k}(T,300)$  will be used in equation (22) for computing the heat conduction through the supports. For a high temperature of 298 K

$$\begin{aligned} (T - 298) \bar{k}(T,298) &= (T - 300) \bar{k}(T,300) - (300 - 298) \bar{k}(298,300) \\ &= (T - 300) \bar{k}(T,300) - 0.1754 \end{aligned}$$

where

$$\bar{k}(T,298) = \frac{1}{298 - T} \int_T^{298} k(T) dT$$

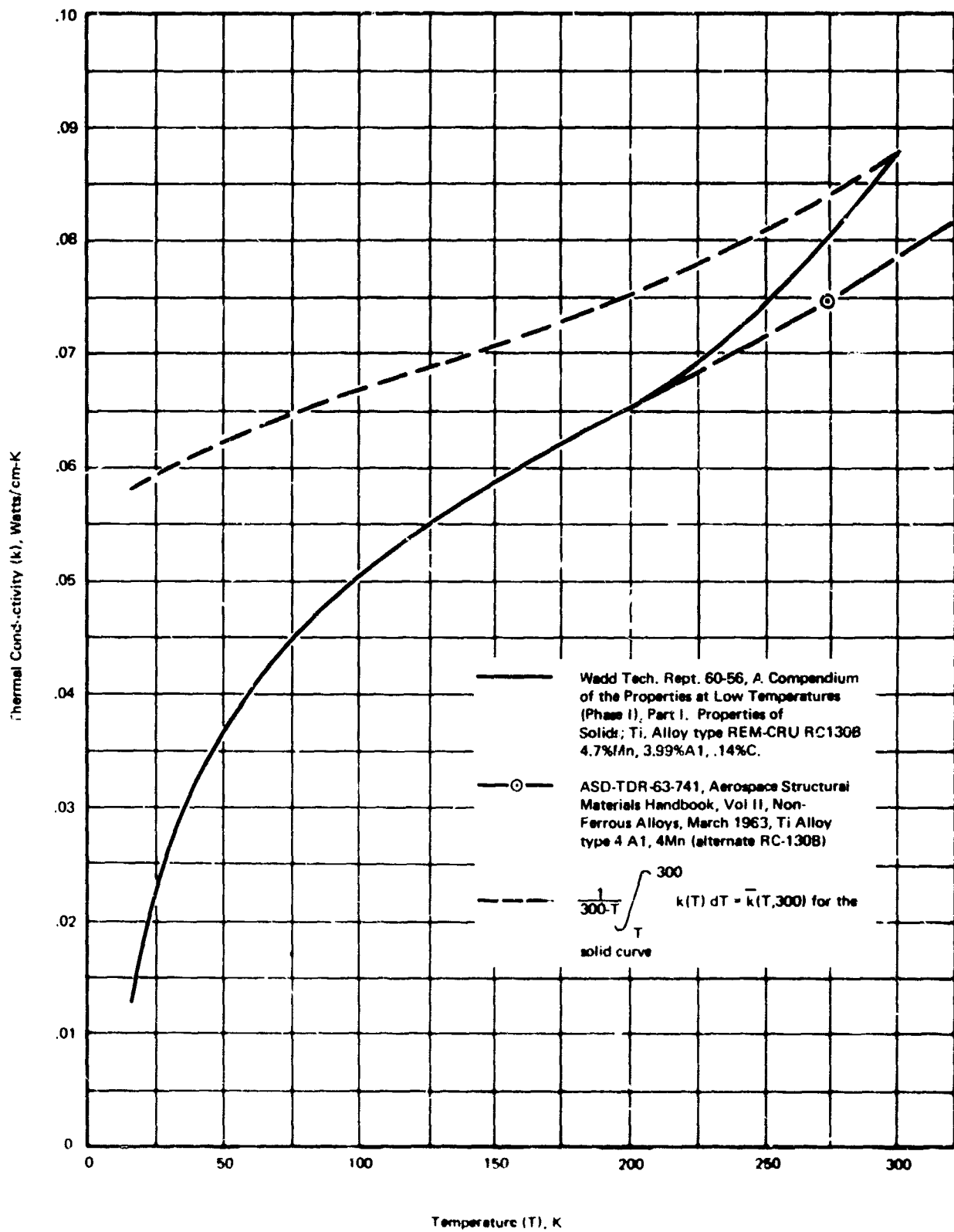


Figure 55. Thermal Conductivity of Titanium Alloy vs Temperature  
Type 4AL 4MN

RESIDUAL-GAS HEAT CONDUCTION (in the rigid radiation shields)

The magnitude of the residual gas conduction is usually very low in a high vacuum; however, a check calculation will be made to compare with the other modes (multilayer insulation). Vance and Duke, (1962, pp. 154 - 156) present the equation for residual gas heat conduction between two surfaces in a vacuum as

$$W_{gc} = K\alpha P (T_2 - T_1) \quad (26)$$

Where

$W_{gc}$  = Net energy transfer per unit time per unit area of inner container surface, w/cm<sup>2</sup>

$K = \frac{\gamma + 1}{\gamma - 1} \frac{R}{8\pi MT} = 0.0159 \text{ w/cm}^2\text{-mm of Hg-K for P measured at 300 K, N}_2 \text{ gas}$

$R$  = Universal gas constant

$M$  = Molecular weight of the gas

$T$  = Temperature of the gas

$\gamma$  = Ratio of specific heats, cp/cv

$P$  = Pressure, mm of Hg

$\alpha = \text{Overall accommodation coefficient} = \frac{\alpha_1 \alpha_2}{\alpha_2 + \alpha_1(1 - \alpha_2)A_1/A_2}$

$A$  = Area

Subscripts 1 and 2 refer to the inner and outer surfaces, respectively.

For the present configuration and for no shields

$$A_1 \approx A_2$$

and from Vance and Duke (1962, p 156)

$$\alpha_2 = 0.85, \alpha_1 = 1.0, \text{ for } T_2 = 300 \text{ K}, T_1 = 77 \text{ K}.$$

The temperature difference is

$$T_2 - T_1 = 300 - 77 = 223 \text{ K}.$$

$$\alpha = \frac{0.85}{1.0} = 0.85$$

$$W_{gc} = 0.0159 (0.85) P (223) = 3.01 P$$

$P$ mm-Hg	$W_{gc}$ w/cm <sup>2</sup>
$10^{-5}$	$3.01 \times 10^{-5}$
$10^{-6}$	$0.301 \times 10^{-5}$
$10^{-7}$	$0.0301 \times 10^{-5}$

Comparing the residual gas conduction with radiation where there are no shields but the inner and outer container have a low emissivity,

$$\epsilon_1 = \epsilon_2 = 0.015 \text{ (average)}$$

$$T_1 = 77 \text{ K}, T_2 = 300 \text{ K}$$

$$\frac{q_r}{A} = \sqrt{F_{1-2}} \sigma (T_2^4 - T_1^4)$$

$$F_{1-2} = \frac{\epsilon_1 \epsilon_2}{\epsilon_2 + (1 - \epsilon_2) \epsilon_1} = \frac{(0.015)^2}{0.015 + 0.015 (0.985)} = \frac{0.015}{1.985}$$

$$= 0.00756$$

$$T_2 = 300 \text{ K}, \sigma T_2^4 = 0.0459 \text{ w/cm}^2$$

$$T_1 = 77 \text{ K}, \sigma T_1^4 = 0.0002 \text{ w/cm}^2$$

$$\sigma (T_2^4 - T_1^4) = 0.0457 \text{ w/cm}^2$$

$$\frac{q_r}{A} = 0.00756 (0.0457) \times 10^{-5}$$

$$= 34.5 \times 10^{-5} \text{ w/cm}^2$$

at  $P = 10^{-4}$  mm of Hg,  $W_{gc}$  is 90% of  $q_r/A$

at  $P = 10^{-5}$  mm of Hg,  $W_{gc}$  is 9% of  $q_r/A$

at  $P = 10^{-6}$  mm of Hg,  $W_{gc}$  is 0.9% of  $q_r/A$

For  $N$  shields:

Assuming,  $W_{gc} = h_{gc} \Delta T$ ,  $\Delta T$  = temperature differential between any two shields are  $h_{gc}$  changes negligibly with temperature,

then

$$W_{gc} = \frac{h_{gc}}{N + 1} (T_2 - T_1)$$

where  $T_2 - T_1$  is the overall temperature difference.

Assuming that the emissivity changes are negligible with temperature of shields, the radiant energy decreases by a factor of  $1/(N + 1)$ . Thus, both radiant energy transfer and residual gas conduction decrease at the same rate as the number of shields is increased.

Looking at the shields on the cold side for the case of many shields,  $P = 10^{-6}$  mm-Hg and  $KP = \text{constant}$  (see Scott, 1959, pp. 145 - 147), conduction by the residual of gas is

$$\left[ \frac{w_{RC}}{\Delta T} \right] = 1.0 (0.0159) (10^{-6}) \quad (\alpha = 1.0)$$

$$= 0.159 \times 10^{-7} \text{ w/cm}^2\text{-K}$$

The radiation between assumed shield temperatures of 77 K and 100 K with surface properties of  $\epsilon_1, \epsilon_2 = 0.006$ ,  $\mathcal{F}_{1-2} = \frac{(0.006)^2}{0.006 + 0.006 (0.995)} = \frac{0.006}{1.99} = 0.00301$ , is (using the linearized radiation equation):

$$\frac{q_r}{A \Delta T} = \mathcal{F}_{1-2} (4\sigma T^3)$$

$$= 4(0.00301) (5.669 \times 10^{-12}) (88)^3$$

$$= 0.466 \times 10^{-7} \text{ w/cm}^2\text{-K}$$

Thus: Radiation is 3 times the residual gas conduction at a pressure of  $10^{-6}$  torr

Radiation is 30 times the residual gas conduction at a pressure of  $10^{-7}$  torr

For the rigid radiation shield insulation, the pressure in the vacuum region will be assumed to be  $10^{-7}$  torr and the residual gas conduction will be neglected.

#### TOTAL HEAT TRANSFER TO THE STORED OXYGEN

The total heat transfer to the stored oxygen ( $Q_{tot}$ ) is given by

$$Q_{tot} = Q_{ins} + Q_s \quad (27)$$

for the flexible multilayer insulation. For the rigid shield insulation, the total heat transfer is given by

$$Q_{tc+} = Q_T + Q_s \quad (28)$$

The component heat transfer relations given in Sections I and II and in equations (27) and (28) were programmed for solution on the IBM 350 digital computer with the storage container size, insulation parameters and support parameters as variables. Results are presented in figures 56 through 59.

Figures 56 and 57 present the total heat transfer (through the insulation and supports) as a function of inner container radius for solid and liquid, respectively. Also shown in figure 56 is the heat transfer with rigid radiation shields with vacuum deposited gold; the results are of the same order of magnitude as with flexible multilayer insulation. The total heat transfer into supercritical oxygen as a function of inner container radius is presented in figures 58 and 59. Figure 58 illustrates the heat transfer to the oxygen at its initial temperature of 104.2 K. Figure 59 presents the same data when the oxygen is at a temperature of 158 K. This latter temperature corresponds to the condition at which minimum heat transfer is required to deliver a constant flow rate,  $\dot{m}$ . This phenomena of a reduction in heat input requirements is due primarily to the reduction in the specific heat capacity of oxygen near the critical point of the material. (See figure 60 and figure 61 of Appendix II, Heating Requirements for Oxygen Delivery.)

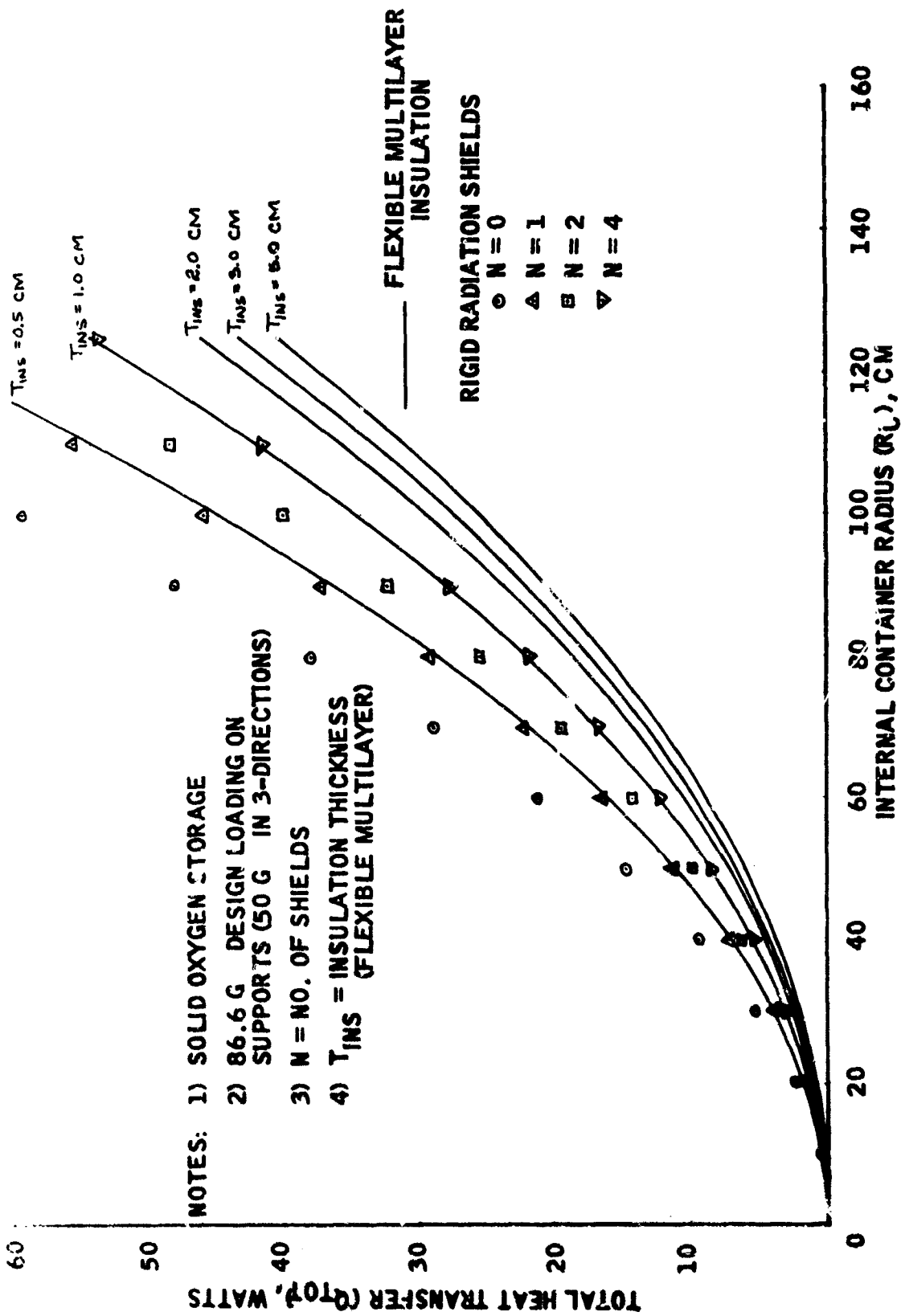


Figure 56. Total Heat Transfer Through Insulation and Supports as a function on Internal Container Radius - Solid Oxygen Storage

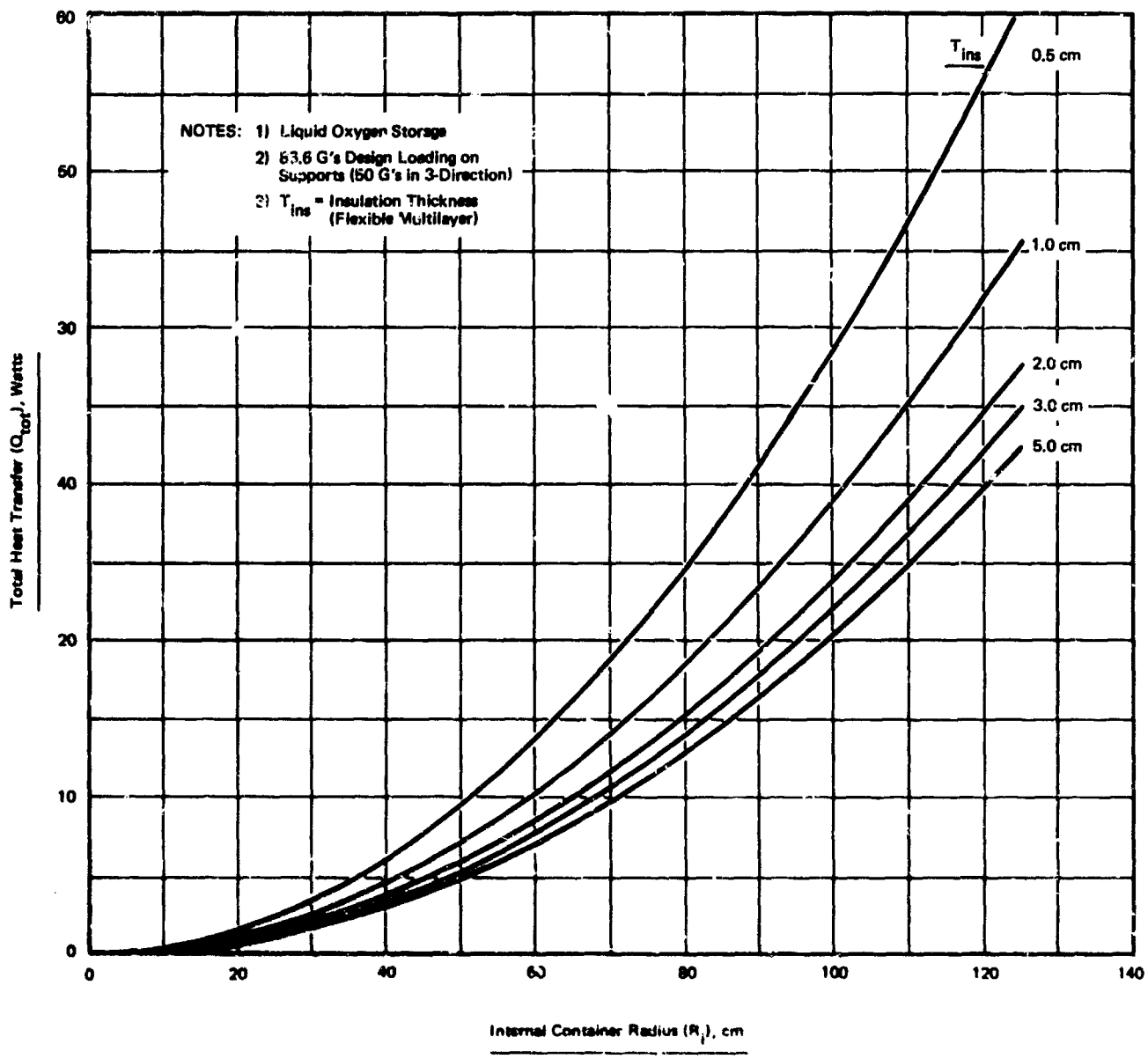


Figure 67. Total Heat Transfer Through Insulation and Supports vs Internal Container Radius

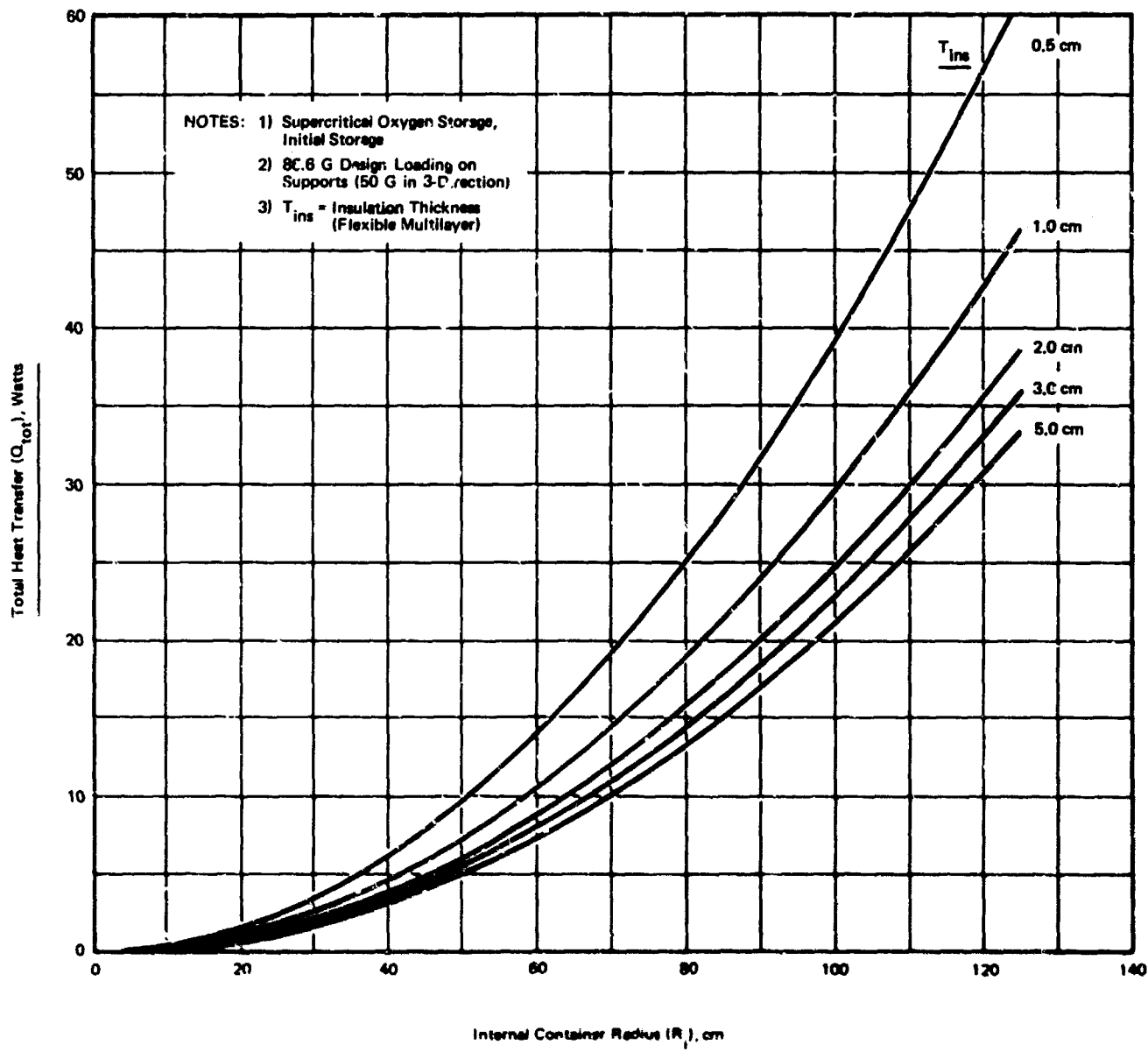


Figure 58. Total Heat Transfer Through Insulation and Supports vs Internal Container Radius

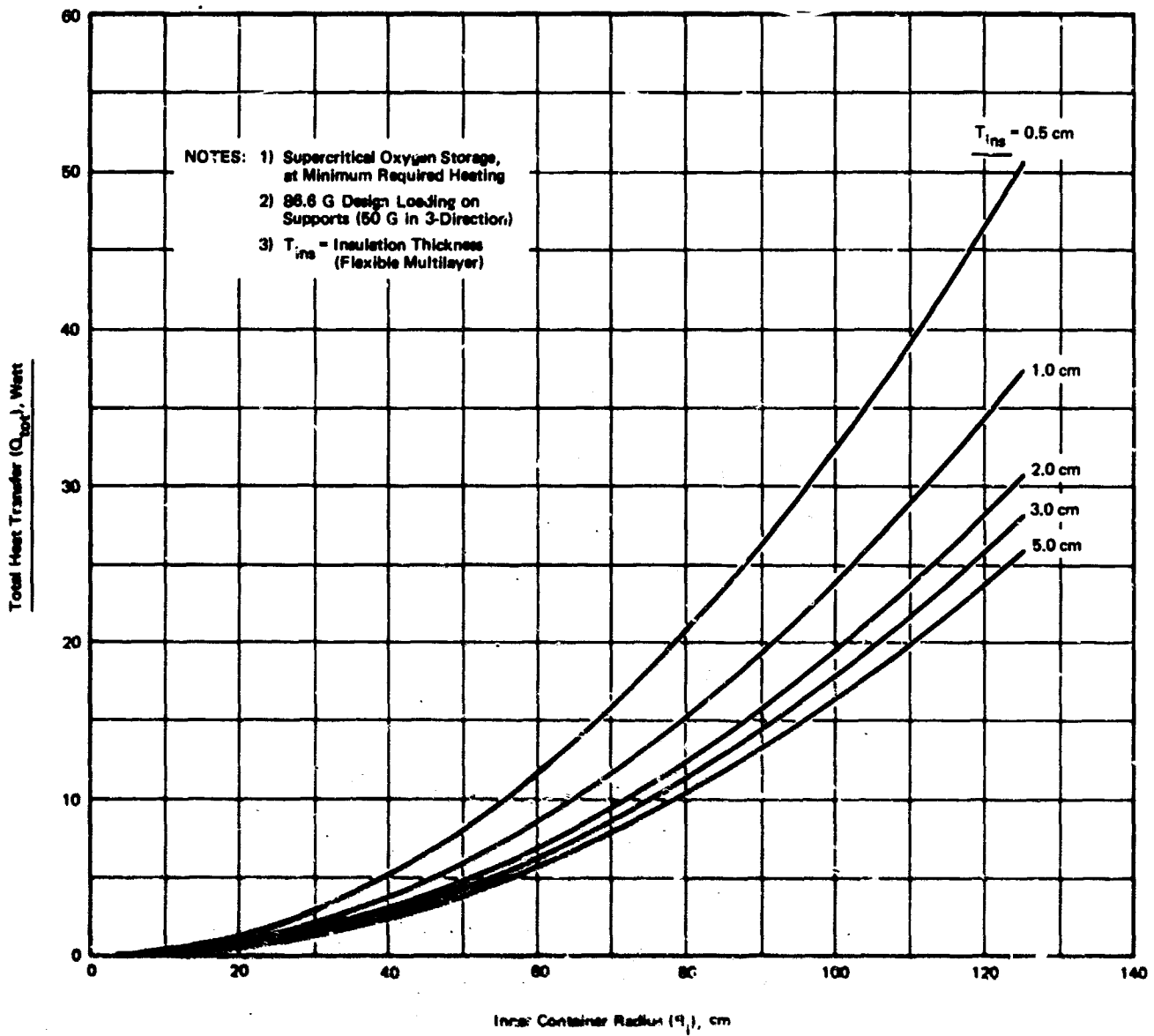


Figure 58. Total Heat Transfer Through Insulation and Supports vs Internal Container Radius

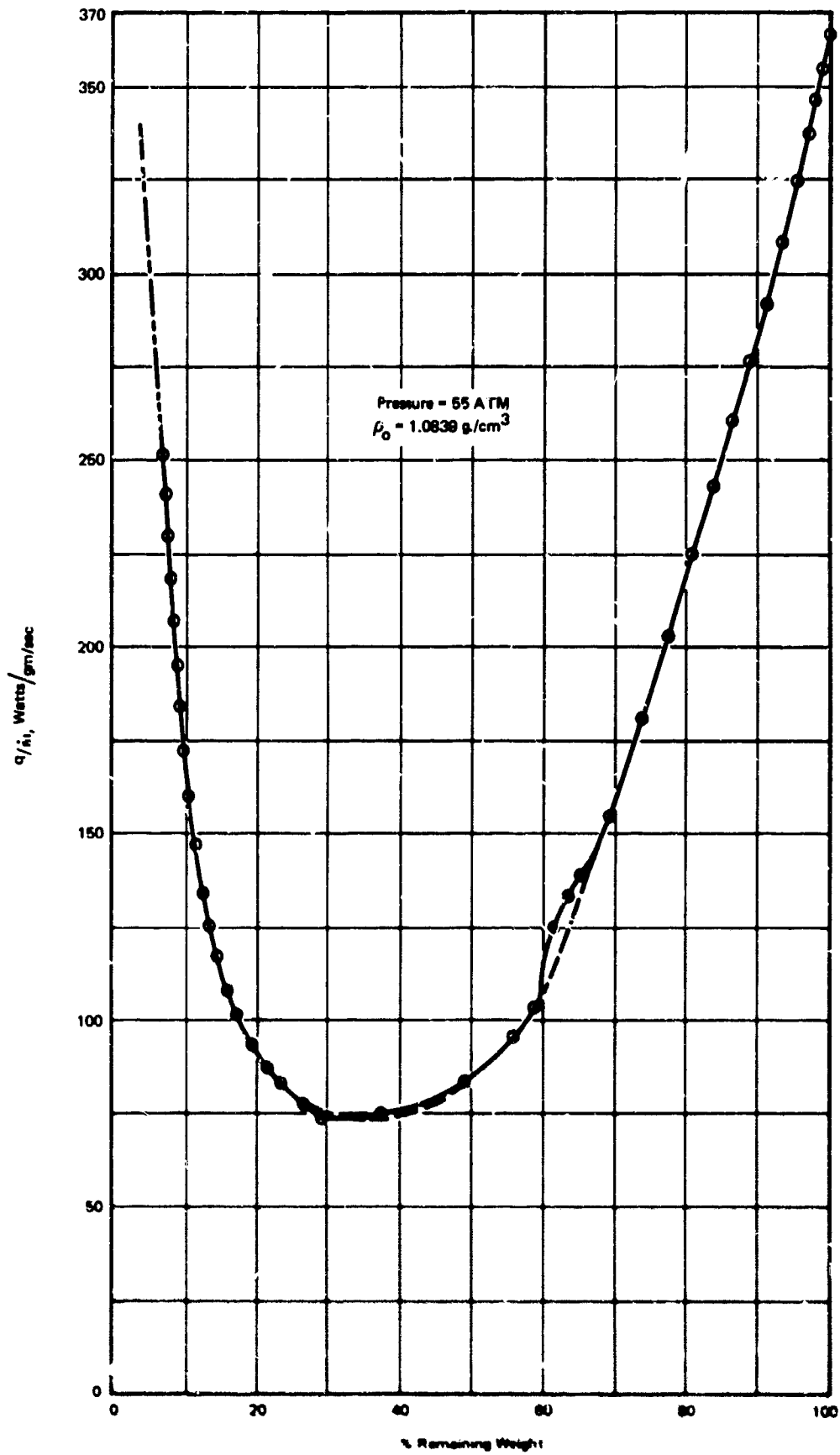


Figure 80. Specific Heat Input for Constant Pressure Delivery - Supercritical Oxygen Storage

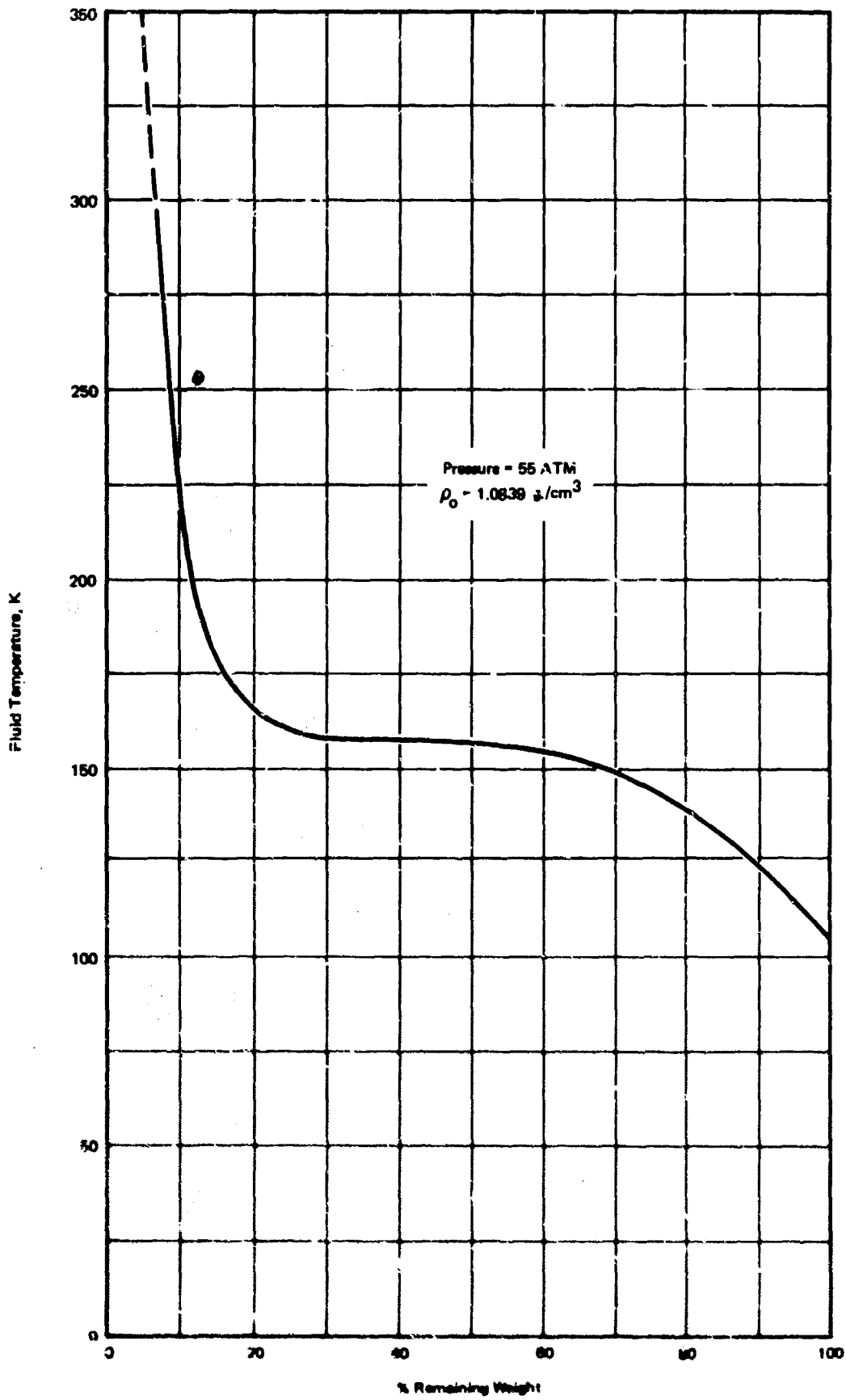


Figure 67. Fluid Temperature for Constant Pressure Delivery - Supercritical Oxygen Storage

## APPENDIX II

### HEATING REQUIREMENTS FOR OXYGEN DELIVERY

#### SUPERCRITICAL OXYGEN HEATING REQUIREMENTS FOR PRESSURIZATION

The pressure in the storage container is to be held constant at 55 atm. The initial density ( $\rho_0$ ) is 1.0839 g/cm<sup>3</sup> or 33.8717 g-mol/liter. This density was calculated assuming the container was initially filled with liquid at one atmosphere to 95% of the container volume.

The fluid heat input required for constant pressure operation in a supercritical storage vessel can be derived from the first law of thermodynamics. The result is given by

$$\frac{q}{\dot{m}} = -\rho \left( \frac{\partial h}{\partial \rho} \right)_P \quad (29)$$

where

q = Rate of heat transfer (by any method) into the vessel, joules/sec or watts

$\dot{m}$  = Weight or mass flow out of the vessel, mol/sec

h = Enthalpy of the fluid in the vessel, joule/mol

P = Pressure of the fluid in the container, atm

$\rho$  = Density of the fluid, g/cm<sup>3</sup> or mol/cm<sup>3</sup>

It is noted that the fluid density is directly proportional to the fill density and the fraction of the initial tank contents remaining in the vessel at any time. Thus the fluid heat input is directly proportional to delivery rate and to a quantity which can be determined from the thermodynamic properties of the fluid stored. This quantity,  $-\rho (\partial h / \partial \rho)_P$ , is a function of fluid density at given constant pressure and thus varies during operation. Fluid temperature also varies during operation.

However, since there is only one phase and pressure is held constant, only one other thermodynamic variable is necessary to define the process, i.e., temperature or density.

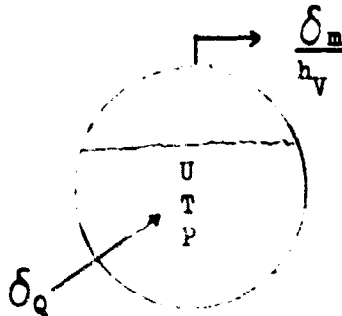
The specific heating rate equation (29) was calculated numerically from tabulated thermodynamic data given by Stewart (1966). The results of equation (29) are plotted in figure 60 as a function of percent weight remaining in the container where

$$\text{Percent Remaining Weight} = 100 \left[ \frac{\rho}{\rho_0} \right]$$

Figure 61 shows the fluid temperature as a function of percent weight remaining in the container for constant pressure delivery of supercritical oxygen at 55 atmospheres. This curve will be used to calculate the heat transfer into the container.

#### LIQUID STORAGE WITH HEATING AND VAPOR REMOVAL

For this study the liquid will be considered to be stored at constant pressure. The two phases will be considered separated in the storage vessel with only the vapor removed.



Pressure and temperature are constant.  
Applying the First Law of Thermodynamics to the process,

$$\delta Q = \delta U + h_v \delta m \quad (30)$$

where

$\delta Q$  = Heat added in time  $\delta \theta$

$\delta U$  = Change in internal energy change of the fluid in the vessel

$h_v$  = Enthalpy of the vented vapor (in this case, enthalpy of the saturated vapor at the pressure P)

$\delta m$  = Vapor removed in time  $\delta \theta$

The change in internal energy is

$$\delta U = U_2 - U_1$$

where

$U_1$  = Internal energy at time  $\theta$

$U_2$  = Internal energy at time  $\theta + \delta\theta$

Also

$$\delta U = m_2 u_2 - m_1 u_1$$

where

$u$  = Internal energy per unit mass

$m$  = Mass (liquid + vapor) in the vessel

In terms of the masses of liquid (L) and vapor (V),

$$\begin{aligned} \delta U &= m_{2L} u_L + m_{2V} u_V - (m_{1L} u_L + m_{1V} u_V) \\ &= u_L (m_{2L} - m_{1L}) + u_V (m_{2V} - m_{1V}) \end{aligned} \quad (31)$$

Performing a mass balance on phases inside the container,

$$m_{1L} - m_{2L} = \delta m + (m_{2V} - m_{1V}) \quad (32)$$

$$\delta m = m_{1L} - m_{2L} - (m_{2V} - m_{1V}) \quad (33)$$

Substituting equation (32) into equation (31) gives

$$\begin{aligned} \delta U &= -\delta m u_L + u_L (m_{1V} - m_{2V}) + u_V (m_{2V} - m_{1V}) \\ &= -\delta m u_L + (m_{2V} - m_{1V}) (u_V - u_L) \end{aligned} \quad (34)$$

Substituting the definition of enthalpy of the liquid ( $h_L = u_L + P/\rho_L$ ) into equation (34), where  $\rho_L$  is the liquid density, gives

$$\delta U = -\delta m h_L + \delta m P / \rho_L + (m_{2V} - m_{1V}) (u_V - u_L) \quad (35)$$

Also

$$u_V - u_L = h_V - h_L - P \left( \frac{1}{\rho_V} - \frac{1}{\rho_L} \right) = h_V - h_L - P \left( \frac{\rho_L - \rho_V}{\rho_V \rho_L} \right) \quad (36)$$

and

$$m_{2V} - m_{1V} = \rho_V \Delta V_L$$

where

$\Delta V_L$  is the volume of liquid evaporated

But

$$\Delta V_L = \frac{1}{\rho_L} (m_{1L} - m_{2V})$$

or

$$m_{2V} - m_{1V} = \frac{\rho_V}{\rho_L} (m_{1L} - m_{2L}) \quad (37)$$

Substituting equation (32) into equation (37) gives

$$m_{2V} - m_{1V} = \frac{\rho_V}{\rho_L} \delta m + \frac{\rho_V}{\rho_L} (m_{2V} - m_{1V})$$

or

$$\frac{\rho_V}{\rho_L} \delta m = (m_{2V} - m_{1V}) \left( 1 - \frac{\rho_V}{\rho_L} \right)$$

and

$$m_{2V} - m_{1V} = \delta m \left( \frac{\rho_V}{\rho_L - \rho_V} \right) \quad (38)$$

Substituting equations (38) and (36) into equation (35) gives

$$\delta U = -\delta m h_L + \delta m P/\rho_L + \delta m \left( \frac{\rho_V}{\rho_L - \rho_V} \right) \left[ h_V - h_L - P \left( \frac{\rho_L - \rho_V}{\rho_V \rho_L} \right) \right]$$

or

$$\delta U = -\delta m h_L + \delta m \left( \frac{\rho_V}{\rho_L - \rho_V} \right) (h_V - h_L) \quad (39)$$

Combining equations (39) and (30) gives

$$\delta Q = -\delta m (h_V - h_L) + \delta m \left( \frac{\rho_V}{\rho_L - \rho_V} \right) (h_V - h_L) = \delta m (h_V - h_L) \left( \frac{\rho_L}{\rho_L - \rho_V} \right)$$

Dividing by the time interval  $\delta \theta$  and letting

$$q = \frac{\delta Q}{\delta \theta}$$

$$\dot{m} = \frac{\delta m}{\delta \theta}$$

$$h_V - h_L = H_{VL}$$

gives

$$q = \dot{m} H_{VL} \left( \frac{\rho_L}{\rho_L - \rho_V} \right) \quad (40)$$

where

$H_{VL}$  = Heat of vaporization of the liquid at the pressure  $P$ , j/g

$\dot{m}$  = Vapor removal rate, g/sec

$q$  = Rate of heat addition, wat's

For liquid-oxygen storage at 1 atm (1.0333 kg/cm<sup>2</sup>)

$$\rho_L = 35.6471 \text{ mol/liter}$$

$$\rho_V = 0.1396 \text{ mol/liter}$$

$$\frac{\rho_L}{\rho_L - \rho_V} = \frac{35.6471}{35.5075} = 1 + \frac{0.1396}{35.5075} = 1.00392$$

$$H_{VL} = 6825.8 \text{ j/mol} = 213.30 \text{ j/g}$$

and from equation (40)

$$q = \dot{m}(213.30) (1.00392)$$

$$q = 214.14 \dot{m} \text{ (liquid storage at 1-atm absolute pressure)}$$

$$\frac{q}{\dot{m}} = 214.14 \text{ w/g/sec (constant)}$$

#### SOLID STORAGE WITH HEATING AND VAPOR REMOVAL

The equation for heating and vapor removal of constant pressure for liquid storage also applies to solid storage (with solid and vapor in equilibrium below the triple point pressure) with the substitution of the heat of sublimation for the heat vaporization and the solid density for the liquid density. Thus for solid storage

$$q = \dot{m} \lambda_S \left( \frac{\rho_S}{\rho_S - \rho_V} \right) \quad (41)$$

where

$q$  = Heat addition, watts

$\dot{m}$  = Mass rate of vapor removal, g/sec

$\lambda_S$  = Heat of sublimation, j/g

$\rho_S$  = Density of the solid at the container pressure and temperature, mol/liter or g/cu cm

$\rho_V$  = Density of the vapor at the pressure and temperature in the container, mol/liter or g/cu cm

For solid-oxygen storage, the pressure will be less than 1.14 mm of Hg absolute where the vapor density will be negligible compared to the density of the solid. Then for the solid-oxygen storage, equation (41) becomes:

$$q \doteq \dot{m} \lambda_S \quad (42)$$

For solid oxygen slightly below the triple point (T.P.) (54.36°K and 1.14 torr), the heat of sublimation is

$$\begin{aligned} \lambda_S &= 8176.0 \text{ j/mol (at T.P.)} \\ &= 255.50 \text{ j/g} \end{aligned}$$

and

$$\frac{q}{\dot{m}} = 255.5 \text{ watts/g/sec (at T.P.)}$$

(19.3% greater than the liquid storage at 1 atm)

### APPENDIX III

## ANALYTIC STUDY, COMPARISON OF LIQUID VERSUS SOLID OXYGEN STORAGE

### INTRODUCTION

A comparison analysis of solid versus liquid oxygen storage life has been made where the solid is reduced to the liquid phase after the extended storage time. By starting with solidified oxygen, instead of the saturated liquid for either the subcritical or supercritical storage systems, advantage can be taken of the sensible heat capacity, heat of fusion, and increased density of the solid to increase its storage life. This can be done by launching it as a solid and then allowing it to liquefy after launch. A combination of methods could be used to achieve maximum usage of the solidified oxygen. An example would be the case in which a portion of the solid oxygen is sublimed to space prior to liquefaction. Instead of wasting that part of the oxygen which would be lost to space, it could be sublimed to adsorbents which would subsequently raise its pressure to a breathable level. However, when the solid is being melted, the container would be sealed.

The general procedure is to start with solid oxygen in a given Dewar where, with the increased density of the solid, a greater loading of oxygen in the container can be realized than is possible with liquid oxygen. (Solid is 14 percent greater.) Using both the latent heat of the solid and the sensible heat of solid and liquid finally ending up with a container of liquid, extended storage time can be achieved. Also, the extended storage time can be increased by cooling the solid below the triple point to achieve a greater density loading of solid oxygen. (Due to solid phase changes, loadings of up to 28 percent by weight greater than liquid can be achieved.) In addition, the cooled solid has a greater heat of sublimation, as well as the increased sensible heat of the cooled solid.

Three procedures were analyzed which involve starting initially with solid oxygen and ending with liquid. The three procedures for calculation purposes, shown schematically in figures 62 and 63, are described in the following paragraphs.

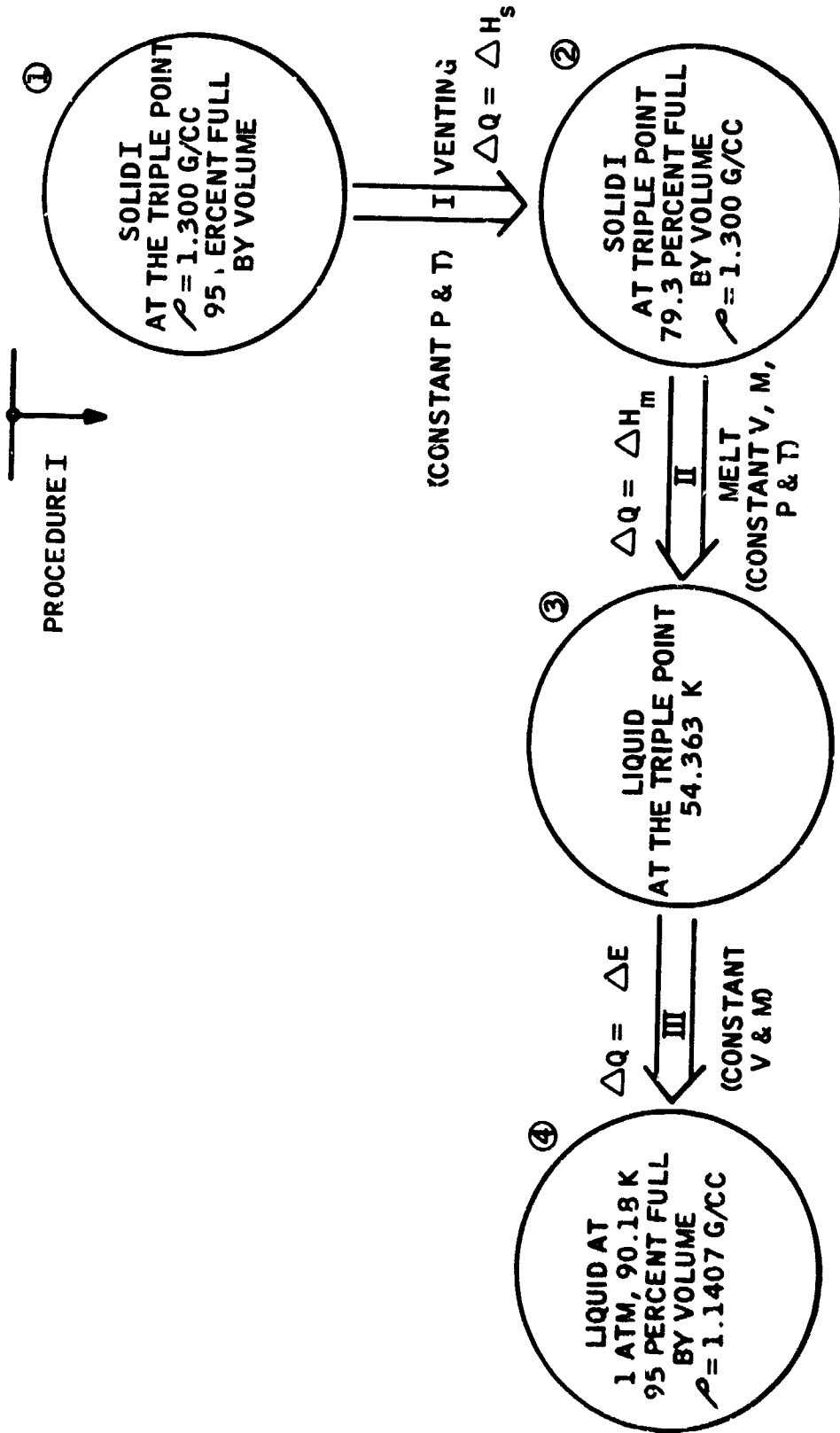


Figure 62. Oxygen Initially Stored as a Solid at the Triple Point

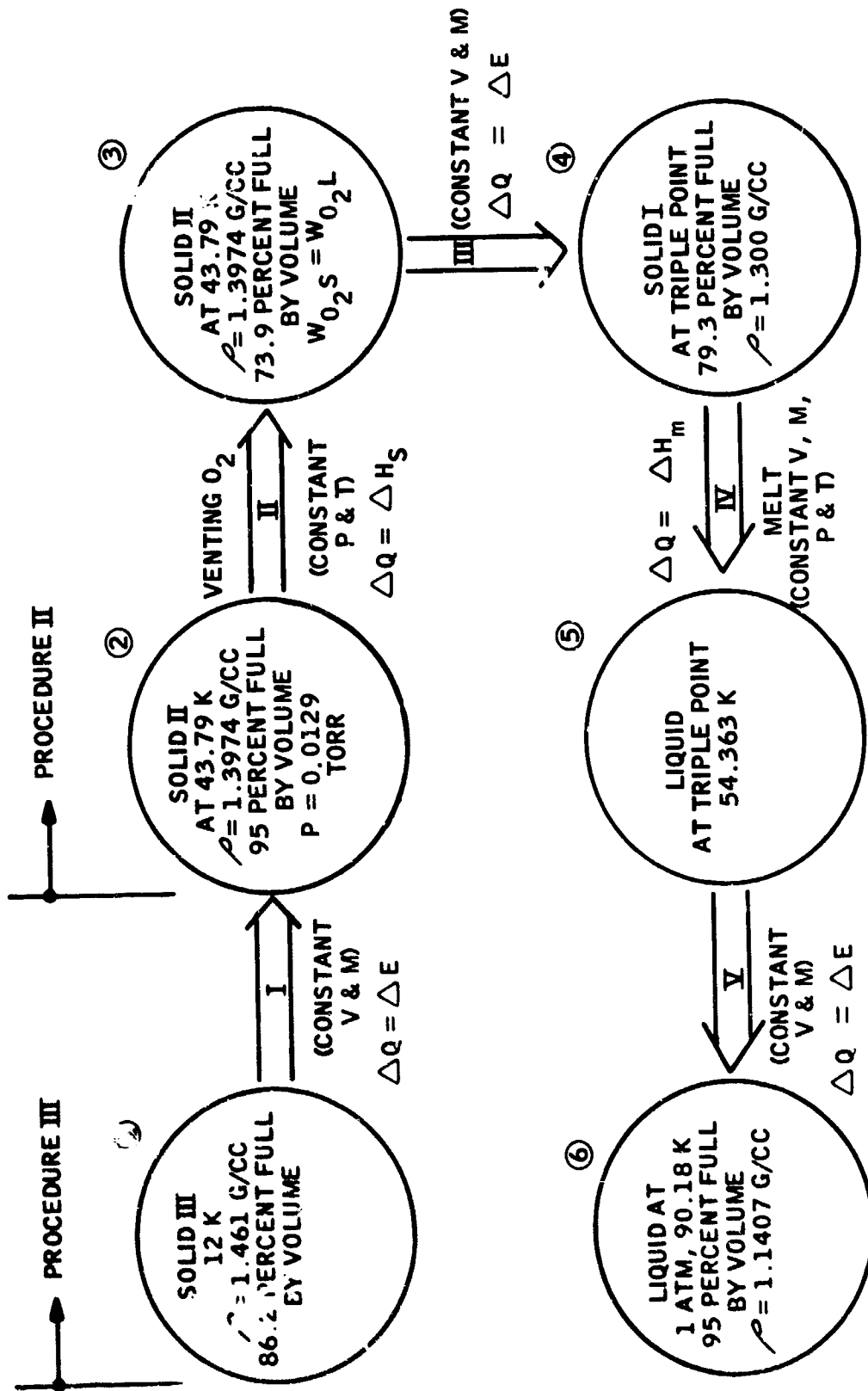


Figure 63. Oxygen Initially Stored as a Solid at 43.79K (Phase II), and 12K (Phase III), Respectively

PROCEDURE I, FIGURE 62

The container starts 95 percent filled (by volume) with solid oxygen at the triple point (Phase I) and having a density of 1.300 g/cc. Enough solid oxygen is allowed to sublime (with venting) to yield a solid oxygen weight equal to the desired liquid oxygen weight (95 percent full by volume). The solid is allowed to melt without venting to yield liquid at the triple point. Thirdly, the liquid pressure and temperature is allowed rise without venting to one atmosphere and 90.2 K, respectively. At this point, the oxygen is stored as a liquid with venting of vapor at one atmosphere inside the container. The density of the liquid oxygen at its normal boiling point is 1.141 g/cc.

The following paragraphs present the formulation of the storage time when a container is initially filled 95% full of solid oxygen and allowed to sublime until the remaining weight is equal to the equivalent of a container 95% full of liquid oxygen.

The remaining (solid or liquid) oxygen after storage time  $\theta$  (with sublimation or evaporation) is given by

$$W_{O_2R} = W_{O_2} - \dot{m}\theta \quad (43)$$

where

$\theta$  = time, days

$\dot{m}$  = vapor removal rate, kg/day

$W_{O_2}$  = initial weight of oxygen, kg

$W_{O_2R}$  = weight of oxygen remaining, kg

The vapor removal will be governed by the total heat leak,  $Q_{tot}$ , into the container. For both solid and liquid storage,

$$q = \dot{m}K \quad (44)$$

where

$q$  = the heating rate necessary to yield a vapor removal rate of  $\dot{m}$  (kg/day), watts

$K$  = a constant, though different for solid and liquid,

$K = 2.4785$  watts/kg/day for liquid storage at the normal boiling point and  $K = 2.9618$  watts/kg/day for solid storage at the triple point.

$$\text{With } q = Q_{\text{tot}} \quad (45)$$

$$\text{The } W_{O_2R} = W_{O_2} - \frac{Q_{\text{tot}} \Theta}{K} \quad (46a)$$

$$= W_{O_2} \left[ 1 - \frac{Q_{\text{tot}} \Theta}{K W_{O_2}} \right] \quad (46b)$$

In general, the information desired is the storage time,  $\Theta$ , for  $W_{O_2R}$  of the solid to be equal to the initial weight of liquid<sup>S</sup> which would fill 95% of the original container.

$$\Theta_S = \frac{K_S}{Q_{\text{tots}}} (W_{O_2S} - W_{O_2L}), \text{ days} \quad (47)$$

Also, the time for the remaining solid to melt,  $\Theta_m$ , is

$$\bar{q} \Theta_m = W_{O_2R} H_f \quad (48)$$

where  $H_f$  = the heat of fusion at the triple point, watt-hr/lg.  
( $H_f = 3.860$  watt-hr/kg for oxygen)

$\bar{q}$  = the average heat leak melting the solid, watt.

Since the temperature is constant during the melting,

$$\bar{q} = Q_{\text{tots}} \quad (49)$$

where  $Q_{\text{tots}}$  = the total heat transfer into the solid oxygen.

Then

$$\theta_m = \frac{W_{O_2 R} (3.867)}{(24) Q_{\text{tots}}}, \text{ days} \quad (50)$$

or when  $W_{O_2 R} = W_{O_2 L}$

$$\theta_m = 0.161 \frac{W_{O_2 L}}{Q_{\text{tots}}}, \text{ days} \quad (51)$$

At this point, the stored oxygen has been raised to the liquid state at the triple point (pressure of 1.14 torr and temperature of 54.36 K), by sealing the container and letting the heat transfer into the container melt the solid oxygen. Additional storage time can be realized by letting heat be absorbed by the liquid (maintaining a sealed container) and raising the pressure and temperature of the liquid. The sensible heat absorbed in changing the saturated liquid at the triple point to a saturated liquid at the normal boiling point is 16.332 watts-hr/kg for oxygen.

The time for this sensible heat change,  $\theta_L$  (days), neglecting the small heat capacity of the container and part of the insulation, is given by

$$\bar{q}_L \theta_L = \frac{16.332}{24} (W_{O_2 L}) \quad (52)$$

where  $\bar{q}_L$  is the average heat leak into the liquid. Since the temperature changes from 54.36 K to 90.18 K in the sensible heat change, the heat leak will vary from  $Q_{\text{tots}}$  for the solid to  $Q_{\text{totl}}$  for the liquid. However, neglecting the small change in thermal conductivity of the insulation and supports with temperature,

$$\bar{q}_L = \frac{1}{2} (Q_{\text{tots}} + Q_{\text{totl}})$$

and the heat leak is proportional to the ambient to oxygen temperature drop, or

$$Q_{\text{totl}} \doteq Q_{\text{tots}} \frac{298 - T_L}{298 - T_S} \quad (53)$$

where

$T_L$  = liquid oxygen temperature, K

$T_S$  = solid oxygen temperature, K

For this case,  $T_L = 90.18$  K and  $T_S = 54.36$  K and

$$Q_{\text{totl}} \doteq Q_{\text{tots}} \left( \frac{207.82}{243.64} \right) = 0.854 Q_{\text{tots}}$$

Then

$$\bar{q}_L \doteq \frac{1.854}{2} q_{\text{tots}} = 0.927 Q_{\text{tots}}$$

and from equation (52)

$$\Theta_L = \frac{16.332}{0.927(24)} \frac{W_{O_2L}}{Q_{\text{tots}}}$$

or

$$\Theta_L = 0.735 \frac{W_{O_2L}}{Q_{\text{tots}}} \quad (\text{days}) \quad (54)$$

The total time is  $\Theta_T = \Theta_S + \Theta_m + \Theta_L$ . Combining equations (47), (51), and (54) gives

$$\Theta_T = \frac{K_s}{Q_{\text{tots}}} [W_{O_2S}] - \frac{K_s}{Q_{\text{tots}}} [W_{O_2L}] + \frac{0.897}{Q_{\text{tots}}} [W_{O_2L}] \quad (55a)$$

For  $K_S = 2.962$  watts/kg/day and  $W_{O_2S} = 1.1395 W_{O_2L}$

(ratio of densities)

$$\theta_T = 1.310 \left[ \frac{W_{O_2L}}{Q_{\text{tots}}} \right] \quad (55b)$$

The derivation of equation (55b) is for the condition  $W_{O_2R} = W_{O_2L}$ ,

a function of the container radius.  $Q_{\text{tots}}$  is a function of  $r_1$  and  $t_{\text{ins}}$ ,

the insulation thickness. The results of equation (55b), using computer generated data, are plotted in figures 26 and 27 of the report.

Figure 26 presents the total storage life as a function of inner container radius when insulated with flexible multilayer insulation. Figure 27 presents similar data when rigid radiation shields are used for insulation. This storage life is based upon starting with the container 95% full of solid and allowing sublimation until the amount of solid is enough such that, when melted, it fills the container to 95% full of liquid. Of this storage time, approximately 34% is accounted for by sublimation and 66% by melting of the solid oxygen and changing the sensible heat of the liquid to form liquid at one atmosphere of pressure. During the sublimation portion, venting would be required, and during the melting portion, no venting would be required.

The time to vaporize the remaining liquid oxygen is given by

$$\theta_V = 2.4785 W_{O_2L} / Q_{\text{totl}} \quad (\text{days}) \quad (56)$$

where  $Q_{\text{totl}}$  = the total heat transfer into the container, watts (liquid oxygen 90.18 K and the supports designed for solid oxygen, 95% full),

$W_{O_2L}$  = the initial weight of liquid oxygen, kg.

Figures 30 through 37 of the report show the relative weight of oxygen as a function of time for this procedure of extending the storage time of oxygen as curve number "2". Curve number "1" is for a container which is designed for initially 95% full of liquid oxygen.

PROCEDURE II, FIGURE 63

The container starts 95% filled (by volume) with solid oxygen at 43.79 K (Phase II) having a density of 1.397 g/cc. Enough solid oxygen is allowed to sublime (with venting) to yield a solid oxygen weight equal to the desired liquid oxygen weight (95% full by volume). The remaining solid is allowed to warm up without venting to the triple point temperature and pressure. At this point, the procedure is the same as in Procedure I, with the melting solid and sensible heat change of the liquid.

There is initially  $1.397/1.300 = 1.075$  times the initial weight of solid oxygen as in Procedure I, and there is an increased heat of sublimation also,  $K_s = 3.300$  watt-day/kilogram (w-day/kg). The weight is

$$W_{O_2S} = \frac{1.397}{1.141} W_{O_2L} = 1.225 W_{O_2L}$$

Equation (47) for this procedure becomes

$$\Theta_S = (1.225 - 1.000) (3.300) W_{O_2L}/Q_{II}$$

giving

$$\Theta_{II} = \Theta_S = 0.7420 W_{O_2L}/Q_{II} \quad (57)$$

where  $Q_{II}$  is the heat transfer experienced on path II.

From state ⑤ to ④ in figure 63, the heat capacity of the solid from figure 3 of the report is

$$\begin{aligned} \Delta E_{III} &= 117.60 + 11.05(10.563) = 294.32 \text{ cal/mol} \\ &= 0.4453 \text{ w-day/kg} \end{aligned}$$

The time for the temperature rise in the solid oxygen is

$$\Theta_{III} = 0.4453 \frac{W_{O_2} L}{Q_{III}} \quad (58)$$

where  $Q_{III}$  is the average heat transfer into the solid along path III (figure 3) where the solid oxygen temperature changes from 43.78 K to 54.36 K.

The remaining state changes are the same as for Procedure I. State ④ to ⑤

$$\Theta_{IV} = 0.1608 \frac{W_{O_2} L}{Q_{IV}} \quad (59)$$

and for state ⑤ to ⑥

$$\Theta_V = 0.6805 \frac{W_{O_2} L}{Q_V} \quad (60)$$

where  $Q_{IV}$  and  $Q_V$  are the heat transfer experienced on paths IV and V, respectively.

Computer results for  $Q_{II}$ ,  $Q_{III}$ ,  $Q_{IV}$ , and  $Q_V$ , equal to the total heat transfer for the temperature experienced at the state points shown on figure 63, were used to compute  $\Theta_{II}$  through  $\Theta_V$ . The total time is plotted on figures 28 and 29 of the report as a function of container radius and insulation thickness. Approximately 1.85 times the extended storage time is achieved by Procedure II as by Procedure I.

Figures 30 through 37 of the report show the relative weight of oxygen as a function of time for Procedure II as curve number "3".

#### PROCEDURE III, FIGURE 63

Procedure III is the same as Procedure II except that the 95% full container at 43.78 K is cooled to 12 K initially to gain the extra sensible heat of the solid from 12 K to 43.79 K.

The added storage time,  $\theta_I$ , to be added to the time for Procedure II, is the time for the solid to rise in temperature from state ① (12 K) to state ② (43.78 K). The heat capacity from figure 3 of the report is

$$\begin{aligned} E_I &= 22.42 + 8.05(19.914) + 2.76 (11.886) \\ &= 215.53 \text{ cal/mod} = 0.3261 \text{ w-day/kg} \end{aligned}$$

The added storage time is

$$\theta_I = 0.3261 W_{O_2 S} / Q_I = 1.225 (0.3261) W_{O_2 L} / Q_I = 0.3995 W_{O_2 L} / Q_I \quad (61)$$

$\theta_I$  extends the total storage of Procedure II by approximately 16%. Figures 30 through 37 of the report show the relative weight of oxygen as a function of time for Procedure III as curve "4".

#### SUPERCRITICAL STORAGE

The container is initially filled to 95% full of liquid; hence, the initial weight of supercritical fluid is the same as for the liquid. The time for the liquid (sealed container) to reach the supercritical state at 55 atmospheres is governed by the mass of oxygen and the change in internal energy of the two states,  $\Delta E_{SC}$ . From Stewart (1966).

$$\Delta E_{SC} = -3574.3 - (-4280.4) = 706.1 \text{ j/mol} = 0.2554 \text{ w-day/kg}$$

The time to reach 55 atmospheres is

$$\theta_{SC} = 0.2554 \frac{W_{O_2 L}}{Q_{SC}} \quad (62)$$

Where  $Q_{SC}$  is the average heat transfer for the oxygen at 90.18 K and 104.2 K, watts.

At this point, the supercritical fluid container would begin to vent (by pressure regulation). However, the vent rate varies with time because of the rise in oxygen temperature (figure 61 of Appendix II), and because of the variation of the specific heat capacity (figure 60 of Appendix II). The calculation is as follows:

The mass flow of supercritical fluid is

$$\dot{m} = \frac{Q_{\text{tot}}(R)}{K_{\text{SC}}(R)} \quad (63)$$

where

$R$  = the fraction remaining in the container, or relative weight of oxygen in the container

$K_{\text{SC}}(R)$  = the specific heat capacity given in figure 60, w-sec/gram

$Q_{\text{tot}}(R)$  = the total heat transfer to the oxygen which is a function of temperature which varies with  $R$  as given in figure 61, watts

Dividing equation (63) by  $W_{\text{O}_2\text{L}}$  gives

$$\dot{m}_r = \frac{\dot{m}}{W_{\text{O}_2\text{L}}} = \frac{Q_{\text{tot}}(R)}{W_{\text{O}_2\text{L}} K_{\text{SC}}(R)} \quad (64)$$

where

$\dot{m}_r$  = the "reduced" mass flow rate, g/sec

$W_{\text{O}_2\text{L}}$  = the initial weight of oxygen, grams.

The  $Q_{\text{tot}}$  variation with temperature is obtained from the IBM 360 computer heat-transfer program. Values for  $\dot{m}_r$  are computed then as a function of  $R$ , using equation (64). The variation of  $R$  with time ( $\theta$ ) is given by a numerical integration of the reciprocal of  $\dot{m}_r$  with respect to  $R$  as follows

$$\theta = \int_{1.0}^R (\dot{m}_r)^{-1} dR \quad (65)$$

or numerically by

$$\theta = \sum (\bar{\dot{m}}_r)^{-1} \Delta R \quad (66)$$

where  $\bar{\dot{m}}_r$  is the average  $\dot{m}_r$  over the interval of  $\Delta R$ .

The relative mass variation for a supercritical fluid was generated for two cases, shown in figures 30 and 31 as curve number "5". The curves steady out at 6.7% (0.067) because the heat transfer goes to zero when the oxygen temperature reaches the ambient temperature (figure 61 of Appendix II).

#### APPENDIX IV

#### ANALYSIS OF WEIGHTS FOR OXYGEN STORAGE SYSTEMS

The weights of the various components which make up the supercritical, subcritical (liquid), and solid oxygen storage systems, are calculated as described herein.

#### STORED OXYGEN

Refer to figure 64.

Subcritical (Liquid)

$$W_{LO_2} = \rho_L VK \quad (67)$$

where:

$W_{LO_2}$  = Weight of liquid oxygen, gm

$\rho_L$  = Density of liquid oxygen, gm/cm<sup>3</sup>

V = Container volume, cm<sup>3</sup>

K = Fill factor, 0.95

for a spherical container, the contained volume is

$$V = \frac{4}{3} \pi r_1^3 \quad (68)$$

where:

$r_1$  = inside radius of the inner container

Then:

$$W_{LO_2} = \frac{4}{3} \pi r_1^3 \rho_L K \quad (69)$$

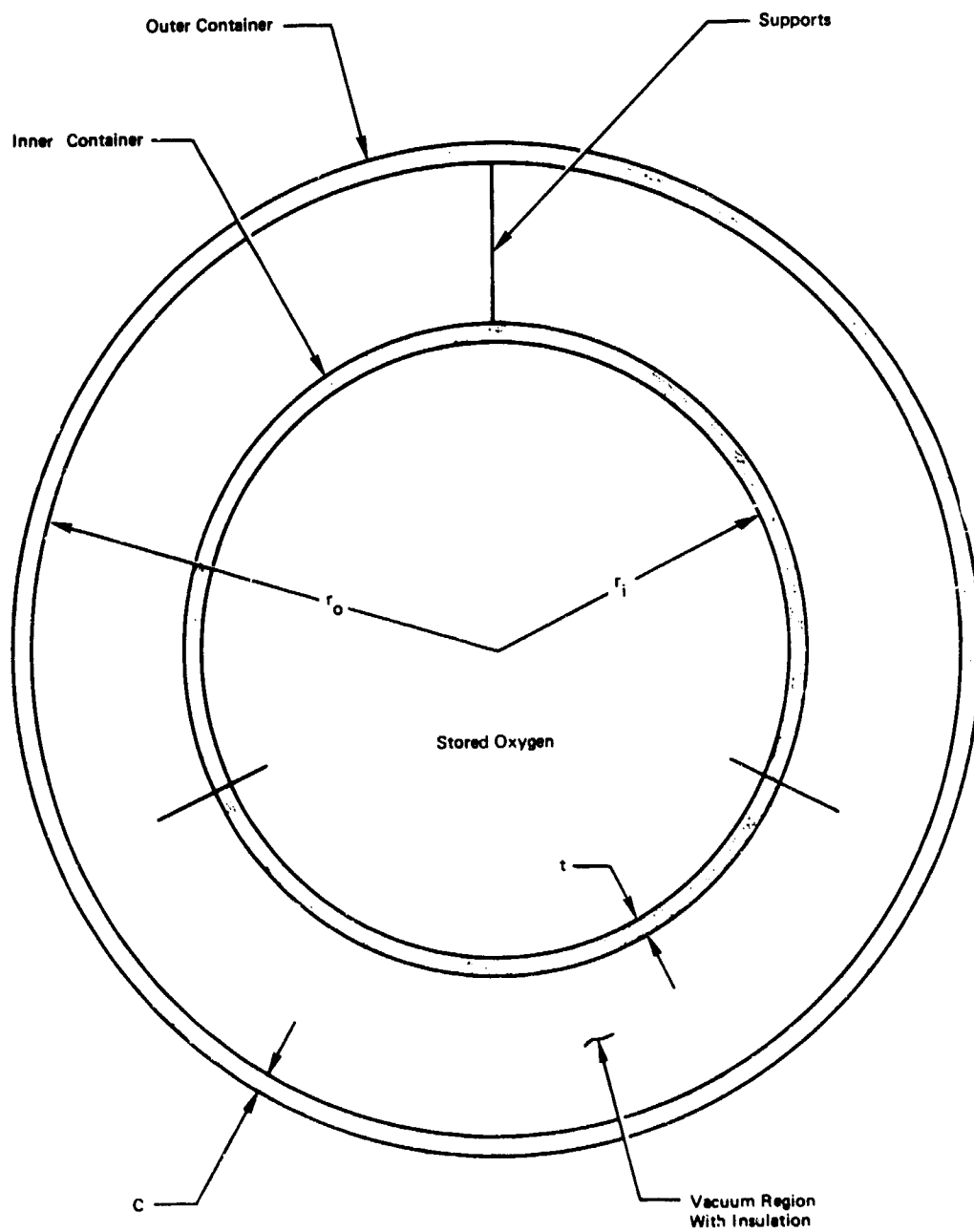


Figure 64. Oxygen Container

Supercritical

$$W_{\text{SCO}_2} = \rho_{\text{SC}} V \quad (70)$$

where

- $W_{\text{SCO}_2}$  = Weight of supercritical oxygen, gm  
 $\rho_{\text{SC}}$  = Density of supercritical oxygen, gm/cm<sup>3</sup>  
K = Fill factor is included in the density

Then

$$W_{\text{SCO}_2} = \frac{4}{3} \pi r_i^3 \rho \quad (71)$$

from equations (68) and (70).

Initially, the Dewar will be filled with saturated liquid oxygen at one atmosphere to 95% of capacity. The pressure will be allowed to rise to 55 atmospheres with no bleed off (constant volume and mass). Then

$$\rho_{\text{SC}} = 0.95 \rho_L + 0.05 \rho_V \quad (72)$$

where

- $\rho_L$  = Density of saturated liquid at one atm,  
 $\rho_V$  = Density of saturated vapor at one atm.  
 $\rho_L = 1.1407 \text{ gm/cm}^3$   
 $\rho_V = 0.0045 \text{ gm/cm}^3$

Then

$$\begin{aligned} \rho_{\text{SC}} &= 0.95(1.1407) + 0.05(0.0045) = 1.142 - 0.05(1.1407 - 0.0045) \\ &\approx 1.0839 \text{ gm/cm}^3 \end{aligned}$$

practically the same as the liquid with the fill factor.

Solid

$$W_{SO_2} = \rho_s V K \quad (73)$$

where

$W_{SO_2}$  = Weight of solid oxygen, gm

$\rho_s$  = Density of solid oxygen, gm/cm<sup>3</sup>

Then:

From equations (68) and (73)

$$W_{SO_2} = \frac{4}{3} \pi r_i^3 \rho_s K \quad (74)$$

Figure 65 presents the weight of contained oxygen as a functions of inner container radius ( $r_i$ ) for solid, liquid, and supercritical storage of oxygen.

#### INNER CONTAINER

The inner container will always be subjected to an internal pressure because of the vacuum jacket for the insulation. Thus, the internal pressure,  $P_i$ , will be the maximum absolute pressure experienced by the inner container for each storage mode considered. The container configuration will be a sphere.

#### Subcritical

The maximum pressure will be one atmosphere absolute  $P_i = 1.0333 \text{ kg/cm}^2$ . A safety factor of 1.67 will be applied to the yield stress. The container material will be Inconel 718, which has a density of  $8.20 \text{ g/cm}^3$  and a yield stress of  $1.23 \times 10^4 \text{ kg/cm}^2$ .

The wall thickness for the spherical container, which is under a "low" internal burst pressure, is given by the relation:

$$t = f P_i r_i / 2S \quad (75)$$

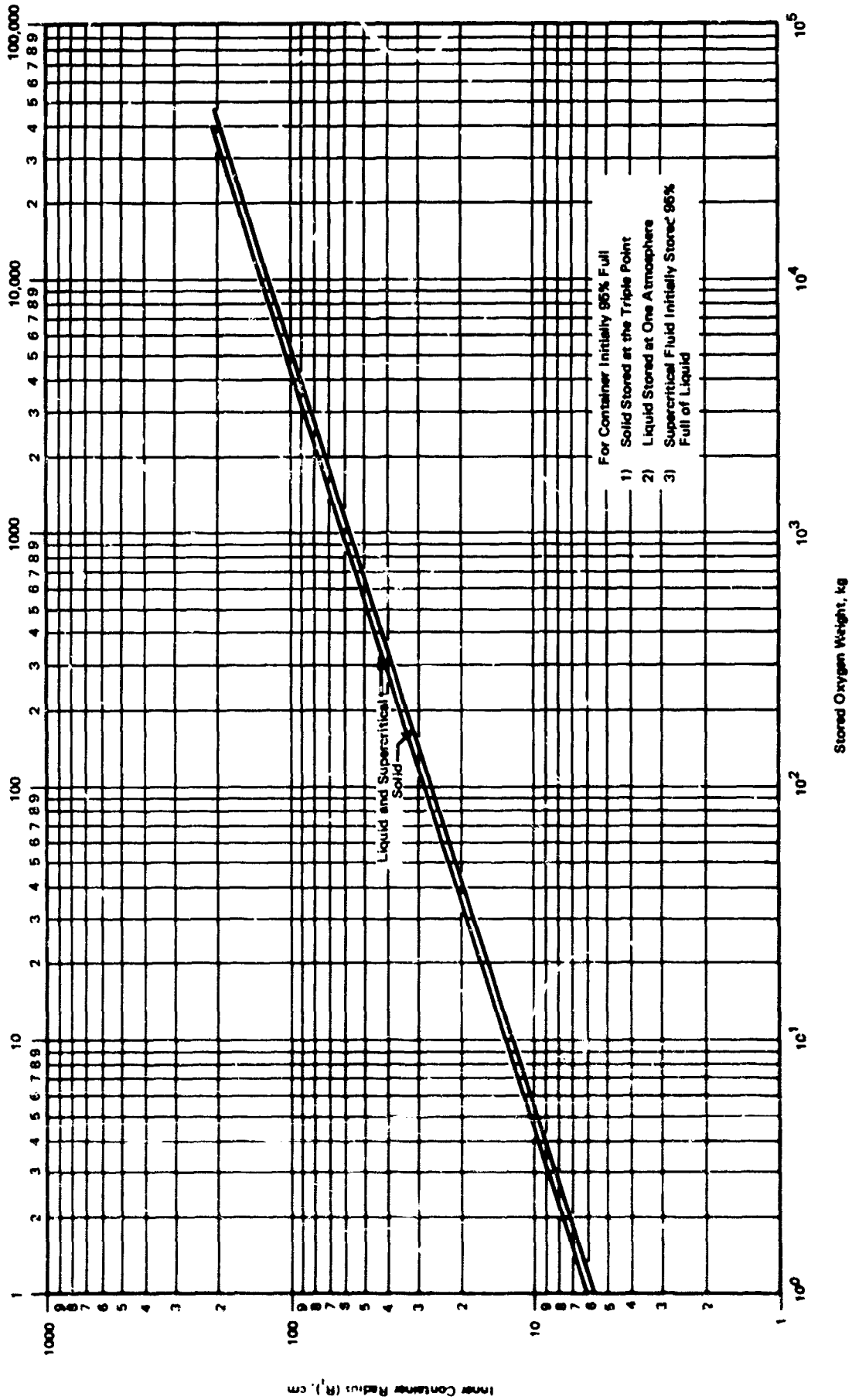


Figure 65. Inner Container Radius vs Stored Oxygen Weight

for a "thin-wall" container ( $t/r_i \ll 1$ ), where:

$t$  = Wall thickness, cm

$P_i$  = The maximum design pressure,  $\text{kg/cm}^2$

$r_i$  = Inside radius of the inner container, cm

$S$  = Yield stress of the container material,  $\text{kg/cm}^2$

$f$  = Safety factor, dimensionless

For the container material given above, equation (75) gives  $t/r_i = 0.70 \times 10^{-4}$ .

The weight of the spherical container is given by the relation:

$$\begin{aligned} W_{\text{ICL}} &= \frac{4\pi}{3} \rho_m \left[ (r_i + t)^3 - r_i^3 \right] \\ &= 4\pi \rho_m r_i^2 t \left[ 1 + \frac{t}{r_i} + \frac{1}{3} \left( \frac{t}{r_i} \right)^2 \right] \end{aligned}$$

With  $t/r_i = 0.70 \times 10^{-4}$ , the last two terms are negligible and inner container weight becomes:

$$W_{\text{ICL}} = 4\pi r_i^2 t \rho_m \quad (76)$$

where

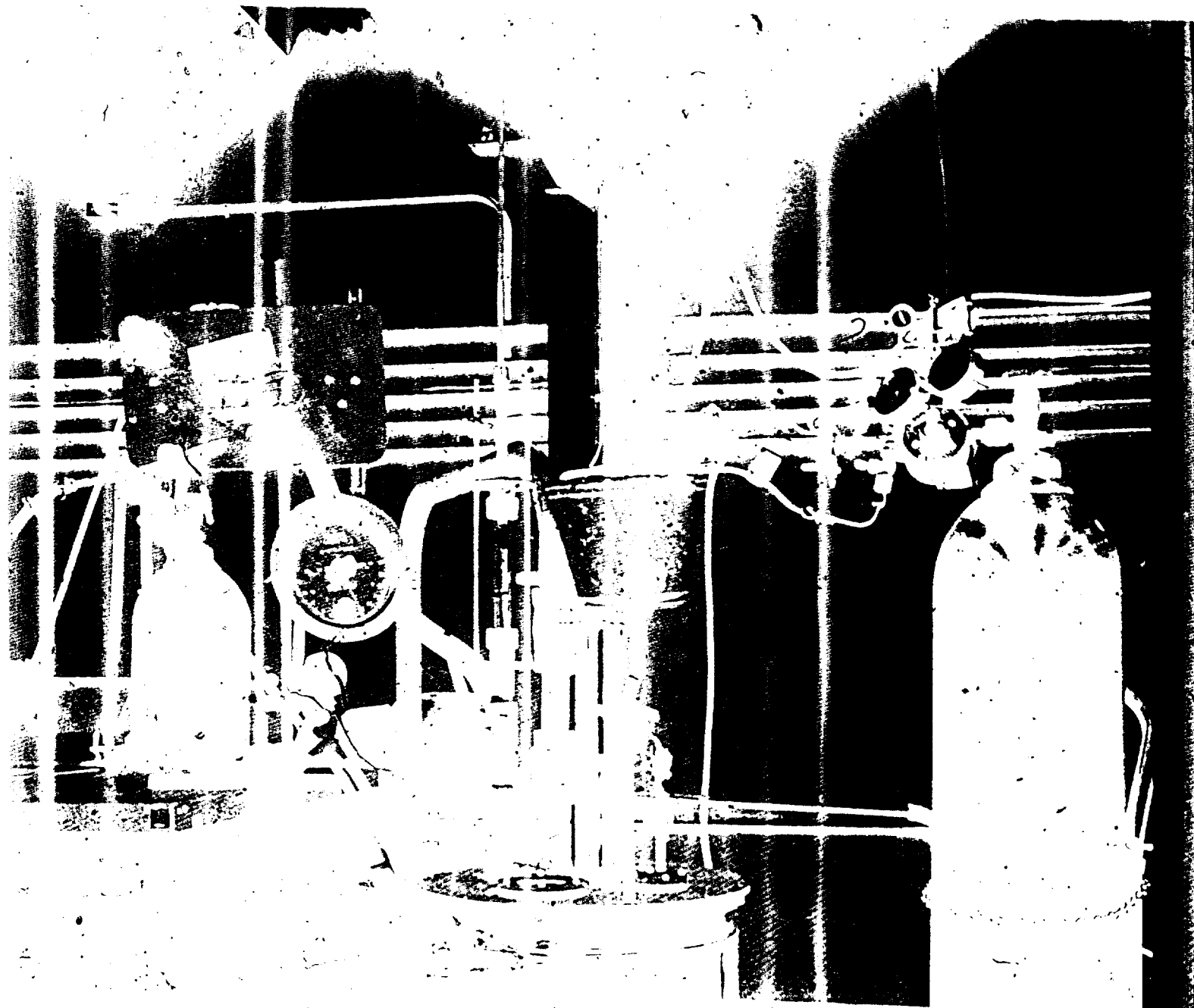
$W_{\text{ICL}}$  = The weight of the inner container, gm

$\rho_m$  = The inner container material, density,  $\text{gm/cm}^3$

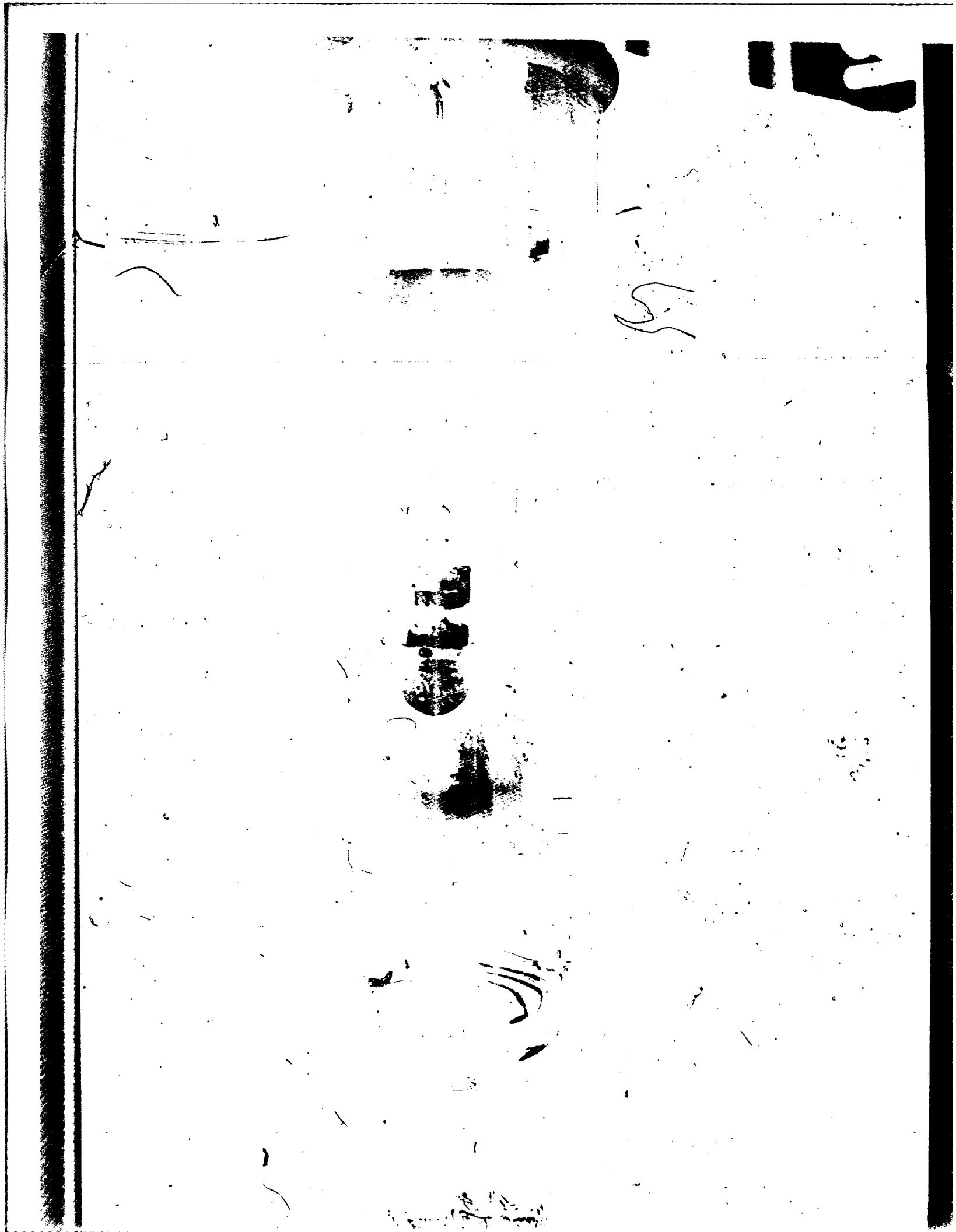
Combining equations (75) and (76) gives

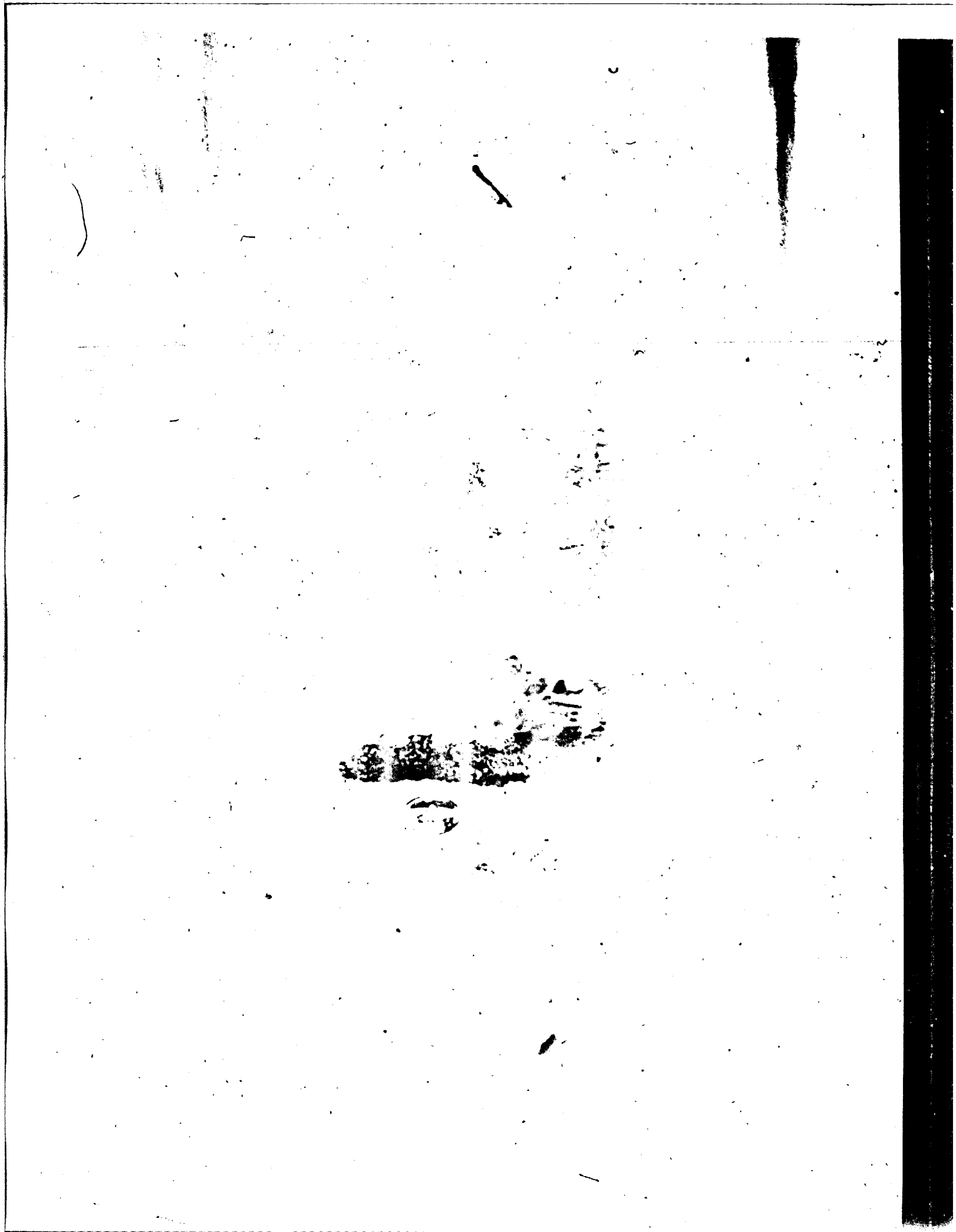
$$W_{\text{ICL}} = 2\pi \frac{f P_i r_i^3}{S} \quad (77)$$

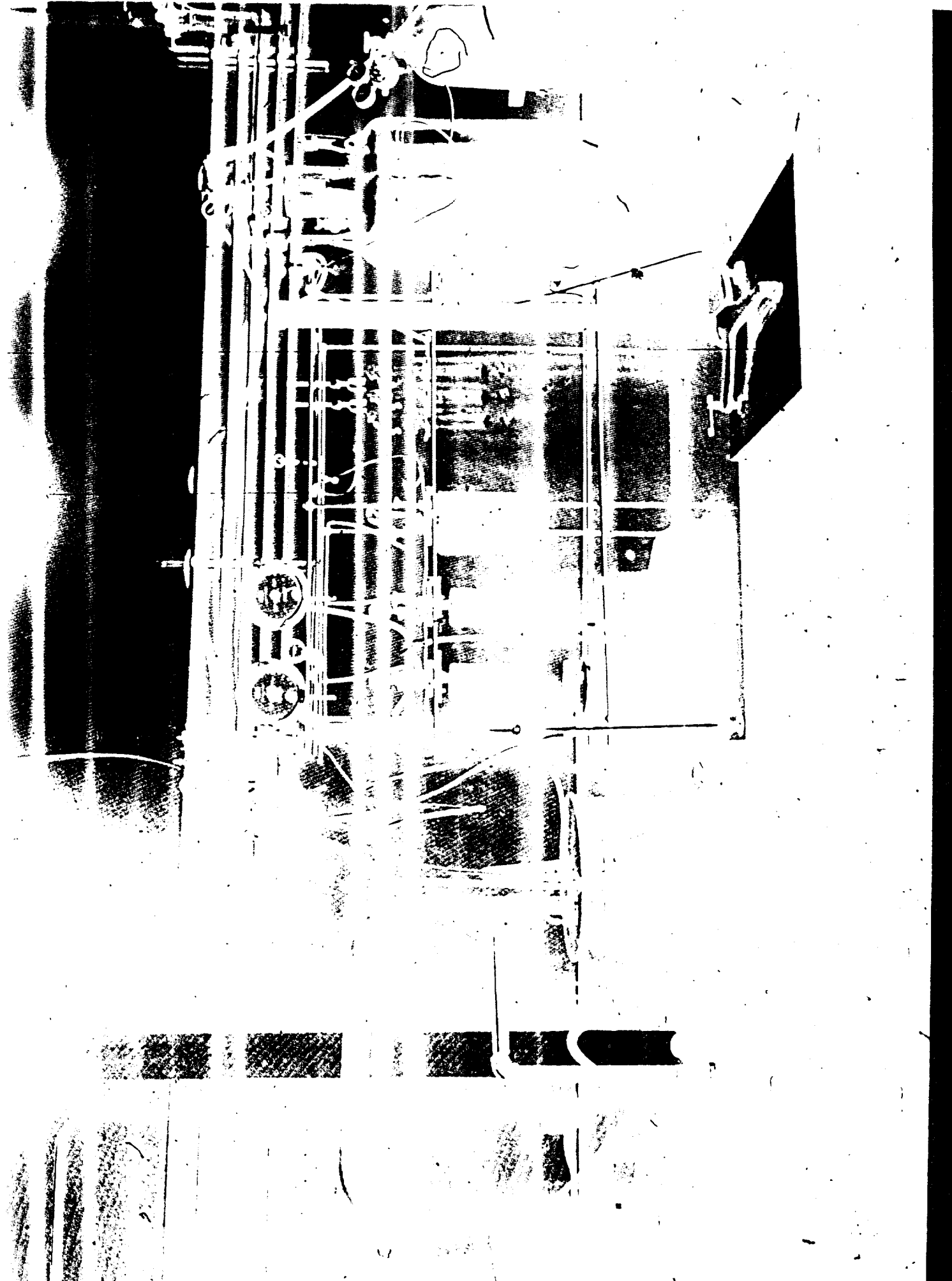












### Supercritical

The maximum pressure will be 55 atmospheres absolute,  $P_i = 56.83 \text{ kg/cm}^2$ . A safety factor of 1.67 will be applied to the yield stress. The container material will be Inconel 718, which has a density of  $8.20 \text{ g/cm}^3$  and a yield stress of  $1.23 \times 10^4 \text{ kg/cm}^2$ .

The wall thickness for the spherical container, which is under a "moderate" internal burst pressures, is given by the relation

$$t = r_i \left[ \sqrt{1 + \frac{P_i f}{S}} - 1 \right] \quad (78)$$

where the symbols have all previously been defined. With the container defined in the first paragraph,  $t/r_i = 0.00385$  and  $P_i f/S = 0.00771$ .

The weight of the spherical container is given by the relation

$$W_{\text{ICSC}} = \frac{4\pi}{3} \rho_m \left[ (r_i + t)^3 - r_i^3 \right] \quad (79)$$

where

$W_{\text{ICSC}}$  = The weight of the inner container with the supercritical oxygen, gm

Combining equations (78) and (79) gives

$$W_{\text{ICSC}} = \frac{4\pi}{3} \rho_m r_i^3 \left[ \left(1 + \frac{P_i f}{S}\right)^{3/2} - 1 \right] \quad (80)$$

Since  $\frac{P_i f}{S} \ll 1$ , then  $\sqrt{1 + \frac{P_i f}{S}} \approx 1 + \frac{P_i f}{2S}$ , and equation (80) becomes

$$W_{\text{ICSC}} = 2\pi \frac{\rho_m P_i f}{S} \left[ 1 + \frac{P_i f}{3S} \right] r_i^3 \quad (81)$$

## Solid

### Solid Continuously

With solid oxygen storage, the maximum internal pressure experienced by the inner container will be one atmosphere. Thus, the inner container weight for the continuous solid O<sub>2</sub> storage will be the same as for the subcritical storage, i.e., equation (77) becomes

$$W_{ICS} = 2\pi \frac{fP_1 \rho_m}{S} r_i^3 \quad (82)$$

where

$W_{ICS}$  = The weight for the inner container for storing solid O<sub>2</sub> continuously, gm

### Solid Initially, Transformed to a Subcritical Liquid

With the O<sub>2</sub> initially stored as a solid and then transformed to the subcritical liquid state with a pressure no greater than one atmosphere, the inner container weight will be given by equation (77).

### Solid Initially, Transformed to a Supercritical Fluid

With the O<sub>2</sub> initially stored as a solid and then transformed to a supercritical state with a pressure of approximately 55 atmospheres, the inner container weight will be given by equation (81), assuming that the pressure in the container is much less than the yield stress of the container material.

## INSULATION

Two types of insulation, flexible multilayer and multiple radiation shields (rigid), will be considered. A vacuum environment will be required for both types of insulation.

### Multilayered Shields

This insulation consists of alternate layers of aluminized mylar and a thin spacer material. The density is approximately 0.033 gm/cm<sup>3</sup> for 80 shields (mylar and spacer) per inch.

The volume of the flexible multilayer insulation, independent of the stored method, is given by

$$V_{INS} = \frac{4}{3} \pi \left[ r_o^3 - (r_i + t)^3 \right] \quad (83)$$

and the weight of the insulation is given by

$$W_{INS} = \frac{4}{3} \pi \rho_{ins} \left[ r_o^3 - (r_i + t)^3 \right] \quad (84)$$

where

$V_{INS}$  = The insulation volume,  $cm^3$

$W_{INS}$  = The insulation weight, gm

$r_o$  = The inside radius of the outer container, cm

$\rho_{ins}$  = The density of the insulation material,  $g/cm^3$

#### Rigid Multiple Radiation Shields

The weight of this type of insulation depends primarily upon the radius and thickness. When there is more than one shield, the total weight of the insulation depends upon the number of shields and their spacing.

$\rho_{sh}$  = Density of the shield material,  $gm/cm^3$

$x$  = Shield spacing, cm

$\delta$  = Shield thickness, cm

$A_{jsh}$  = Area of the  $j^{th}$  shield,  $cm^2$

$t$  = Inner container thickness, cm

If it is assumed that  $\delta \ll x$ , the volumes and weight are, respectively,

$$V_{sh} = \delta \sum_{j=1}^N A_{jsh} \quad (85)$$

$$W_{sh} = \rho_{sh} \delta \sum_{j=1}^N A_{jsh} \quad (86)$$

For one shield

$$A_{1sh} = 4\pi R^2$$

where R is the "mean" radius of the shield; then

$$A_{1sh} = 4\pi (r_i + t + x)^2$$

For two shields

$$\begin{aligned} A_{2sh} &= A_{1sh} + 4\pi (r_i + t + 2x)^2 \\ &= 4\pi [(r_i + t + x)^2 + (r_i + t + 2x)^2] \end{aligned}$$

Then for N shields

$$\begin{aligned} A_{Nsh} &= \sum_{j=1}^N A_{jsh} \\ A_{Nsh} &= 4\pi [(r_i + t + x)^2 + (r_i + t + 2x)^2 + (r_i + t + 3x)^2 + \dots \\ &\quad + (r_i + t + Nx)^2] \end{aligned}$$

$$= 4\pi \left[ N(r_i + t)^2 + 2x(r_i + t) (1 + 2 + 3 + \dots + N) + x^2 (1 + 4 + 9 + \dots + N^2) \right]$$

or finally

$$A_{Nsh} = 4\pi \left[ N(r_i + t)^2 + 2x(r_i + t) (N) \left(\frac{N+1}{2}\right) + x^2 \sum_{j=1}^N j^2 \right] \quad (87)$$

The term  $\sum_{j=1}^N j^2$  can be expanded thusly

$$\begin{aligned} \sum_{j=1}^N j^2 &= 1^2 + 2^2 + 3^2 + \dots + N^2 = 1 + 4 + 9 + \dots + N^2 \\ &= \frac{N}{6} (N+1) (2N+1) \end{aligned}$$

Substituting this into equation (87) gives

$$A_{Nsh} = 4\pi N \left[ (r_i + t)^2 + x (r_i + t) (N+1) + \frac{1}{6} x^2 (N+1) (2N+1) \right] \quad (88)$$

Substituting equation (88) into equation (86) gives

$$W_{sh} = 4\pi N \int \rho_{sh} \left[ (r_i + t)^2 + x (r_i + t) (N+1) + \frac{1}{6} x^2 (N+1) (2N+1) \right] \quad (89)$$

The outer container is considered a part of the insulation since its sole purpose is to provide the vacuum region for the insulation. However, it is treated as a separate entity in the next section.

Several small holes would be provided in each shield to allow trapped air to be removed during vacuum pumping. The weight of the "holes" is assumed to be approximately balanced by small plastic (nylon, teflon, dacron, etc.) shield supports between each shield.

## OUTER CONTAINER

The outer container will be subjected to an external collapsing pressure because of the vacuum region with the insulation. The weight of the outer container depends upon the radius ( $r_0$ ), the external pressure, and the container material and its strength. The outer container weight does not depend upon the method of oxygen storage or the size of the internal hardware. The outer container configuration will be spherical for this study.

The maximum external pressure tending to collapse the outer container will be one atmosphere,  $P_0 = 1.0333 \text{ kg/cm}^2$ . A safety factor of 1.67 will be applied to the computed wall thickness. The container material will be:

Material:	Aluminum - 6061-T6
Density:	$2.76 \text{ g/cm}^3$
Yield Stress:	$2.810 \times 10^3 \text{ kg/cm}^2$
E =	$7.03 \times 10^5 \text{ kg/cm}^2$
$\nu$ =	0.33 (Poisson's ratio)

Assuming that the spherical shell is thin, the weight is given by

$$W_{oc} = \rho_{mo} (4\pi r_0^2) c \quad (90)$$

where

$c$  = Thickness of outer container wall, cm

$\rho_{mo}$  = Density of the outer container material,  $\text{g/cm}^3$

The compressive stress in a thin spherical shell under a uniform external pressure is

$$S = \frac{P_0 r_0}{2c} \quad (91)$$

However, the critical stress at which buckling would occur is given by (see Timoshenko and Gere (1962) )

$$S_{cr} = \frac{EC}{r_o \sqrt{3(1 - \nu^2)}} \quad (92)$$

where

$E$  = Modulus of elasticity,  $g/cm^2$

$\nu$  = Poisson's ratio

Applying a safety factor,  $f$ , to the wall thickness after equating  $S_c$  to  $S$  in equation (91) gives

$$\frac{P_o r_o}{2C} = \frac{EC}{r_o \sqrt{3(1 - \nu^2)}}$$

$$C = fr_o \left\{ \frac{P_o}{2E} \sqrt{3(1 - \nu^2)} \right\}^{\frac{1}{2}} \quad (93)$$

Combining equations (93) and (90) gives

$$W_{oc} = 4\pi f \rho_{mo} \left[ \frac{P_o}{2E} \sqrt{3(1 - \nu^2)} \right]^{\frac{1}{2}} r_o^3 \quad (94)$$

The radius  $r_o$  is related to the inner container and insulation dimensions by  $r_o = r_i + t + (N + 1)x$  for shields, and

$r_o = r_i + t + t_{ins}$  for multilayer insulation in which

$t_{ins}$  = insulation thickness. All other terms have been previously defined.

## INNER CONTAINER SUPPORTS

The weight or size of the inner container supports depend upon the mass being supported and the acceleration (G's - shock or acceleration) and the strength of the support material. Titanium alloy having a yield strength of 9150 kg/cm<sup>2</sup> will be used as the support material for all the storage applications. A safety factor of 1.67 will be applied to the calculated support cross-section area.

The dynamic load on the inner container will be varied from 10 to 50 G's (in three directions). This dynamic load is the result of all launch loading (including shock, vibration, acceleration, and any amplification through the supports due to the "spring-mass" action).

The mass supported includes

1. Stored oxygen
2. Inner container
3. Insulation
4. Phase separator (for the liquid only)

but does not include the outer container. The total weight is:

$$W_T = W_{O_2} + W_{IC} + W_{INS} \quad (95)$$

where

- $W_T$  = Total weight, gm  
 $W_{O_2}$  = Stored oxygen weight (any method), gm  
 $W_{IC}$  = Inner container weight (any method), gm  
 $W_{INS}$  = Insulation weight (either insulation), gm

For the subcritical liquid storage, the weight of the phase separator must also be included in equation (95).

The support system will be as shown in figure 64. Each support is being radial, the support length is given by

$$L_s = r_o - r_i - t \quad (96)$$

i.e., each support extends from the inner container to the outer container. There are four supports located such that the ends form the four corners of a tetrahedron. Any one support can take the full load. Assuming that the loads will range from 10 to 50 G in three directions, the "full" load could vary from a minimum of 10 G to a maximum of  $50\sqrt{3}$  G (50 G in 3 - 86.6 G directions simultaneously).

Assuming the dynamic loading to be a (G), the maximum force in any support will be

$$F_s = W_T a (980) \quad (97)$$

where

$F_s$  = force in a support, dynes

$a$  = G-loading, G

980 = acceleration of one-G, cm/sec<sup>2</sup>

The stress in the support is given by

$$S_s = \frac{F_s}{A_s} = \frac{W_T a (980)}{A_s g_c} \quad (98)$$

where

$S_s$  = The stress (tension), gram/cm<sup>2</sup>

$A_s$  = The support cross-sectional area, cm<sup>2</sup>

$g_c$  = The conversion factor of dynes to grams force,  
980 gm-cm/gm<sub>f</sub>-sec<sup>2</sup>

The yield stress will be designated by  $S_y$ , and with the safety factor,  $f$ , the support stress must be such that

$$fS_s \leq S_y$$

Using the "equal" relation, then

$$\frac{S_y}{f} = \frac{W_T a}{A_s}$$

Solving for  $A_s$  gives

$$A_s = \frac{fW_T a}{S_y} \quad (99)$$

With  $L_s$  as the support length, then the volume is

$$V_s = A_s L_s$$

The weight of four supports is

$$W_s = 4 \rho_s L_s \left[ \frac{fW_T a}{S_y} \right] \quad (100)$$

As shown in Appendix I, Analysis of Heat Transfer to the Stored Oxygen, the support length will be calculated by:

$$L_s = 3r_o - r_i - t$$

With

$$S_y = 9150 \text{ kg/cm}^2$$

$$\rho_s = 4.52 \text{ gm/cm}^3$$

$$a = 86.6 \text{ G}$$

$$L_s = 200 \text{ cm maximum}$$

$$\begin{aligned}\frac{W_S}{W_T} &= 4(86.6)(1.67)(4.52)(200)/(9150 \times 10^3) \\ &= 0.064 = 6.4\%\end{aligned}$$

Or thus, the support weight is only a small part of the total weight. However, equation (99) will be used in calculating the support heat leak in Appendix I.

## APPENDIX V

### ANALYSIS OF OXYGEN USAGE

For this study, oxygen usage will be by three methods

- Crew breathing
- Space cabin leakage
- Extra-vehicular activities; air lock operation

#### CREW BREATHING

The oxygen usage rate for crew breathing has been set for this study at 1.13 kg/day/man. When  $M$  is the number of men in the crew, the combined oxygen breathing rate ( $\dot{W}_B$ ) can be expressed as follows:

$$\dot{W}_B = 1.13M \text{ (kg/day)} \quad (101)$$

#### SPACE CABIN LEAKAGE

The space cabin leakage rate ( $L_e$ ) will be varied from 0 to 1 kg/day.

#### EXTRA-VEHICULAR ACTIVITIES

For this study, a 1.5 m<sup>3</sup> air lock will be opened once per day for 0 to 100% of the mission days. A cabin oxygen partial pressure (or total pressure when no diluent is used) of 150 to 250 torr will be considered.

With the space cabin at 298 K, the oxygen densities for the 2 cabin pressures are

$$\begin{aligned} P_c &= 150 \text{ torr} = 0.19737 \text{ atm}; \rho_c = 0.003073 \text{ mol/liter} \\ &= 0.0002583 \text{ g/cm}^3 \end{aligned}$$

$$\begin{aligned} P_c &= 250 \text{ torr} = 0.32895 \text{ atm}; \rho_c = 0.013456 \text{ mol/liter} \\ &= 0.0004306 \text{ g/cm}^3 \end{aligned}$$

where

$P_c$  = Cabin oxygen pressure, torr

$\rho_c$  = Cabin oxygen density, g/cm<sup>3</sup>

The mass of oxygen lost with each air-lock operation is

$$W_{AL(1)} = \rho_c (1.5) \cdot 10^3 \text{ (kg)} \quad (102)$$

where  $W_{AL(1)}$  is the mass of oxygen lost for one air-lock operation.

Since the air lock is used only once per day,  $W_{AL}$  is also the oxygen loss per day of use. Letting  $F_u$  be the air lock use fraction (0 to 1.0) of the total mission days (duration), the total oxygen loss from the air-lock operation is

$$W_{AL} = 1.5 F_u \rho_c D_L \cdot 10^3 \text{ (kg)} \quad (103)$$

where

$D_L$  = Mission length, days

$W_{AL}$  = Total oxygen loss from the air-lock operation, kg

#### TOTAL OXYGEN USAGE

When there is no oxygen "dumped" to space the total oxygen used in the whole mission is

$$W_{O_2u} = D_L \left[ 1.13M + L_e + 1.5 F_u \rho_c \cdot 10^3 \right] \text{ (kg)} \quad (104)$$

and

$$D_L = \frac{W_{O_2u}}{1.13M + L_e + 1.5 F_u \rho_c \cdot 10^3} \quad (105)$$

The total oxygen usage rate is

$$\dot{W}_{O_2u} = 1.13M + L_e + 1.5 F_u \rho_c \cdot 10^3 \quad (106)$$

Figures 66 and 67 present the oxygen usage rate,  $\dot{W}_{O_2u}$ , equation (106), as a function of the number of men, leakage rate, and air-lock usage factor for chamber oxygen pressures of 150 and 250 torr, respectively.

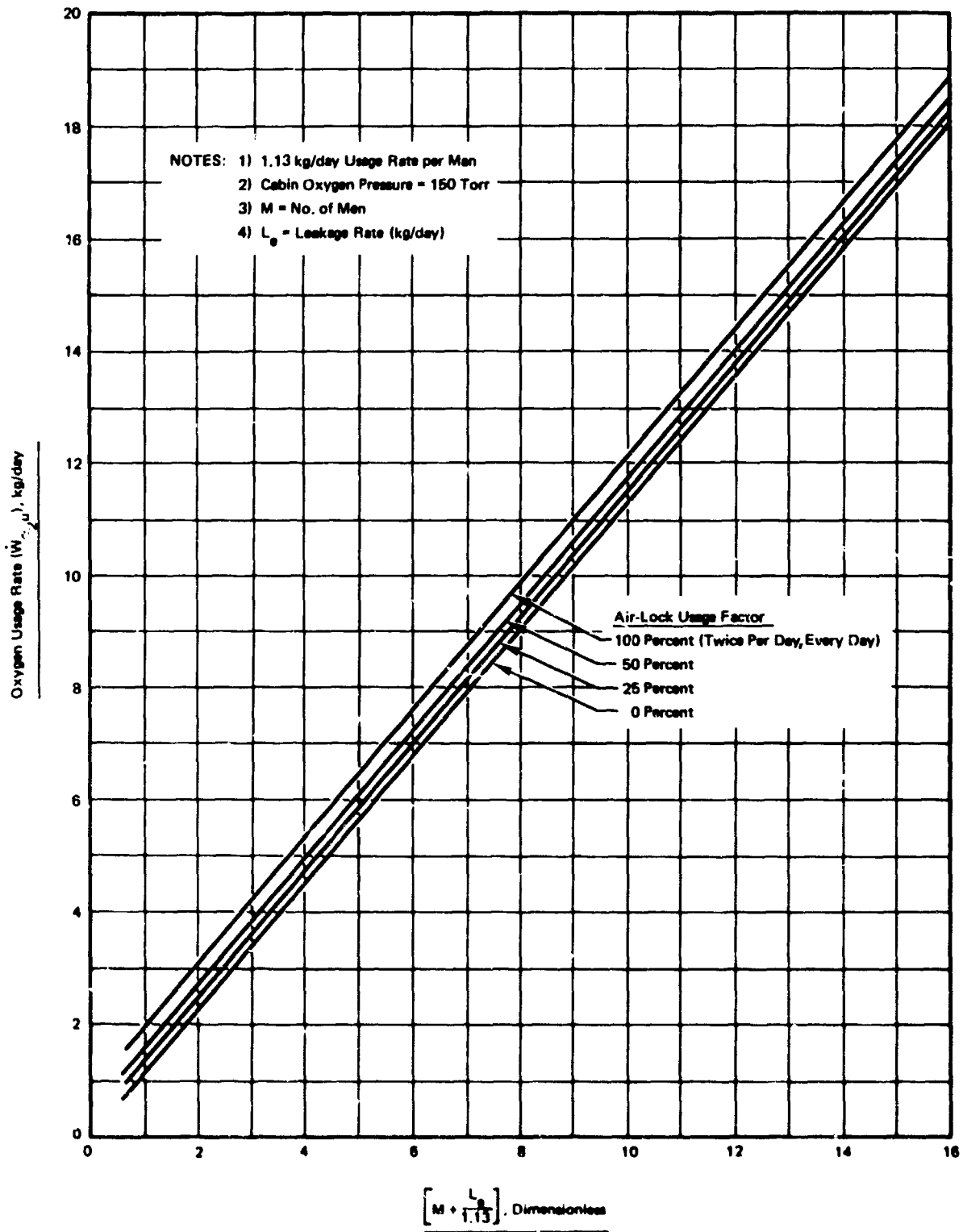


Figure 86. Oxygen Usage Rate as a Function of No. of Men, Leakage Rate and Air-Lock Usage Factor

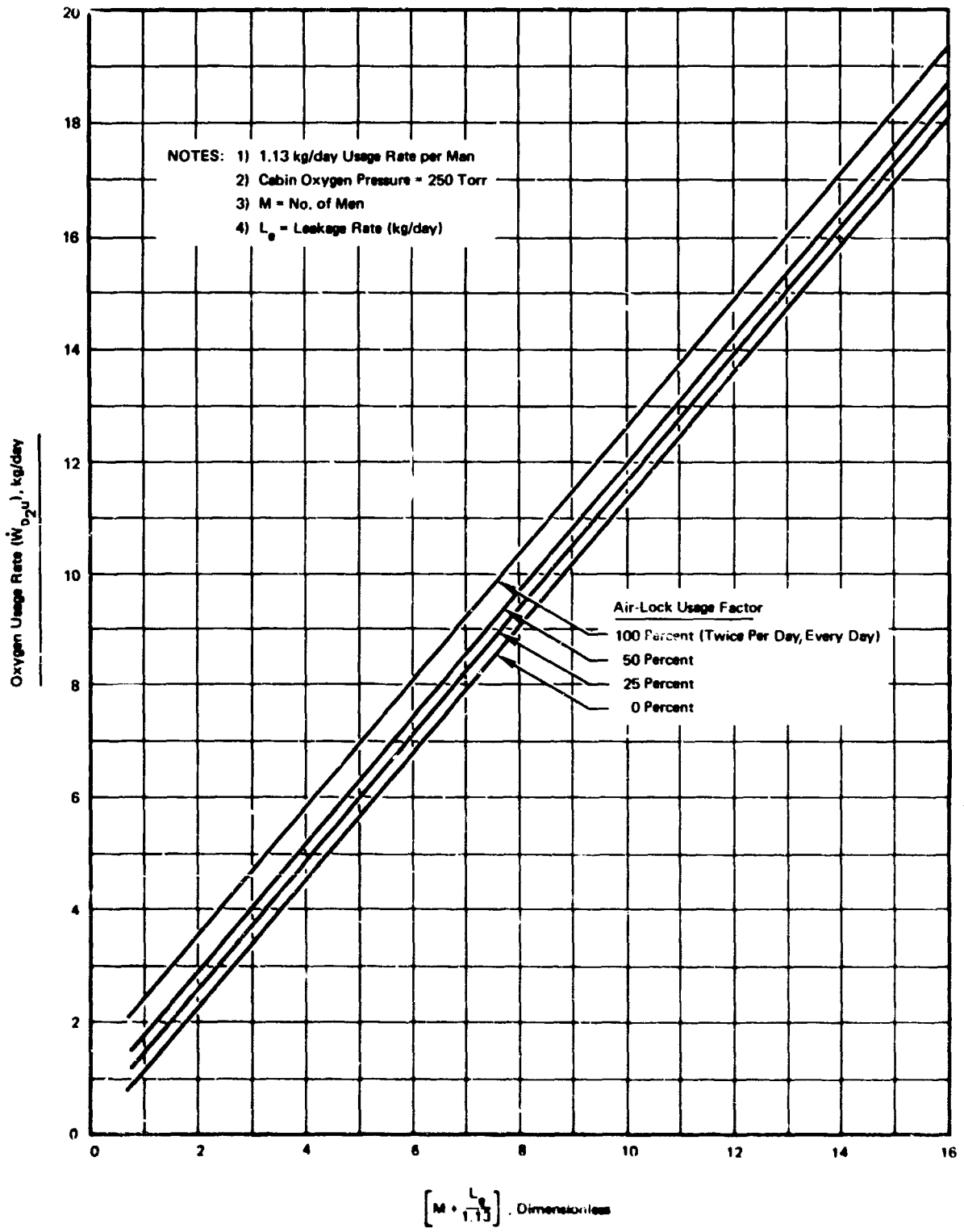


Figure 67. Oxygen Usage Rate as a Function of No. of Men, Leakage Rate and Air-Lock Usage Factor

AD 687852

Security Classification

DOCUMENT CONTROL DATA - R & D

(Security classification of title, body of abstract and indexing annotation must be entered when the overall report is classified)

1. ORIGINATING ACTIVITY (Corporate author) Aerojet-General Corporation Electronics Division Azusa, California		2a. REPORT SECURITY CLASSIFICATION UNCLASSIFIED	
		2b. GROUP N/A	
3. REPORT TITLE CRYOGENIC SOLID OXYGEN STORAGE AND SUBLIMATION INVESTIGATION			
4. DESCRIPTIVE NOTES (Type of report and inclusive dates) Final Report (1 July 1967 - 31 March 1968)			
5. AUTHOR(S) (First name, middle initial, last name) John E. Ahern Truman W. Lawson, Jr.			
6. REPORT DATE December 1968	7a. TOTAL NO. OF PAGES 158	7b. NO. OF REFS 14	
8a. CONTRACT OR GRANT NO. F33615-67-C-1849		9a. ORIGINATOR'S REPORT NUMBER(S) Aerojet-General Report No. 3545	
b. PROJECT NO. 6373			
c. Task No. 637302		9b. OTHER REPORT NO(S) (Any other numbers that may be assigned this report) AMRL-TR-68-105	
d. Work Unit No. 637302045			
10. DISTRIBUTION STATEMENT This document has been approved for public release and sale; its distribution is unlimited.			
11. SUPPLEMENTARY NOTES		12. SPONSORING MILITARY ACTIVITY Aerospace Medical Research Laboratories Aerospace Medical Div., Air Force Systems Command, Wright-Patterson AFB, OH 45433	
13. ABSTRACT The use of solid oxygen for storage and supply systems in space applications was studied both analytically and experimentally. The analysis indicated that the use of solid oxygen could provide substantially longer storage times over that obtainable with subcritical and supercritical oxygen. Oxygen transport from the vacuum storage condition of solid oxygen to a condition suitable for breathing was demonstrated experimentally by two methods, vapor transport using cryosorption pumps and solid transport by mechanically moving the solid through a vapor lock. A preliminary analysis of the transport methods indicates that the mechanical system should be the most suitable.			

DD FORM 1473

Security Classification

14. KEY WORDS	LINK A		LINK B		LINK C	
	ROLE	WT	ROLE	WT	ROLE	WT
Atmosphere regeneration Cryogenic solid oxygen Oxygen Supply Oxygen storage Space systems						